

**CONSTRUCTIVE TISSUE REMODELING BY EXTRACELLULAR MATRIX  
BIOSCAFFOLDS WITHIN THE AGING SKELETAL MUSCLE  
MICROENVIRONMENT**

by

Brian Matthew Sicari

Bachelor of Science in the Biological Sciences, University of Pittsburgh, 2004

Submitted to the Graduate Faculty of  
The School of Medicine in partial fulfillment  
of the requirements for the degree of  
Doctor of Philosophy

University of Pittsburgh

2013

UNIVERSITY OF PITTSBURGH

School of Medicine

This dissertation was presented

by

Brian Matthew Sicari

It was defended on

November 26<sup>th</sup>, 2013

and approved by

Donna Beer Stolz, PhD, Associate Professor, Department of Cell Biology

Johnny Huard, PhD, Professor, Department of Orthopedic Surgery

James L. Funderburgh, PhD, Professor, Department of Cell Biology and Physiology

Jon Piganelli, PhD, Associate Professor, Department of Immunology

Dissertation Advisor: Stephen F. Badylak, DVM, PhD, MD, Professor, Department of

Surgery

**CONSTRUCTIVE TISSUE REMODELING BY EXTRACELLULAR MATRIX  
BIOSCAFFOLDS WITHIN THE AGING SKELETAL MUSCLE  
MICROENVIRONMENT**

Brian Matthew Sicari, PhD

University of Pittsburgh, 2013

Copyright © by Brian Matthew Sicari

2013

**CONSTRUCTIVE TISSUE REMODELING BY EXTRACELLULAR MATRIX  
BIOSCAFFOLDS WITHIN THE AGING SKELETAL MUSCLE  
MICROENVIRONMENT**

Brian Matthew Sicari, PhD

University of Pittsburgh, 2013

Adult mammalian skeletal muscle tissue retains inherent regenerative capability in response to injury. This regenerative response is contingent upon an activated progenitor cell population and a temporal transition from pro-inflammatory M1 to immunomodulatory and constructive M2 polarized macrophages at the site of injury. Specifically, pro-inflammatory effector molecules secreted by M1 macrophages promote the expansion of skeletal muscle progenitor cells, while resolution of the inflammatory response and myogenic differentiation of skeletal muscle progenitor cells is dependent upon immunomodulatory effector molecules secreted by M2 macrophages.

The decline in the regenerative capacity of skeletal muscle tissue associated with advanced age is largely a consequence of progenitor cell dysfunction. Furthermore, advanced age is accompanied with immunosenescence of the innate immune system resulting in an impaired macrophage polarization potential.

Biologic scaffold materials composed of mammalian extracellular matrix (ECM) have been successfully used in both pre-clinical animal studies and in human clinical applications to promote constructive tissue remodeling in a variety of anatomic locations including skeletal muscle. The presence of ECM bioscaffolds at sites of skeletal muscle injury has been associated with a predominant M2 macrophage phenotype and downstream site-appropriate or constructive,

functional tissue remodeling. The mechanisms responsible for this constructive tissue remodeling response are only partially understood.

The present dissertation shows that the age of source animals from which ECM bioscaffold materials are harvested represents a determinant factor of the constructive tissue remodeling potential induced by these materials. The present work also shows that degradation products of mammalian ECM promote the constructive M2 macrophage phenotype in both young and age-impaired macrophages. Moreover, effector molecules from macrophages exposed to ECM degradation products are chemotactic and myogenic for skeletal muscle progenitor cells. The present dissertation describes a new rodent model of volumetric muscle loss (VML) and an ECM bioscaffold based approach for tissue replacement associated with modulation of macrophage phenotype and the endogenous recruitment of perivascular stem cells.

## TABLE OF CONTENTS

<b>1.0 INTRODUCTION AND SPECIFIC AIMS .....</b>	<b>1</b>
<b>1.1. BIOLOGIC SCAFFOLDS COMPOSED OF MAMMALIAN EXTRACELLULAR MATRIX .....</b>	<b>1</b>
<b>1.1.1. Native Mammalian Extracellular Matrix .....</b>	<b>1</b>
<b>1.1.2. Extracellular Matrix as a Scaffold Material .....</b>	<b>2</b>
<b>1.1.3. Default mammalian injury response vs. constructive tissue remodeling ...</b>	<b>3</b>
<b>1.1.4. Mechanisms of extracellular matrix bioscaffold mediated constructive tissue remodeling.....</b>	<b>4</b>
<b>1.1.4.1. Degradation of Extracellular Matrix Bioscaffolds.....</b>	<b>4</b>
<b>1.1.4.2. Recruitment of Progenitor Cells by Extracellular Matrix Bioscaffolds.....</b>	<b>5</b>
<b>1.1.4.3. The Innate Immune Response to Extracellular Matrix Bioscaffolds</b>	<b>6</b>
<b>1.2. TISSUE ENGINEERING AND REGENERATIVE MEDICINE APPROACHES TO ENHANCE THE FUNCTIONAL RESPONSE TO SKELETAL MUSCLE INJURY .....</b>	<b>8</b>
<b>1.2.1. Background.....</b>	<b>9</b>
<b>1.2.1.1. The Skeletal Muscle Response to Injury.....</b>	<b>9</b>

1.2.1.2.	Myogenic Progenitor Cells .....	10
1.2.1.3.	Tissue Engineering and Regenerative Medicine .....	10
1.2.2.	Cell-Therapy Approach .....	12
1.2.2.1.	Overview .....	12
1.2.2.2.	Muscle-Derived Progenitor Cells.....	13
1.2.2.3.	Limitations Associated with Cell-Therapy .....	19
1.2.3.	TEMC Approach.....	21
1.2.3.1.	Synthetic Scaffold Based TEMC .....	22
1.2.3.2.	Naturally Occurring Scaffold Based TEMC .....	23
1.2.4.	Acellular Scaffold Approach .....	26
1.2.4.1.	Implanted Acellular ECM Scaffolds Influence the Host Tissue Microenvironment .....	27
1.2.4.2.	Process of Acellular ECM Scaffold Remodeling.....	27
1.2.4.3.	Acellular ECM Scaffolds Recruit Progenitor Cells .....	28
1.2.4.4.	Acellular ECM Scaffolds Influence the Host Innate Immune Response .....	30
1.2.4.5.	Limitations Associated with Acellular ECM Scaffolds .....	31
1.2.4.6.	Clinical Translation of ECM Scaffolds .....	31
1.2.5.	Conclusions .....	33
1.3.	THE ROLE OF THE INNATE IMMUNE SYSTEM FOLLOWING SKELETAL MUSCLE INJURY .....	33
1.4.	AGE-ASSOCIATED PATHOLOGIES AFFECTING THE SKELETAL MUSCLE INJURY RESPONSE.....	35

1.4.1. Age-Related Changes in Skeletal Muscle Myogenesis .....	36
1.4.2. Age-Related Changes in Macrophage Physiology .....	36
1.5. CENTRAL HYPOTHESIS.....	37
1.6. SPECIFIC AIMS .....	37
<b>2.0 THE HOST REMODELING RESPONSE, INCLUDING MACROPHAGE PHENOTYPE INDUCED BY ECM SCAFFOLDS DERIVED FROM YOUNG AND AGED SOURCE ANIMALS .....</b>	<b>38</b>
2.1 BACKGROUND.....	38
1.7. MATERIALS AND METHODS.....	40
2.1.1 Overview of Experimental Design.....	40
2.1.2 Source and preparation of ECM scaffold material .....	41
2.1.3 Surgical procedure .....	42
2.1.4 Euthanasia and specimen harvest .....	43
2.1.5 Histologic and immunolabeling analysis .....	44
2.1.6 Quantification of histologic and immunolabeling analysis .....	46
2.1.7 Mechanical testing .....	47
2.1.8 Statistical analysis.....	48
2.2 RESULTS.....	48
2.2.1 Histomorphologic and immunolabeling findings .....	48
2.2.1.1 Untreated defect .....	50
2.2.1.2 Autologous tissue graft .....	52
2.2.1.3 Neonate aged SIS-ECM scaffold.....	54
2.2.1.4 Feeder aged SIS-ECM graft.....	55

2.2.1.5	Market aged SIS-ECM graft.....	57
2.2.1.6	Sow aged SIS-ECM scaffold.....	59
2.2.2	Mechanical testing.....	60
2.3	DISCUSSION AND CONCLUSIONS.....	61
2.4	LIMITATIONS AND FUTURE DIRECTIONS.....	65
3.0	THE ABILITY OF ECM TO ENHANCE THE POLARIZATION OF MACROPHAGES ISOLATED FROM YOUNG AND AGED SUBJECTS AND THE EFFECT OF ECM AND POLARIZED MACROPHAGES UPON SKELETAL MUSCLE PROGENITOR CELLS.....	66
3.1	BACKGROUND.....	66
3.2	MATERIALS AND METHODS.....	69
3.2.1	Overview of Experimental Design.....	69
3.2.2	Preparation of ECM degradation products.....	69
3.2.3	Isolation and culture of murine bone marrow derived macrophages .....	70
3.2.4	Polarization and immunolabeling of bone marrow derived macrophages 70	
3.2.5	Validation of Macrophage Phenotype with Western Blots.....	71
3.2.6	Progenitor Cell Culture.....	72
3.2.7	Preparation of Boyden Chamber Test Articles .....	72
3.2.8	Chemotaxis Assay.....	73
3.2.9	Mitogenesis Assay.....	73
3.2.10	Myogenesis Assay.....	74
3.2.11	Statistical analysis.....	75

<b>3.3</b>	<b>RESULTS.....</b>	<b>75</b>
3.3.1	Degradation Products from ECM Bioscaffolds Promote the M2 Macrophage Phenotype .....	75
3.3.2	ECM-Treated and IL-4 induced M2 Macrophages are Chemotactic and Myogenic for Skeletal Muscle Progenitor Cells. ....	77
3.3.3	Degradation Products from Market Weight and Young ECM are Chemotactic and Myogenic for Skeletal Muscle Progenitor Cells .....	79
<b>3.4</b>	<b>DISCUSSION AND CONCLUSIONS.....</b>	<b>80</b>
<b>3.5</b>	<b>LIMITATIONS AND FUTURE DIRECTIONS .....</b>	<b>85</b>
<b>4.0</b>	<b>ECM MEDIATED CONSTRUCTIVE REMODELING IN A MOUSE MODEL OF VOLUMETRIC MUSCLE LOSS .....</b>	<b>88</b>
<b>4.1</b>	<b>BACKGROUND.....</b>	<b>88</b>
<b>4.2</b>	<b>MATERIALS AND METHODS.....</b>	<b>90</b>
4.2.1	Overview of Experimental Design.....	90
4.2.2	Scaffold Preparation.....	90
4.2.3	Surgical Procedure .....	91
4.2.4	Specimen Harvest and Histology.....	92
4.2.5	Immunolabeling Studies.....	93
4.2.6	Statistical Analysis.....	94
<b>4.3</b>	<b>RESULTS.....</b>	<b>95</b>
4.3.1	Surgical Procedures.....	95
4.3.2	Macroscopic and Microscopic Findings .....	96
4.3.2.1	Control Group.....	96

4.3.2.2	SIS-ECM Treated Group .....	98
4.4	DISCUSSION AND CONCLUSIONS.....	100
4.5	LIMITATIONS AND FUTURE DIRECTIONS .....	107
5.0	CLINICAL TRANSLATION OF EXTRACELLULAR MATRIX BIOSCAFFOLDS	
	109	
5.1	BACKGROUND.....	109
5.2	MATERIALS AND METHODS.....	111
5.2.1	Mouse Model of Volumetric Muscle Loss .....	111
5.2.2	Patient Selection and Screening Examination .....	111
5.2.3	Physical Therapy Screening .....	113
5.2.4	Pre-Surgical Physical Therapy.....	114
5.2.5	Surgical Procedure .....	114
5.2.6	Post-Surgical Physical Therapy .....	115
5.2.6.1	Imaging .....	115
5.2.7	Tissue Biopsy.....	116
5.2.8	Immunolabeling Studies.....	116
5.3	RESULTS.....	119
5.3.1	Mouse Model of Volumetric Muscle Loss .....	119
5.3.2	Clinical Cohort Study Design .....	122
5.3.3	Subjects with Volumetric Muscle Loss .....	125
5.3.4	Histomorphologic Findings.....	126
5.3.5	Pre- & Post-Surgical Imaging .....	128
5.3.6	Post-Surgical Function .....	129

<b>5.4 DISCUSSION AND CONCLUSIONS.....</b>	<b>132</b>
<b>5.5 LIMITATIONS AND FUTURE DIRECTIONS .....</b>	<b>136</b>
<b>6.0 DISSERTATION SYNOPSIS .....</b>	<b>139</b>
<b>6.1 MAJOR FINDINGS .....</b>	<b>139</b>
<b>APPENDIX.....</b>	<b>142</b>
<b>BIBLIOGRAPHY .....</b>	<b>146</b>

## LIST OF TABLES

Table 1: A summary of the pre-implantation properties of the differently aged ECM scaffolds..	40
Table 2: Tissue assessment. ....	41
Table 3: Patient exclusion and inclusion criteria. ....	113
Table 4: Quantification of Histological Findings from the Mouse Model of VML.. ....	118
Table 5: Patient information.. ....	125
Table 6: Patient Biopsy Procedure and Findings.. ....	126

## LIST OF FIGURES

Figure 1: Tissue Engineering and Regenerative Medicine Approaches Aimed at Augmenting the Skeletal Muscle Response To Injury. ....	12
Figure 2: The Implantation of an Acellular ECM Scaffold Promotes the Recruitment of Host Cells. ....	28
Figure 3: Common Populations of Cells with Myogenic Potential Employed In Exogenous Cell-Therapy, Exogenous Tissue Engineered Muscle Construct (TEMC) Therapy, and Acellular ECM Scaffold Mediated Endogenous Cell Recruitment.....	30
Figure 4: Host cellular response at the surgical site at 14 days post-surgery. ....	50
Figure 5: Quantitative immunohistochemical analysis of vascularity.....	51
Figure 6: Trichrome staining (A) and collagen content quantified (blue staining) using spectral unmixing (B). ....	53
Figure 7: Scaffold composition at 14, 28, and 180 days post-surgery.....	55
Figure 8: Connective tissue deposition within each surgical site over time. ....	56
Figure 9: Distribution of slow and fast skeletal muscle fibers within the remodeled tissue at 180 days post-surgery. ....	58
Figure 10: Innervation of remodeled tissue at 180 days post-surgery. ....	60
Figure 11. Mechanical properties of explanted surgical sites at 180 days post-surgery.....	61

Figure 12: Mammalian ECM promotes the M2 macrophage phenotype. ....	77
Figure 13: Mammalian ECM promotes the M2 macrophage phenotype in aged macrophages...78	
Figure 14: Polarized macrophages retain phenotype after growth-factor withdrawal.....	80
Figure 15: M2 and ECM-treated macrophages are chemotactic for progenitor cells.....	81
Figure 16: M1 macrophages are mitogenic for progenitor cells.....	82
Figure 17: Media conditioned by polarized M2 and ECM-treated macrophages are myogenic for myoblasts. ....	83
Figure 18: Degradation Products from ECM are chemotactic for progenitor cells.....	84
Figure 19: Degradation Products from ECM are not mitogenic for PVSCs.....	86
Figure 20: Degradation products from ECM are myogenic for PVSCs.....	86
Figure 21: Degradation products from ECM are myogenic for C2C12 skeletal muscle myoblasts. ....	87
Figure 22: Induction of VML injury. ....	92
Figure 23: VML injury is of critical size. ....	95
Figure 24: Defect site at 7 days post-surgery.....	97
Figure 25: Defect site at 14 days post-surgery.....	98
Figure 26: Macrophage phenotype.. ....	100
Figure 27. Perivascular stem cell activation. ....	101
Figure 28. Defect site at 28 days post-surgery.....	102
Figure 29. Vascularity of treated versus untreated VML defects. ....	103
Figure 30. Evidence of innervation within treated versus untreated VML defects. ....	104
Figure 31. Site-appropriate remodeling by ECM scaffolds. ....	106

Figure 32: Progenitor cells are present at the site of constructive remodeling by ECM scaffolds surgically placed within sites of VML injury. ....	120
Figure 33: Schematic of clinical study design.. ....	124
Figure 34: Constructive tissue remodeling by ECM scaffolds in a human clinical application. ....	127
Figure 35: Imaging of affected extremity pre- and post-surgical implantation. ....	129
Figure 36: ECM-mediated constructive remodeling was associated with functional improvements.....	130
Figure 37: Force production data from each individual patient.....	131
Figure 38: Functional task data from each individual patient.....	134

## PREFACE

This dissertation is dedicated to my parents, Tony and Debbie Sicari, and to my late grandparents, Jack and Elaine Dakas. Any success I achieve is directly a result of their love, support, and inspiration.

I would like to thank my first mentors: Drs. Andrew F. Stewart and Nathalie Fiaschi-Taesch who encouraged me to always “surround yourself with people smarter than you.”

Dr. Badylak, thank you for giving me the opportunity to take their advice and work in your laboratory. The knowledge and opportunities you have provided cannot be expressed in words. I am forever grateful for the multidisciplinary training I have received under your mentorship.

I would like to especially thank the “people smarter than me,” my colleagues in the Badylak Laboratory: Dr. Neill Turner, Dr. Vineet Agrawal, Dr. Chris Dearth, Dr. Chris Medberry, Matt Wolf, Dr. Chris Carruthers, Ricardo Londono, Lisa Carey, Tim Keane, Denver Faulk, Scott Johnson, Dr. Li Zhang, Janet Reing, Dr. Peter Slivka, Dr. Fan Wei Meng, Dr. Steve Tottey, Dr. Beth Kollar, John Freund, Dr. Hongbin Jiang, and Dr. Bryan Brown.

Special thanks to Jocelyn Runyon, Eve Simpson, and Allyson Lacovey for all of your help and support.

Thank you to Shawn Bengston, Joe Hanke, Terri Horgan, Diane Rossi and all other staff members of the McGowan Center for Preclinical Studies.

I have also been lucky enough to work with exceptional undergraduate students who are well on their way to successful scientific / medical careers. This work would not exist without you. Thank you Jenna Dziki and Bernard Siu.

Special thanks to my committee members: Dr. Johnny Huard and the entire Huard Laboratory, Dr. Jon Piganelli and the entire Piganelli Laboratory, Dr. Donna Beer Stolz, and Dr. James Funderburgh. Your input into this body of work has been invaluable.

I would also like to thank the National Institutes of Health and specifically the National Institute on Aging for funding this body of work.

## **1.0 INTRODUCTION AND SPECIFIC AIMS**

This section will introduce biologic scaffolds composed of extracellular matrix (ECM) and discuss current tissue engineering and regenerative medicine therapeutic strategies, including the use of surgically placed ECM bioscaffolds, for the reconstruction of skeletal muscle tissue. The role of the innate immune system and myogenic progenitor cells in the context of skeletal muscle regeneration and how the aging process negatively affects this system will also be discussed. Finally, the central hypothesis and specific aims of the present dissertation will be introduced.

### **1.1. BIOLOGIC SCAFFOLDS COMPOSED OF MAMMALIAN EXTRACELLULAR MATRIX**

#### **1.1.1. Native Mammalian Extracellular Matrix**

Mammalian extracellular matrix (ECM) is composed of the secreted products produced by the resident cells of each tissue or organ. The composition of the ECM is dependent on factors that affect resident cell phenotype such as mechanical forces, biochemical milieu, oxygen tension, and patterns of gene expression among others. The ECM, in turn, influences the phenotype, chemotaxis, mitogenesis, and differentiation of resident cells, and serves as a medium for crosstalk between cells (*1*). For these reasons, the ECM is considered to be in a state of dynamic reciprocity with the resident

cell population and to play an important role in normal tissue and organ morphogenesis and homeostasis (1, 2). Mammalian ECM is composed of: collagen, fibronectin, laminin, elastin, glycosaminoglycans, growth factors, and cryptic peptides among others (1, 3). Collagen is the most abundant molecule within mammalian ECM and comprises nearly 90% of its dry weight (4). In addition to maintaining the structure of each tissue; cryptic peptides derived from parent collagen molecules are known to possess significant biologic activity (5-11). Other functional molecules within ECM include growth factors such as vascular endothelial growth factor (VEGF), fibroblast growth factor (FGF), stromal derived growth factor (SDF-1), epidermal growth factor (EGF), transforming growth factor beta (TGF- $\beta$ ), keratinocytes growth factor (KGF), hepatocyte growth factor (HGF), platelet derived growth factor (PDGF), and bone morphogenetic protein (BMP) among others (12-16).

### **1.1.2. Extracellular Matrix as a Scaffold Material**

Biologic scaffolds composed of extracellular matrix are derived through the decellularization of mammalian tissues. The decellularization process incorporates mechanical, chemical, and enzymatic processes designed to efficiently promote the dissociation and removal of pro-inflammatory immunogenic cellular material while preserving the native constituents and ultrastructure of the ECM. Upon their surgical placement at sites of tissue injury, ECM bioscaffolds have been shown to promote constructive tissue remodeling. Constructive tissue remodeling alters the default scar tissue forming mammalian response to injury and promotes site-appropriate tissue formation.

### **1.1.3. Default mammalian injury response vs. constructive tissue remodeling**

The default mammalian response to injury is highly conserved among tissue types and occurs in three overlapping yet distinct phases: the inflammatory phase, the proliferative phase, and the remodeling phase (17). The inflammatory phase occurs immediately after tissue damage and is marked by activation of the coagulation cascade and the subsequent influx of innate inflammatory cells that facilitate the removal of cellular debris and infection prevention. Specifically, hemostasis is achieved through the deposition of a provisional fibrin matrix which acts as a scaffold for infiltrating neutrophils and macrophages (18). The proliferative phase is characterized by angiogenesis as well as the migration, proliferation and differentiation of different cell types (19, 20). During the remodeling phase macrophages and endothelial cells are subject to apoptosis while fibroblasts and myofibroblasts produce and deposit a collagenous extracellular matrix. This relatively acellular fibrous matrix is the precursor of scar tissue, which typically replaces site appropriate functional tissue within the injury site.

In contrast, host constructive tissue remodeling is a process by which the default healing response to injury is modified from one that results in scar tissue formation to one that results in the formation of site appropriate functional tissue. Mechanisms behind an ECM scaffold mediated constructive remodeling response to injury are discussed below and include the participation of an activated host progenitor cell population and a predominant M2/Th2 restricted immune response among others (8, 21, 22).

#### **1.1.4. Mechanisms of extracellular matrix bioscaffold mediated constructive tissue remodeling**

While the exact mechanisms behind the ability of ECM based bioscaffolds to promote constructive tissue remodeling remain only partially understood, there are a number of processes which are believed to be key contributors. Among these processes are the ability of the scaffold material to degrade rapidly with concomitant release of bioactive matricryptic peptides, the ability of the scaffold material to recruit stem / progenitor cells, and the ability of the scaffold material to elicit a constructive host response which does not result in a foreign body response or immunologic rejection of the implant. Each of these processes is discussed below, and explored in further detail in the studies which comprise the present dissertation.

##### **1.1.4.1. Degradation of Extracellular Matrix Bioscaffolds**

ECM scaffolds degrade rapidly *in vivo*. Studies have shown that surgically placed ECM scaffolds become 60% degraded at 30 days post-implantation and 100% degraded after 90 days (23). During this period, the scaffold becomes populated and degraded by host-derived mononuclear cells and ultimately results in the formation of site-specific functional host tissue histologically indistinguishable from native tissue. The scaffold degradation process is mediated by inflammatory cells, such as macrophages, which produce proteolytic enzymes that facilitate the degradation of the matrix scaffold material (23-25).

ECM scaffolds have also been degraded *ex vivo* by chemical and physical methods (26). Recent findings suggest that the degradation products of ECM scaffolds are bioactive (6, 7, 9, 10). Studies have shown antimicrobial activity associated with the degradation products of ECM scaffolds; however, in the absence of degradation, antimicrobial activity was not seen,

suggesting that some of the bioactive properties of the ECM are derived from its degradation products rather than from whole parent molecules present within the ECM (9, 26). Furthermore, a low molecular weight peptide derived from the collagen III parent molecule has been shown to possess osteogenic potential (6). Degradation products of ECM scaffolds have also been shown to be chemotactic for progenitor and non-progenitor cell populations (5, 7, 8, 10, 27, 28) and to influence the host innate immune response (9, 21, 22, 29-31).

#### **1.1.4.2. Recruitment of Progenitor Cells by Extracellular Matrix Bioscaffolds**

Surgically placed ECM scaffolds and their degradation products have been associated with the recruitment of endogenous stem / progenitor cells. This phenomenon, including recruited cell-types, is discussed in detail under section 1.2 of the present dissertation. In general, biologic scaffolds composed of mammalian ECM have been shown to be chemotactic for a diverse array of stem / progenitor cells with robust differentiation potentials. For example, primitive Sox2<sup>+</sup> cells were shown to be present at the site of ECM implantation in an adult mammalian model of digit injury (5, 27), while multipotent bone-marrow derived cells were shown to participate in the remodeling of ECM scaffold mediated Achilles tendon repair (32). Specifically, in the preclinical Achilles tendon injury model, ECM scaffold explants promoted chemotaxis of progenitor cells after 3, 7, and 14 days of *in vivo* remodeling (8). The results of the study showed greater migration of progenitor cells towards tendons repaired with ECM scaffolds compared to tendons repaired with autologous tissue and uninjured normal contralateral tendon. These results suggest that ECM scaffolds are capable of recruiting progenitor cells to the site of implantation to participate in constructive tissue remodeling over the long-term.

### ***Perivascular Stem Cells***

ECM scaffold materials have been shown to influence specialized populations of progenitor cells including multipotent perivascular stem cells (PVSC). Specifically, degradation products from ECM bioscaffolds have been shown to be chemotactic for PVSCs (5, 7, 11, 33). PVSC's are CD146<sup>+</sup>, NG2<sup>+</sup> cells found in all vascularized tissues of adult mammals and reside in a niche encircling microvessels and capillaries where they regulate vasoconstriction (33). Outside their niche, these cells are multipotent and give rise to cells from the adipogenic, osteogenic, and chondrogenic cell lineages. Furthermore PVSC's (isolated as CD146<sup>+</sup>, CD56<sup>-</sup>, CD45<sup>-</sup>, CD34<sup>-</sup>, CD144<sup>-</sup>) have been shown to be highly myogenic and when transplanted into areas of injured muscle induce a higher regenerative index when compared to other myogenic cell-types (33, 34). Endogenous PVSCs have also been shown to give rise to skeletal muscle myoblasts and participate in the adult mammalian regenerative response to skeletal muscle injury (35, 36). PVSCs, and other myogenic cell populations, are further discussed under section 1.2 of the present dissertation.

#### **1.1.4.3. The Innate Immune Response to Extracellular Matrix Bioscaffolds**

The host innate immune system and specifically macrophages play a pivotal role in the host response to biomaterial implantation. In fact, macrophage depletion prevents the degradation of ECM biologic scaffolds *in vivo* (31). Macrophages have been shown to respond to many different implanted biomaterials, including those composed of metals (37), ceramics (38), polymers (39), and biologic proteins such as collagens and xenogeneic ECM (31, 40). Macrophage mediated foreign body giant cell formation and pro-inflammatory cytokine

production are frequently associated with the implantation of non-degradable or synthetic biomaterials. However, several recent studies suggest that immunomodulatory macrophages can facilitate constructive and site-appropriate tissue remodeling in response to ECM bioscaffold implantation (31, 41). Specifically, surgically placed ECM bioscaffolds have been associated with a constructive macrophage phenotype. Mechanisms behind this association are examined by the present dissertation.

Innate immunology has previously characterized macrophages as mononuclear phagocytes responsible for microbicidal activity and antigen presentation, the removal of cellular debris following acute tissue injury, and propagation of a type-I pro-inflammatory immune response (42-44). Macrophages are now recognized as a heterogeneous cell population capable of immunomodulation and tissue repair (24, 45-51). Specifically, following the Th1/Th2 nomenclature, macrophages have been categorized according to their functional properties as either M1 or M2 (47, 48). M1 or “classically activated” macrophages propagate a pro-inflammatory response while M2 or “alternatively activated” macrophages promote immunomodulation and are constructive. These opposing macrophage phenotypes will be discussed throughout this dissertation. Most relevant to the present introduction, is the phenomenon of surgically placed ECM bioscaffolds to be associated with the constructive M2 macrophage phenotype. Moreover, the phenotype of responding macrophages has been found to be an important determining factor in the success of an implanted biomaterial scaffold and its ultimate remodeling outcome (21, 22).

## **1.2. TISSUE ENGINEERING AND REGENERATIVE MEDICINE APPROACHES TO ENHANCE THE FUNCTIONAL RESPONSE TO SKELETAL MUSCLE INJURY**

The well-recognized ability of skeletal muscle for functional and structural regeneration following injury is severely compromised in degenerative diseases, diabetes, advanced age, and following volumetric muscle loss (VML). Tissue engineering and regenerative medicine strategies to support muscle reconstruction have typically been cell-centric with approaches that involve the exogenous delivery of cells with myogenic potential. These strategies have been plagued by poor cell viability and engraftment into host tissue among other limitations. Alternative approaches have involved the use of biomaterial scaffolds as substrates or delivery vehicles for exogenous myogenic progenitor cells. Acellular biomaterial scaffolds composed of mammalian extracellular matrix (ECM) have also been used as an inductive niche to promote the recruitment and differentiation of endogenous myogenic progenitor cells. An acellular approach, which activates or utilizes endogenous cell sources, obviates the need for exogenous cell administration and provides an advantage for clinical translation. The present section examines the state of tissue engineering and regenerative medicine therapies directed at augmenting the skeletal muscle response to injury and presents the pros and cons of each with respect to clinical translation.

## **1.2.1. Background**

### **1.2.1.1. The Skeletal Muscle Response to Injury**

Skeletal muscle has a robust capacity for remodeling, repair, and regeneration following injury (52, 53). This inherent regenerative response consists of three phases: the destruction phase, the repair phase, and the remodeling phase (54-56). The degeneration phase involves necrosis of parenchymal cells, stromal disruption, hematoma formation, and the influx of inflammatory cells. (54, 57). The repair phase is characterized by the activation of quiescent myogenic progenitor cells that enter the cell cycle, migrate to the site of injury and become proliferative (58, 59). These activated progenitor cells then differentiate and fuse to form multinucleated myofibers (55, 60). During the final phase of the skeletal muscle response to injury, referred to as the remodeling phase, the regenerated myofibers organize, mature and obtain the ability to contract. However, this response is often inadequate to replace functional tissue in certain conditions such as inheritable muscle degenerative disease, advanced age, or volumetric muscle loss (VML).

The above phases of skeletal muscle regeneration rely heavily on a population of cells, defined anatomically, as satellite cells. Satellite cells constitute the putative muscle stem cell compartment and when quiescent, are located between the plasma and basal membrane of myofibers (61, 62). Satellite cells asymmetrically divide and, in response to injury, give rise to skeletal muscle myoblasts (55). Myoblasts then proliferate, differentiate and fuse to form multinucleate and functional contractile skeletal muscle myofibers to complete the regenerative response (55, 63).

### **1.2.1.2. Myogenic Progenitor Cells**

In addition to satellite cells and myoblasts, progenitor cells with high myogenic potential have been identified within adult skeletal muscle. These cell types include CD133<sup>+</sup> progenitor cells, muscle-derived stem cells (MDSC's), multipotent perivascular progenitor cells, and muscle derived side-population (SP) cells among others. Multipotent cells with myogenic potential have also been isolated from tissues other than skeletal muscle such as bone marrow, adipose, and umbilical cord.

The present section of this dissertation will examine tissue engineering and regenerative medicine approaches which utilize the above myogenic cell types through exogenous cell-therapy or endogenous cell-recruitment. The eventual goal of all therapies is the augmentation of the inherent regenerative response of diseased or injured skeletal muscle.

### **1.2.1.3. Tissue Engineering and Regenerative Medicine**

Despite the well-accepted ability of skeletal muscle to regenerate following injury, the decline in the regenerative capacity associated with age, congenital defects such as Duchenne muscular dystrophy (DMD), and massive loss of muscle tissue from trauma, tumor ablation, or prolonged denervation resulting in VML represent skeletal muscle pathologies for which the inherent repair mechanisms are inadequate. In such cases, the current standard of care includes corticosteroid therapy for DMD (64-66) and autologous tissue transfer for VML (67-69). These treatment options show limited efficacy and are associated with severe pharmacologic side effects and donor site morbidity for DMD and VML, respectively.

Tissue engineering and regenerative medicine approaches aimed at augmenting the skeletal muscle injury response have traditionally involved the *in vitro* propagation and

subsequent injection or implantation of myogenic progenitor cells into areas of injured muscle (70-73). More recently, myogenic cells or their precursors have been combined with biologic scaffolds in attempts to promote the muscle regenerative response. These approaches attempt to develop an implantable tissue engineered muscle construct (TEMC) and typically require a period of *ex-vivo* culture necessary for efficient cellular-scaffold integration. Despite recent advancements, the *in vitro* culture and/or *ex-vivo* engineering followed by subsequent implantation of muscle cells and/or tissue has both technical limitations and associated translational hurdles. An engineered functional skeletal muscle construct requires integration with the host tissue including functional vascularization, and neuromuscular innervation. In addition, any cell-based approach subjects the therapy to more rigorous regulatory standards that are associated with both cost and time for the manufacturer/provider.

An alternative approach has been investigated in which decellularized xenogeneic or allogeneic mammalian tissues have been used to create inductive bioscaffolds composed of extracellular matrix (ECM). Such scaffolds provide no external source of new cells but rather recruit endogenous progenitor cells to sites of scaffold placement/muscle injury. The relative efficacy of the cell-based vs. acellular approaches has not been compared in head to head studies. Therapies which use cell based approaches, TEMC's, and acellular scaffolds will be discussed herein (Figure 1).

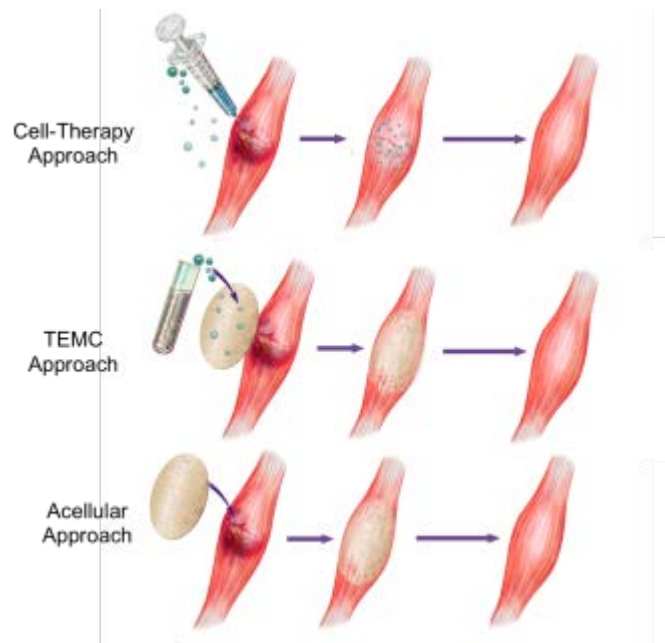


**Figure 1: Tissue Engineering and Regenerative Medicine Approaches Aimed at Augmenting the Skeletal Muscle Response To Injury.** The cell-therapy approach employs the administration of exogenous myogenic progenitor cells into sites of skeletal muscle injury via intramuscular injection. The second approach seeks to develop an implantable tissue engineered muscle construct (TEMC) composed of exogenous myogenic cells coupled with a biomaterial scaffold. The acellular approach employs the implantation of biologic scaffolds composed of decellularized mammalian tissue, which upon their degradation, recruit endogenous myogenic progenitor cells. These approaches share the same goal in that they seek to restore site appropriate and functional skeletal muscle tissue.

## 1.2.2. Cell-Therapy Approach

### 1.2.2.1. Overview

The concept of a purely cell-based approach is designed to increase the local pool of cells with myogenic potential; an approach which would logically augment and support the inherent

regenerative response of injured skeletal muscle. A variety of stem/progenitor cells are candidates for such an approach.

#### **1.2.2.2. Muscle-Derived Progenitor Cells**

##### ***Myoblasts***

Satellite cells reside beneath the basal lamina of normal adult skeletal muscle fibers and comprise only 2-7% of muscle associated cells (55, 59). These quiescent muscle progenitor cells become activated in response to stress from muscle overstimulation or injury and enter the cell cycle. Through asymmetric division, activated satellite cells replenish the quiescent satellite cell pool and give rise to committed myogenic precursor cells known as myoblasts (55). Skeletal muscle myoblasts proliferate, differentiate, and fuse with other myoblasts or to existing damaged myofibers to form new skeletal muscle. Following recoverable injuries such as weight bearing or exercise, myoblasts are able to fully repair damaged muscle fibers and eventually restore normal structure-function relationships. Pathologic conditions such as DMD or irrecoverable volumetric muscle loss (VML) involve types of muscle defects for which endogenous myoblasts are unable to fully compensate (74-76).

It is now well accepted that other muscle-derived stem cells or circulating progenitor cells possess myogenic potential and can contribute to new skeletal muscle formation. However, the satellite cell derived myoblast represents the primary cell type responsible for inherent skeletal muscle repair and regeneration. Transplantation of allogeneic myoblasts into injured muscle has been extensively investigated, especially as therapy for DMD. The initial preclinical demonstration that myoblast transplantation could restore dystrophin expression in animal models occurred as early as 1989 (77). A series of clinical trials resulting in unfavorable

outcomes were soon to follow (70, 71, 78-82). Although largely unsuccessful, these early clinical trials provided valuable insights surrounding the pathobiology of muscle cell implantation. The following fundamental problems with the current myoblast implantation procedures were identified: (1) At 3 days post-implantation less than 25% of the donor myoblasts remained viable (83, 84); (2) Donor myoblasts were incapable of significant migration from the injection site (85); (3) Inadequate immunosuppressive therapy resulted in the rapid rejection of donor cells (86); and (4) Cyclosporine mediated immunosuppression induced myoblast apoptosis (87, 88).

There are now partial solutions for these problems. The transfer of a greater number of cells can compensate for the poor post-implantation cell viability (85). A subset of pre-myoblast satellite cells has been identified that, when injected into models of DMD, result in an efficient and functional engraftment (89, 90). The low migration pattern associated with injected myoblasts has been partially addressed by transplant protocols that utilize an increased number of adjacent intramuscular injections resulting in more evenly distributed cell delivery (91). Moreover, Riederer and colleagues postulated that precocious differentiation of injected myoblasts prevented their post-transplantation proliferation and migration (92). Indeed, in pre-clinical models, when myoblasts were prevented from premature cell-cycle exit by using serum prior to and during administration, these cells were able to increase in number and colonize a much larger area within the recipient's muscle (92). As for problems associated with the prevention of graft rejection, some studies have shown that FK506 mediated immunosuppression results in favorable cell transplant outcomes when tested in mice and non-human primate models (93, 94). Although less than ideal, when some of these strategies were concurrently employed in a human patient clinical trial, they resulted in a 30% restoration of dystrophin expression. (91, 95, 96).

### ***CD133<sup>+</sup> Progenitor Cells***

As mentioned above, attempts to transplant cells into injured muscle via intramuscular injection have been hampered by the low migratory potential of the injected cells. An alternative approach would be to deliver myogenic progenitor cells via the systemic circulation if a mechanism for homing the cells to the site of interest were available. To this end, CD133<sup>+</sup> progenitor cells represent a promising myogenic cell type. Freshly isolated human CD133<sup>+</sup> progenitor cells express patterns of adhesion molecules commonly associated with cells capable of extravasation through the blood vessel wall (76). When enriched CD133<sup>+</sup> progenitor cells were injected into the systemic circulation of dystrophic mice, the CD133<sup>+</sup> cells contributed to muscle repair, increased dystrophin expression, and were able to replenish the endogenous satellite cell pool (97). In a head to head comparison, muscle derived CD133<sup>+</sup> cells injected into injured mouse muscle showed a greater replenishment of the satellite cell pool and higher regenerative capacity when compared to myoblasts injected in a similar fashion (98). To evaluate safety, Torrente and colleagues designed a DMD patient phase I clinical trial in which transplantation of autologous, and thus still dystrophic, muscle derived CD133<sup>+</sup> cells was conducted. Results of this trial showed no adverse events (99). Future studies will attempt delivery of healthy CD133<sup>+</sup> cells within the clinical setting.

### ***Muscle-Derived Stem Cells***

Early myogenic progenitor cells distinct from satellite cells can be separated from other muscle cell types based on their adherence to collagen coated flasks *in vitro* (100). Specifically, early adhering cells express satellite cell markers, while late adhering cells express stem cell markers. These cells, isolated from muscle digests and capable of long-term proliferation and myogenic potential, have been distinctly identified as muscle derived stem cells (MDSC's) (101). The

transplantation of enriched MDSC's into injured mouse skeletal muscle results in a more favorable outcome than the transplantation of skeletal muscle myoblasts (101). Genetically engineered MDSC's transduced with vectors overexpressing different growth factors prior to transplantation into dystrophic mouse models, have been associated with higher engraftment and better outcomes when compared to native MDSC's (102). One mechanism behind the improved transplantation outcomes of MDSC's over myoblasts, may be the increased antioxidant levels in MDSC's which allow them to survive oxidative stress associated with the harsh injury and transplantation microenvironment (103, 104).

### ***Multipotent Perivascular Progenitor Cells***

Perivascular cells encircle the endothelial cells that comprise capillaries and microvessels in all vascularized tissues (105). Perivascular cells have been traditionally associated with the control and constriction of microvasculature networks (105). In addition however, perivascular cells or subsets of perivascular cells are now accepted to be multipotent (33). It is plausible that multipotential perivascular progenitor cells represent a ubiquitous cell-type present throughout the microvasculature and represent a reserve cell population capable of responding to injury in all tissues. These perivascular stem cells are distinct from other endothelial, hematopoietic, and myogenic cells and can be isolated and enriched from human skeletal muscle according to their unique surface marker phenotype (33). Perivascular progenitor cells have been shown to contribute to developing myofibers in postnatal skeletal muscle development and during the inherent response to injury (35). Multipotent perivascular cells are myogenic *in vitro*, and when

injected into cardiotoxin injured mouse skeletal muscle, were able to induce a higher regenerative index when compared to enriched and injected myoblasts (33).

### ***Muscle Side Population Cells***

Muscle side population (SP) cells have been purified from mouse and human skeletal muscle using a similar approach originally optimized for the isolation of bone marrow SP cells (106). Muscle derived SP cells represent a heterogeneous population of cells distinct from bone marrow cells and other muscle derived progenitor cells (107). SP cells have been shown to give rise to satellite cells and myoblasts *in vivo* when injected into models of skeletal muscle injury (108, 109). Studies have shown that the systemic delivery of SP cells can result in engraftment within dystrophic mouse muscle (107).

### ***Mesenchymal Stem Cells***

Stem and progenitor cells from outside the skeletal muscle tissue compartment have been examined as potential sources of myogenic cells for skeletal muscle tissue engineering. Most of these cell populations can be generically categorized as mesenchymal stem cells (MSC's). Tissue sources of MSC's include bone marrow (110), adipose (111), hair follicles (112), placenta (113), umbilical cord (114), and others. MSC's give rise to tissues of mesodermal origin such as adipogenic, osteogenic, chondrogenic, and myogenic differentiation (115). Furthermore, MSC's are pluripotent and have been shown to differentiate into tissues of ectodermal and endodermal origin as well (116, 117). Following their isolation and expansion *in vitro*, lineage specific differentiation media is used to drive MSC's toward different phenotypes. MSC's derived from bone marrow, adipose, and umbilical cord tissues and their use as cell therapy for augmentation of the skeletal muscle injury response are discussed herein.

### ***Bone Marrow-Derived Cells***

Bone marrow-derived MSC's (BM-MSCs) expand rapidly in culture from bone marrow aspirates, and like MSC's from other sources have been shown to be pluripotent (110). It has been shown that, albeit to a small extent, endogenous circulating BM-MSCs contribute to native skeletal muscle myofiber remodeling in healthy (118, 119) and injured muscle (120, 121). A study by Winkler and colleagues showed a dose-response correlation between the number of transplanted BM-MSCs and the amount of functional recovery resulting from treatment by intramuscular injection within a skeletal muscle crush injury model (122). BM-MSCs delivered to injured muscle via intravenous or intra-arterial injection may contribute to host angiogenesis and myogenesis (123, 124). Recently, studies have shown that many exogenous BM-MSCs mediated cell-therapies have potentiated their positive effects through paracrine interactions with the host microenvironment rather than engraftment within host tissue (125, 126).

### ***Adipose-Derived cells***

Adipose tissue is now recognized as an abundant and readily accessible source of adult pluripotent cells. In adult mammals adipose tissue is composed of mesodermally derived adipocytes associated within a network of loose, areolar collagenous connective tissue. In addition to parenchymal tissue and in similar fashion to bone marrow, adipose tissue contains a stromal vascular cell population. Adipose tissues' stromal vascular compartment is comprised of endothelial, smooth muscle, and progenitor cell populations (111). Following enzymatic digestion, the stromal cellular fraction can be separated from adipocytes and connective tissue and the resulting cell populations can be cultured *in vitro*. Tissue culture plastic adhering cells comprise the progenitor cell compartment and are commonly referred to as adipose derived stem cells (ADSC's). In the presence of lineage specific inductive culture media, ADSC's can

differentiate into adipogenic, chondrogenic, osteogenic, and myogenic cells (127). ADSC's have been shown to spontaneously display myogenic potential *in vitro* and have been examined as potential donor cells aimed at augmenting skeletal muscle regeneration *in vivo* (128). For example, following injection into injured skeletal muscle, ADSC's modulate inflammation, increase angiogenesis, and restore dystrophin expression in mouse models of muscular dystrophy (129). Kang and colleagues investigated the ability of ADSC's to repair tissue damage in a murine ischemic hindlimb model (130). At four weeks post-injury and implantation, ADSC-transplanted limbs showed increased vascular density and reduced muscle atrophy. Treated limb musculature was comprised of donor derived differentiated myocytes (130).

### ***Umbilical Cord Blood-Derived Cells***

As an alternative to bone marrow, human umbilical cord blood (UCB) has been explored as a source of MSC's (114). Some data suggests UCB derived MSC's possess a higher proliferative capacity when compared to BM-MSC's or ADSC's (131). Unlike bone marrow aspiration, human UCB is obtained by a simple and painless procedure after birth, ameliorating any ethical concerns. UCB derived MSC's are pluripotent and some studies have shown that subpopulations of UCB cells display high myogenic potential (132). Injections of myogenic human UCB derived MSC's have promoted myogenesis in mouse models of muscular dystrophy and hindlimb ischemia (133, 134).

#### **1.2.2.3. Limitations Associated with Cell-Therapy**

One limitation of cell-based therapies lies in the potential routes of administration. Typically, injected cells display an impaired ability to redistribute and do not migrate more than 200 $\mu$ m from the intramuscular injection site (85). The systemic delivery of cells via intravenous

injection has resulted in unintentional cell engraftment at sites such as the liver and spleen (76). Another limitation to cell-therapy-based strategies is the inadequate supply of fresh donor cells. Regardless of the auto- or allogeneic progenitor cell source (muscle derived, MSC, or others), cells typically must be expanded in culture to obtain an adequate cell number. Most cell therapy trials in skeletal muscle have utilized *ex vivo* expanded myoblasts, which most likely undergo culture-induced changes with associated deleterious effects upon the differentiation potential of the pre-transplanted cells. Consistent with this notion, a study by Montarras et al. reported that an *ex vivo* culture period of as little as three days, of satellite cells or myoblasts, negatively impacts their ability to contribute to skeletal muscle repair upon transplantation *in vivo* (135). Clonal assays comparing freshly isolated cells versus culture-expanded cells indicated that short-term culture decreases proliferative and differentiation potentials (135). A potential safety concern associated with the use of pluripotent MSC's mediated cell therapy is the risk of transdifferentiation (136). It is now well accepted that some genes that confer pluripotency also confer oncogenicity. Studies determining the risk:benefit ratio associated with these cell-types are still in their infancy and need to be further studied prior to FDA consideration. These perspectives provide an overview of the significant hurdles to clinical translation. Perhaps the most significant limitation associated with cell-therapy approaches is the general poor engraftment of donor cells into host tissue (83, 84, 137-139).

After over 3 decades of study, it is widely accepted that myogenic progenitor cell transplantation and stem cell transplantation typically does not result in a significant engraftment of donor cells into host tissue. It has also been demonstrated that the low number of viable engrafted cells are not typically correlated with the levels of functional improvement in host tissue. For these reasons, it is now widely accepted that favorable outcomes resulting from stem

and progenitor cell transplantation, whether alone or in the context of a TEMC, are most likely associated with a paracrine effect of the donor cells upon the host injured microenvironment (140-145). The release of cytokines or other signaling molecules by donor cells most likely play a role in the recruitment of host cells and/or the modulation of the host innate immune response. For example, many of the above myogenic cell types have been shown to secrete growth factors which, through their paracrine effects, have the potential to stimulate angiogenesis and modulate the host pro-inflammatory response (146-149).

### **1.2.3. TEMC Approach**

Limitations associated with cell-based therapies provide the impetus for innovative tissue engineering approaches, which can augment the innate skeletal muscle response to injury. Since *in vivo* myogenic cells differentiate within a three-dimensional environment, one approach involves the incorporation of myogenic cells or precursor cells within an appropriate three-dimensional biomaterial scaffold; i.e., a microenvironmental niche. A biomaterial scaffold in conjunction with a myogenic cell component is referred to as a tissue engineered muscle construct (TEMC). Ideal biomaterials for skeletal muscle engineering should be able to support the propagation and expansion of myogenic progenitor cells *in vitro* and also, for *in vivo* implantation purposes, be able to integrate into host tissue. Scaffolds with a variety of compositional and biological features have been developed. Although several studies have examined the efficacy of non-biodegradable scaffolds, such as phosphate-based glass (150), biodegradable scaffolds are preferred (151). Following *in vivo* implantation, biodegradable scaffolds promote host tissue integration, and have the potential to be replaced with host skeletal

muscle tissue (152). Both synthetic and natural biodegradable scaffolds have been examined as described below.

#### **1.2.3.1. Synthetic Scaffold Based TEMC**

The copolymer poly-lactide-co-glycolide (PLG) is FDA approved and has been used clinically as a source material for biodegradable sutures for more than 30 years (153). Biodegradable PLG has also been described as a suitable scaffold material that promotes cell adherence, proliferation and formation of new three-dimensional tissues (154, 155). Porous PLG scaffolds have also been shown to promote host mediated vascularization and cell infiltration upon their *in vivo* implantation (156). These characteristics suggest that PLG may hold potential as a biomaterial for TEMC's. In a study by Thorrez et al., human skeletal muscle myoblasts were cultured within collagen coated porous PLG scaffolds and showed significant myogenic differentiation *in vitro* (157). However, when implanted subcutaneously in a mouse model after 4 weeks, these PLG based TEMC's resulted in only 22% donor cell viability (157). Results showed that despite their incorporation within the scaffold, implanted cells were depleted due to host derived NK cells.

Polymers composed of poly( $\epsilon$ -caprolactone) (PCL) and polylactic-co-glycolic acid (PGA) have also been examined as synthetic biodegradable three-dimensional scaffolds for skeletal muscle tissue engineering (158, 159). PCL based scaffolds with uni-directionally oriented nanofibers were able to promote muscle cell alignment and myotube formation (159). Following the implantation of neonatal rat myoblasts seeded onto PGA scaffolds, viable skeletal muscle and neo-vascularization could be identified within the TEMC at 45 days (158).

### **1.2.3.2. Naturally Occurring Scaffold Based TEMC**

TEMC's have been created from naturally occurring scaffolds as an alternative to the above mentioned synthetic polymers. The extracellular matrix (ECM) consists of structural and functional molecules which support cell-cell interactions (160). For these reasons, most TEMC's with a naturally occurring scaffold component are composed of ECM materials.

Native ECM is composed of the secreted products of the resident cells of each tissue and organ within the body. Furthermore, each tissue's ECM contains a distinct structural and compositional blueprint of proteins, proteoglycans, glycosaminoglycans (GAG), and growth factors that are in a continuous state of dynamic reciprocity with the resident cells as microenvironmental conditions change (161). The conventional role of ECM has been to provide mechanical support; however, the tissue specific composition and architecture of the ECM also plays a central role in directing cell communication and behavior by providing an instructive ligand landscape (162, 163). A preferred tissue engineered biomaterial would preserve these characteristics to effectively promote tissue remodeling. Most naturally occurring scaffolds used in TEMC design consist of components of ECM or whole mammalian ECM itself.

#### ***Collagen I Based TEMC's***

Type I collagen is the predominant component of the ECM and represents the most abundant protein within mammalian tissue (164). As a substrate *in vitro*, collagen I can enhance the viability and proliferation of myogenic progenitor cells (165, 166). TEMC's collagen I based scaffolds have been injected as hydrogels and as implanted as three-dimensional scaffolds (167, 168). In several studies, the implantation of a myoblast-collagen I based TEMC within a VML injury model was associated with a minimal inflammatory response and a donor cell contribution that enhanced host-mediated myogenesis (169, 170). In a head-to-head comparison, when

implemented within a DMD mouse model, a collagen I TEMC seeded with myogenic precursor cells restored dystrophin more efficiently when compared to cell-therapy-alone based injections of the same cells (171).

### ***Hyaluronic Acid Based TEMC's***

Hyaluronic Acid (HA) is a major component of the ECM and has been shown to have biologic activity including the ability to promote angiogenesis and prevent apoptosis (172). Myoblasts seeded within a three-dimensional HA based culture system were able to proliferate and fuse (173). In a study by Rossi and colleagues, satellite cells and myoblasts were incorporated into a photo-cross-linked HA-based hydrogel and delivered to injured skeletal muscle in a pre-clinical model of VML (174). This HA-based TEMC resulted in functional recovery as assessed by contractile force measurements and was associated with the formation of new neural and vascular networks.

### ***Decellularized Mammalian Whole- ECM Based TEMC's***

While individual purified components of the ECM such as collagen I and HA have been used as substrates or vehicles for cell delivery, the most extensively investigated naturally occurring scaffold in TEMC design is decellularized native mammalian tissue; i.e., ECM. Acellular ECM scaffolds are essentially free from DNA and xenogeneic and antigenic epitopes when manufactured by methods that meet stringent criteria (175), and therefore will not elicit an adverse immune response. A three-dimensional matrix derived by decellularization of skeletal muscle or other native mammalian tissue may be advantageous because the differentiation of myogenic progenitor cells can be influenced by natural tissue specific factors including the three-dimensional ultrastructure, surface ligands, and chemical and mechanical microenvironment

(176, 177). Myoblasts cultured on ECM derived from skeletal muscle showed enhanced growth rates and differentiation potentials compared to myoblasts on tissue culture plastic (178). These data supports the use of intact ECM scaffolds as a suitable substrate for TEMC's. In a study by Merritt et al., a rat model of VML injury was repaired with a TEMC composed of bone marrow derived MSC's seeded onto an acellular muscle ECM scaffold. The construct was implanted into injured gastrocnemius muscles and showed the presence of vascularized regenerating skeletal muscle after 42 days. In addition, the TEMC repaired muscle was associated with a partial functional recovery (179).

Studies have shown that a conditioning period of *in vitro* mechanical loading upon whole ECM TEMC's can affect the biologic properties of the scaffold and influence myogenesis and improve cell-scaffold integration prior to transplantation (180-182). Vandeburgh *et al.* conducted pioneering work in which a mechanical cell stimulator device applied mechanical stimulation to a TEMC composed of skeletal muscle myoblasts incorporated into a Matrigel:collagen scaffold (183). This approach resulted in improved myofiber diameter and alignment, increased elasticity of the muscle fibers, and improved cell-generated passive force compared to static cultures. A study by Borschel et al. showed that TEMC's composed of skeletal muscle myoblasts seeded onto decellularized muscle scaffolds produced specific forces that were approximately 5% of that observed for the native muscle after 3 weeks of culture (184). In a similar fashion, Christ and colleagues seeded primary human muscle precursor cells onto acellular bladder submucosa and subjected the constructs to cyclic strain for up to 4 weeks, followed by subcutaneous implantation of the cell-seeded construct within the latissimus dorsi muscle of mice. This study showed that specific forces of 1% of that observed for native latissimus dorsi were produced when the constructs were preconditioned in an *in vitro* bioreactor

(182). Although the observed maximal contractility was only 1% of that of native muscle, this result was still 75-fold greater than in previous reports (182).

### ***Limitations Associated with TEMC's***

The formation of TEMC's through the incorporation of myogenic cells into biomaterial scaffolds has, as discussed above, been occasionally able to enhance donor cell viability and myogenicity. Many limitations associated with TEMC cell-scaffold integration have been at least partially resolved by the practice of *ex vivo* mechanical loading prior to implantation. However, the practical and regulatory hurdles associated with the TEMC approach will limit clinical translation in the near term. Because TEMC's involve the use of a cellular component, the same challenges associated with pure cell-based therapies apply.

#### **1.2.4. Acellular Scaffold Approach**

Limitations associated with the use of a cell-based therapy, including the TEMC approach, provide the stimulus for alternative cell-free approaches. The use of decellularized tissues as (acellular) ECM bioscaffolds has been explored as a therapeutic approach for functional skeletal muscle reconstruction. The approach is based upon the concept of the ECM providing an instructive and conducive microenvironment that can modulate the default scar tissue response to injury toward a constructive regenerative response. Obviously for such a cell-free based approach to be viable, endogenous cells must serve as the source of myogenic precursors.

#### **1.2.4.1. Implanted Acellular ECM Scaffolds Influence the Host Tissue Microenvironment**

The *in vivo* placement of an ECM bioscaffold affects the injured tissue response by several mechanisms including: 1) provision of an ultrastructure environment that is cell-friendly (28, 33, 185, 186), 2) release of bound growth factors, chemokines and cytokines during the process of degradation (15, 173), 3) release of bioactive cryptic peptides generated by the degradation of matrix parent molecules (7-10, 15, 23, 186-192), and 4) modulation of the host innate immune response toward a regulatory and constructive phenotype (21, 22, 193).

Preclinical and clinical examples of these processes have been shown in a number of tissues including esophagus (194, 195), lower urinary tract (196, 197), myocardium (198, 199), and skeletal muscle (32, 200-207) among others. The natural tendency of skeletal muscle to regenerate following mild injury involves a temporally orchestrated series of similar events that have been recently reviewed by Tidball (57). Stated differently, the use of acellular matrix scaffolds appears to provide an environment that augments the natural response of skeletal muscle to injury including activation, recruitment and differentiation of endogenous stem/progenitor cells and minimization of a prolonged pro-inflammatory reaction.

#### **1.2.4.2. Process of Acellular ECM Scaffold Remodeling**

Biologic scaffolds composed of ECM are rapidly infiltrated by host polymorphonuclear and mononuclear cells *in vivo*, which initiate the scaffold degradation process. Macrophages, in particular, are key facilitators of this degradation, as their depletion prevents the degradation of ECM scaffolds (31). Quantitative studies of <sup>14</sup>C-labeled ECM scaffolds show that approximately 50% of the ECM scaffold is degraded after 28 days and virtually all of the ECM is replaced with host tissue by 60 - 90 days post-implantation (23, 191, 192); a process partially dependent upon

the anatomic site of placement. The degradation of ECM scaffolds *in vivo* is critical to the constructive remodeling process (5-8, 186). Degradation of ECM generates cryptic oligopeptides with potent *in vitro* and *in vivo* bioactivity not present in the parent ECM molecules. These “matri-cryptic” peptides have shown chemotactic activity for a number of stem/progenitor cells *in vitro* and have been shown to induce the endogenous recruitment of host progenitor cells *in vivo* (5, 11, 27, 186, 200, 208-210). A large number of these multipotential cell-types influenced by the degradation products of ECM scaffold, both *in vitro* and *in vivo*, have myogenic potential (Figure 2).

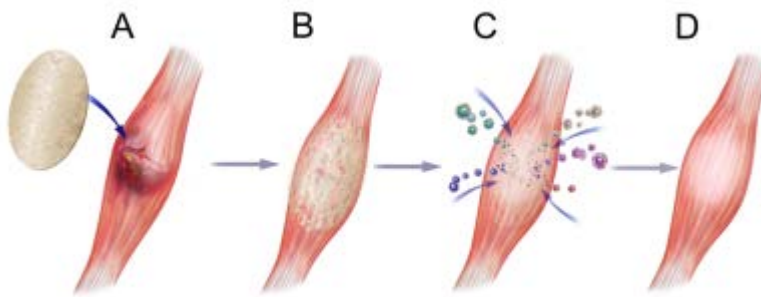


**Figure 2: The Implantation of an Acellular ECM Scaffold Promotes the Recruitment of Host Cells.** Upon their implantation into areas of skeletal muscle injury (A), ECM scaffolds are subjected to rapid host-mediated proteolytic degradation (B). The degradation process releases cryptic peptides, which influence the local tissue microenvironment, including the recruitment of distinct populations of myogenic cells (C). The implantation of acellular ECM scaffolds ultimately results in constructive tissue remodeling, characterized by the formation of site-appropriate and functional tissue (D).

#### 1.2.4.3. Acellular ECM Scaffolds Recruit Progenitor Cells

The accumulation of potentially therapeutic progenitor cells into sites of injury, whether administered via direct injection (cell based approach) or implanted in context with a TEMC, is associated with several limitations including the poor engraftment of donor cells into host tissue.

However, the *in vivo* recruitment of endogenous stem/progenitor cells may partially obviate this limitation, either because of the selection of appropriate precursor cells and/or the lack of external manipulation of the cells. Matrix generated chemotactic peptides have been shown to be chemotactic for several distinct populations of myogenic stem and progenitor cells *in vitro* including: multipotential progenitor cells (186); Sox2+ cells (27); skeletal muscle myoblasts (210) ; and multipotent perivascular progenitor cells (5, 11, 33, 208). Endogenous cells with myogenic potential have been recruited to sites of ECM scaffold implantation and degradation *in vivo*. For example, endogenous CD133+ progenitor cells (200, 209), multipotent perivascular progenitor cells (211), and BM-MSC's (28, 32, 212) have been recruited to sites of ECM implantation within pre-clinical models of skeletal muscle VML. These same cells have previously been used, with limited success, as cell sources for exogenous cell-therapy and in the context with scaffolds as TEMC's (Figure 3) ECM scaffolds have also been shown to recruit CD34+ progenitor cells (209), Sox2+, Sca1+, Rex1+ progenitor cells (5), and cardiomyocytes (213, 214) upon their implantation *in vivo*. These results show the ability of acellular ECM scaffolds to induce endogenous cell-therapy and recruit progenitor cells to sites of injury.

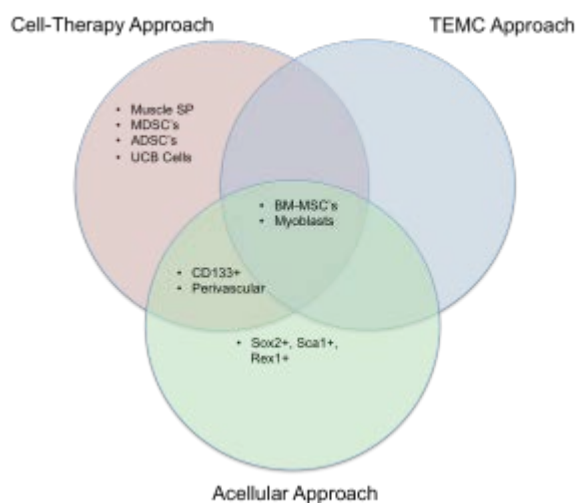


**Figure 3: Common Populations of Cells with Myogenic Potential Employed In Exogenous Cell-Therapy, Exogenous Tissue Engineered Muscle Construct (TEMC) Therapy, and Acellular ECM Scaffold Mediated Endogenous Cell Recruitment.** Several ideal cell-types investigated for exogenous cell-therapy are recruited endogenously by ECM scaffolds.

#### **1.2.4.4. Acellular ECM Scaffolds Influence the Host Innate Immune Response**

The innate immune system has recently been shown to play a pivotal role in both the activation and propagation of the inherent regenerative response of skeletal muscle (57). Following injury, a heterogeneous population of responding macrophages is necessary for muscle's regenerative plasticity (57). Specifically, after injury a population of cells consisting primarily of pro-inflammatory (M1) macrophages not only facilitates pathogen control and debris clearance, but also stimulates the activation of quiescent muscle satellite cells (215, 216). For efficient regeneration and restoration of function, at 48 hours after injury, the primary cell population responding to skeletal muscle injury must be composed of constructive (M2) macrophages (217). M2 macrophages are essential in propagating the inherent regenerative response of skeletal muscle by promoting myogenesis (215, 218).

As stated above, interventions with a cellular component are plagued by the lack of donor cell engraftment are typically associated with less than favorable outcomes. However, limited positive results of cell-based interventions have been associated with donor cell-mediated production of soluble factors capable of affecting the host innate immune system (219-221). Similar to these paracrine effects, acellular ECM scaffolds, upon their implantation *in vivo*, have been shown to influence the local host innate immune response. Specifically, correctly prepared ECM scaffolds promote the constructive M2 macrophage phenotype (21, 22). The ECM scaffold-mediated predominant M2 macrophage response is associated with constructive

remodeling outcomes downstream of the initial participation of the innate immune system (173, 222). Stated differently, ECM scaffolds induce host constructive macrophages and result in favorable remodeling outcomes.

#### **1.2.4.5. Limitations Associated with Acellular ECM Scaffolds**

Outcomes resulting from preclinical and clinical applications of acellular ECM scaffolds have varied considerably and have ranged from poor to excellent (195, 223-228). A potential explanation for these discrepancies may lie within the preparation methods for such materials. For example, numerous decellularization strategies exist for each source tissue; all varying in their effectiveness of removing cellular material as well as altering the ECM structure and composition. Effective decellularization with preservation of native structure function relationships of the component ECM molecules has been shown to be critical for *in vivo* constructive remodeling outcomes (229). For example, *in vivo* implantation of biologic scaffold materials with notable residual DNA amounts was directly correlated to a negative host response (229). Thus, the clinical performance of biologic scaffolds is largely dependent on the preparation and processing techniques.

#### **1.2.4.6. Clinical Translation of ECM Scaffolds**

Biologic scaffolds are commonly used as an alternative to synthetic scaffolds in tissue engineering and regenerative medicine applications (195, 200, 202-206, 230, 231). There exist numerous commercially available ECM based products which are derived from a variety of species including human, porcine, and bovine; as well as an array of tissue sources such as small intestinal submucosa (SIS), urinary bladder, dermis, pericardium, heart valves, and peritoneum, among others.

More than 4 million patients have been implanted with an ECM scaffold for a variety of conditions including: hernia repair (232, 233), diabetic ulcers (234, 235), rotator cuff repair (236-238), breast reconstruction (239, 240), musculotendinous reinforcement (201), pelvic floor reconstruction (241, 242), and urologic defects (243, 244), among others.

A recent clinical case study highlighted the ability of an acellular ECM scaffold to promote skeletal muscle constructive remodeling within a wounded soldier suffering from VML of the quadriceps femoris muscle (201). At 16 weeks post-implantation, the patient showed a 30% increase in muscle function that was concomitant with the presence of soft tissue resembling skeletal muscle on CT.

A clinical study is in progress which evaluates the effect of ECM implantation at the site of VML in 80 patients. The outcome measures of this trial include mechanical strength and function, the cell populations involved in the process, quality of life in these patients, as well as to examine the cellular composition of the remodeled tissue. Preliminary results show the presence of multipotent perivascular cells, desmin+ skeletal muscle cells, neovascularization, and regenerating skeletal muscle tissue (centrally located nuclei) widely distributed throughout the remodeling ECM (245). Furthermore, at 16 weeks post-operatively these patients have exhibited at least a 20% increase in strength compared to pre-ECM implantation values [Unpublished data]. Taken together, these results demonstrate the potential clinical efficacy of ECM scaffolds in promoting the recruitment of perivascular progenitor cells and facilitating restoration of structure and function in volumetric skeletal muscle defects.

### **1.2.5. Conclusions**

Tissue engineering and regenerative medicine approaches aimed at augmenting the regenerative response of skeletal muscle to injury have included both cell-based and acellular strategies. The cell-based interventions face significant hurdles to clinical translation including poor donor cell viability, engraftment, migration and regulatory challenges among others. Acellular strategies include the use of ECM scaffolds, which constructively influence the host injured skeletal muscle microenvironment. ECM scaffolds are presently FDA approved for many clinical applications and have been shown to recruit endogenous myogenic progenitor cells to sites of injury and implantation. Although cell based and acellular approaches have not been compared in head to head studies, it is clear that each approach has pros and cons that are worthy of consideration. In the near term, acellular approaches may be preferable because of their existing regulatory approval. Moreover the studies presented in the present dissertation show further mechanisms of action behind the favorable remodeling outcomes associated with ECM bioscaffolds.

## **1.3. THE ROLE OF THE INNATE IMMUNE SYSTEM FOLLOWING SKELETAL MUSCLE INJURY**

Macrophages are a plastic cell population capable of acquiring diverse phenotypes. They can be classified as either classically activated and pro-inflammatory (M1) or alternatively activated and immunomodulatory (M2) (46-49, 246). Classically activated macrophages, designated M1 after the T cell Th1/Th2 nomenclature, produce pro-inflammatory cytokines and reactive oxygen

intermediates; and are responsible for pathogen killing, cell clearance, and the general propagation of a pro-inflammatory response (46). Alternatively activated macrophages, designated M2, deposit collagen; produce anti-inflammatory cytokines; and facilitate tissue remodeling and repair (247). Although histologically indistinguishable, M1 and M2 macrophages can be identified and distinguished by their species specific and distinct cytokine, gene expression, and cell surface marker profiles (47, 248). Classically activated, pro-inflammatory (M1) macrophages are activated by IFN- $\gamma$  alone or in combination with LPS or TNF. M1 macrophages express IL-12<sup>high</sup>, IL-23<sup>high</sup>, IL-10<sup>low</sup> and produce high levels of inducible nitric oxide synthase (iNOS). They also secrete pro-inflammatory effector molecules and cytokines such as reactive oxygen species and IL-1 $\beta$ , IL-6, and tumor necrosis factor (TNF). These pro-inflammatory products are inducers of Th1 type inflammatory responses {Mantovani, 2005 #135}. In contrast, M2, alternatively activated, macrophages are activated by immunomodulatory cytokines such as IL-4, IL-13, and IL-10, and glucocorticoid or secosteroid (vitamin D3) hormones. M2 activated macrophages express IL-12<sup>low</sup>, IL-23<sup>low</sup>, and IL-10<sup>high</sup> and express high levels of scavenger, mannose, and galactose receptors. M2 macrophages and are involved in polarized Th2 reactions (46).

The role of a heterogeneous host macrophage response to injury has recently been reviewed (57, 249, 250). Immediately following acute skeletal muscle injury, pro-inflammatory cytokines polarize responding host macrophages towards a predominant M1 phenotype. To facilitate appropriate skeletal muscle regeneration, a shift in macrophage polarization takes place and after approximately three days macrophages within the injury site display a predominant M2 phenotype (22). Furthermore, when an M2 macrophage response is inhibited, the host injury response is characterized by a severe lack of muscle regeneration and an accentuation of

inflammation and necrosis (217). In the context of biomaterial implantation, recent studies have shown that a predominant M2 macrophage response to degradable biologic scaffolds is associated with a constructive remodeling outcome. Conversely, a predominant M1 response typically correlates with a foreign body response, the presence of foreign body giant cells, and a poor remodeling outcome in non-degradable biologic scaffolds (22, 31).

#### **1.4. AGE-ASSOCIATED PATHOLOGIES AFFECTING THE SKELETAL MUSCLE INJURY RESPONSE**

Sarcopenia (from the Greek meaning "poverty of flesh") is the degenerative loss of skeletal muscle mass and strength in senescence. In the United States alone, approximately one third of women and two-thirds of men older than age 60 have sarcopenia (251). The direct healthcare cost of sarcopenia in the U.S. has been estimated at over \$18.5 billion annually (252). The morbidity of sarcopenia is associated not only with the degenerative loss of muscle mass, but also with an impaired regenerative response to skeletal muscle injury (253). With age and the associated loss of inherent regenerative capacity, injured skeletal muscles are replaced with scar and connective tissue (254, 255). This impaired regenerative response complicates treatment options and orthopedic procedures in elderly individuals.

#### **1.4.1. Age-Related Changes in Skeletal Muscle Myogenesis**

With age, there is a gradual decline in the regenerative response of skeletal muscle to injury (256). The decline is associated with satellite cell and myoblast dysfunction (257). This decrease in satellite cell function with age is caused by a decline in extrinsic microenvironmental cues rather than a decrease in satellite cell pool (258, 259). In addition, parabiotic studies revealed that exposure to a young systemic milieu resulted in increased satellite cell activation and subsequent rejuvenation of the age-impaired skeletal muscle regenerative niche(260). Thus it appears that the loss of myogenic potential of aged satellite cells is reversible and therefore mediated via partially extrinsic cues within the regenerative microenvironment.

#### **1.4.2. Age-Related Changes in Macrophage Physiology**

Immunosenescence associated with advanced age negatively impacts the innate immune system (261, 262). Specifically, the effect of aging on macrophages appears to be multifaceted and affects many different macrophage functions. Aged subjects display defects in various signaling pathways affecting diverse macrophage activity (263-265). Macrophages from aged humans and mice display a reduced capacity for chemotaxis and phagocytosis (266-270). These functional defects cause an inefficient clearance of apoptotic muscle fiber and tissue debris, resulting in decreased myogenesis in response to injury. In addition, evidence suggests that age-impaired macrophages display a decreased production of cytokines (264, 271-273). Like their younger counterparts macrophages derived from aged subjects can also be exogenously polarized, however requiring higher concentrations of polarizing factors. (274). These reports suggest an

impairment in the susceptibility for polarization in macrophages from aged subjects (275) and therefore an altered myogenic response to skeletal muscle injury.

## **1.5. CENTRAL HYPOTHESIS**

The central hypothesis of the present dissertation states: bioscaffolds composed of extracellular matrix mitigate age-related changes to the skeletal muscle injury microenvironment through modulation of macrophage phenotype and increased myogenic progenitor cell activation.

## **1.6. SPECIFIC AIMS**

**Aim 1:** To evaluate the host remodeling response, including macrophage phenotype induced by extracellular matrix (ECM) scaffolds derived from young and aged source animals.

**Aim 2:** To determine the ability of ECM to enhance the polarization of macrophages isolated from young and aged subjects.

**Sub-Aim:** To evaluate the effect of ECM and polarized macrophages upon the chemotaxis, mitogenesis, and differentiation of skeletal muscle progenitor cells.

**Aim 3:** To determine if an ECM scaffold induced progenitor cell participation and constructive macrophage phenotype correlate with a constructive tissue remodeling outcome in a mouse model of volumetric muscle loss (VML).

## **2.0 THE HOST REMODELING RESPONSE, INCLUDING MACROPHAGE PHENOTYPE INDUCED BY ECM SCAFFOLDS DERIVED FROM YOUNG AND AGED SOURCE ANIMALS**

### **2.1 BACKGROUND**

Biologic scaffolds composed of xenogeneic extracellular matrix (ECM) are derived by the decellularization of mammalian tissues and have been used in both preclinical and clinical settings for the reconstruction of damaged or missing tissues (195, 201, 276). ECM scaffolds can alter the default wound healing response from the well described pro-inflammatory and scarring events toward a more constructive remodeling response, i.e., the site appropriate formation of functional tissue, in a variety of anatomic locations including dermis (277), esophagus (278, 279), skeletal muscle (202, 276, 280), and heart (213, 214, 281), among others. Results of such clinical applications have varied considerably (195, 223-228), and the variables which affect outcome are only partially understood. Two intuitively important determinants of the remodeling outcome are the physical and biologic properties of the ECM scaffold material itself, and the innate immune response of the recipient. Modulation of macrophage phenotype, a critical component of the innate immune response, has been shown to play a prominent role in the scaffold remodeling outcome (21, 22), but the effect of the age of tissue from which the ECM scaffold is prepared has been largely ignored.

Mammalian fetal wound healing is characterized by site-specific regeneration and minimal scar tissue formation; a distinct contrast to wound healing in adults (282). This tissue regeneration response is associated with selected pro-inflammatory events (283, 284), increased capacity for wound closure (285, 286), and a distinct ECM composition (287-290). The ECM present in fetal tissues is enriched in glycosaminoglycans which facilitate the proliferation and migration of a number of cell types (287, 291, 292). The collagen content of fetal ECM is less mature and contains fewer cross-links when compared to adult ECM (293). Minimal collagen cross-linking facilitates rapid ECM turnover and remodeling. Because of these characteristics, it is plausible that biologic materials derived from neonatal or newborn tissues may be better suited as inductive scaffolds than biologic scaffold materials derived from older animals.

The diverse remodeling outcomes associated with ECM scaffold use can also be attributed to variables such as processing methods (202), source species and tissue origin of the ECM (294), post-implantation mechanical load (295), and decellularization efficacy (229). Because the response to tissue injury is known to be more favorable and robust in young vs. aged mammals, some biologic scaffolds use source materials that include ECM derived from fetal cells or mammals (296, 297). It has been previously reported that distinct differences exist in the mechanical, structural, and *in vitro* biologic properties of ECM harvested from different aged animals (208) (Table 1). However, the effect of donor animal age upon the *in vivo* remodeling characteristics of xenogeneic ECM scaffolds has not been systematically examined.

The objective of the present chapter was to compare the *in vivo* remodeling outcome of ECM scaffolds that differ only in source animal age. An established rodent model of abdominal wall muscle reconstruction [18, 39] was used to evaluate the host remodeling response, including

the phenotype of responding macrophages, scaffold induced vascularity, innervation, and myogenesis over time, and the mechanical properties of the remodeled injury site after 26 weeks.

**Table 1: A summary of the pre-implantation properties of the differently aged ECM scaffolds.** Adapted from Tottey et al, 2011 with permission.

Age (Weeks)	Elastic Modulus (MPa)	Stress (MPa)	Thickness ( $\mu$ m)	bFGF (ng / g dry weight material)	VEGF (pg/ g dry weight material)	sGAG ( $\mu$ g / mg dry weight material)
3	0.8 $\pm$ 0.6	13.76 $\pm$ 12.70	14.00 $\pm$ 1.65	49.27 $\pm$ 1.70	510 $\pm$ 52	12.84 $\pm$ 0.09
12	1.9 $\pm$ 0.9	28.18 $\pm$ 13.05	23.15 $\pm$ 2.33	113.90 $\pm$ 0.36	810 $\pm$ 26	13.33 $\pm$ 0.33
26	2.0 $\pm$ 0.6	31.24 $\pm$ 9.93	24.75 $\pm$ 2.61	95.06 $\pm$ 0.86	825 $\pm$ 42	11.09 $\pm$ 0.36
>52	1.2 $\pm$ 0.7	22.20 $\pm$ 8.69	33.97 $\pm$ 2.16	77.93 $\pm$ 0.19	490 $\pm$ 10	10.06 $\pm$ 0.48

## 1.7. MATERIALS AND METHODS

### 2.1.1 Overview of Experimental Design

Small intestinal submucosa (SIS) ECM was prepared from the small intestine of 4 distinctly different aged pigs of identical gene pool and husbandry: 3 weeks (neonatal), 12 weeks (feeder), 26 weeks (market), and greater than 52 weeks of age (sow). The different aged tissues were collected, decellularized, and processed at the same time using identical methods and the resulting SIS-ECM was used to repair a 1.0 cm by 1.0 cm partial thickness abdominal wall musculature defect in a Sprague-Dawley rat model. Treatment groups were equally and randomly subdivided and sacrificed at 14, 28, 120, or 180 days post-surgery. Following euthanasia and explantation of the remodeled scaffold materials, mechanical testing and histologic and immunolabeling methods were used to determine the mechanical and morphologic characteristics of the remodeled tissue (Table 2).

**Table 2: Tissue assessment.** All samples received Masson's trichrome and vasculature (CD31) staining with associated histologic assessment (×). Staining for macrophages was done at a time point consistent with a robust host macrophage response (14 days). Mechanical testing, along with staining for muscle fiber phenotype (myosin) and innervation ( $\beta$ -tubulin III), was included where trichrome staining confirmed the presence of skeletal muscle within the defect site (180 days).

Analysis	Harvest time point			
	14 days	28 days	120 days	180 days
Trichrome staining ( $n = 3$ )	×	×	×	×
CD31 staining ( $n = 3$ )	×	×	×	×
Macrophage staining ( $n = 3$ )	×	–	–	–
Fast/slow myosin staining ( $n = 3$ )	–	–	–	×
$\beta$ -tubulin III staining ( $n = 3$ )	–	–	–	×
Mechanical testing ( $n = 5$ )	–	–	–	×

### 2.1.2 Source and preparation of ECM scaffold material

The jejunum from Whiteshire Hamroc pigs of 4 distinctly different ages (3, 12, 26 and >52 weeks) were harvested immediately following euthanasia (Tissue Source, Lafayette, IN). The animals were of identical genetic heritage, and were raised and kept in identical husbandry conditions including diet and vaccination history. All tissues were harvested on the same day and stored on ice prior to processing to create SIS-ECM as previously described (3, 298). Briefly, the intestines were rinsed with water and the mesenteric tissues were removed. The intestines were cut longitudinally and mechanically delaminated to remove the tunica serosa, tunica muscularis

externa, and the luminal portion of the tunica mucosa including most of the lamina propria. After delamination, the tunica submucosa and the basilar layer of the tunica mucosa including the muscularis mucosa and the stratum compactum of the lamina propria remained. The material was further decellularized using 0.1% peracetic acid (Rochester Midland Corporation, Rochester, NY) followed by multiple rinses with saline and deionized water as previously described (298). The SIS-ECM material was then vacuum pressed to form 4-layer constructs and cut to 1 cm<sup>2</sup> in size before being terminally sterilized with ethylene oxide.

### **2.1.3 Surgical procedure**

All procedures were performed in accordance with the National Institute of Health (NIH) guidelines for care and use of laboratory animals, and with approval of the Institutional Animal Care and Use Committee (IACUC) at the University of Pittsburgh. Adult female Sprague-Dawley rats weighing approximately 300 g (Charles River Laboratory, Wilmington MA) were subjected to partial thickness abdominal wall defect surgery (22, 31). Animals were separated into groups based on treatment type: (1) uninjured control, (2) untreated defect, (3) autologous tissue graft (excised and immediately replaced oblique musculature), (4) sow aged scaffold (>52 weeks), (5) market aged scaffold (26 weeks), (6) feeder aged scaffold (12 weeks), (7) neonate aged scaffold (3 weeks); and harvest time point: 14, 28, 120 and 180 days (n = 3 body walls per treatment group at 14, 28, and 120 days; n = 8 body walls per treatment group at 180 days; 119 total surgeries were performed). Five implant sites per treatment group were used for mechanical testing at 180 days only, and three implant sites per treatment group were used for histologic analysis at each time point.

Each animal was anesthetized with 2% isoflurane in oxygen and the ventral abdomen was prepared by hair clipping and scrubbing with Betadine (povidone-iodine) before the placement of sterile drapes around the surgical site. A ventral midline abdominal skin incision was created. The subcutaneous tissues were bluntly dissected from the underlying muscle tissues on one side of the midline for a distance of approximately 4 cm to the anterior axillary line exposing the oblique musculature. A 1.0 cm<sup>2</sup> partial thickness defect consisting of the internal and external oblique layers of the abdominal wall musculature was excised while leaving the underlying transversalis fascia and peritoneum intact. The defect was left untreated or repaired with a 1.0 cm<sup>2</sup> piece of the chosen test article. A single 4-0 prolene suture was placed at each of the four corners of the test article to secure it to the adjacent abdominal wall musculature, allowing it to be exposed to a physiologic mechanical load and identifying the boundary of the implant at the time of necropsy. Interrupted subcuticular 4-0 Vicryl suture was used for skin closure. Each animal was allowed to recover from anesthesia on a heating pad and was returned to the housing unit.

Each animal received 0.06 mg Buprenex (buprenorphine hydrochloride) by subcutaneous injection the day of surgery and for two additional days. Baytril (5 mg) was given orally the day of surgery and for two additional days. The dietary habits, general health status, and the surgical site were monitored daily and recorded.

#### **2.1.4 Euthanasia and specimen harvest**

Animals were sacrificed at 14, 28, 120, or 180 days. Each rat was euthanized with 5% isoflurane in oxygen followed by an intracardiac injection of 5 mL of potassium chloride to induce cardiac arrest. Implants for histologic evaluation (n = 3), including ~2 mm of surrounding native

abdominal wall musculature, was excised, mounted on corkboard to maintain *in situ* size and shape, and placed in 10% neutral buffered formalin. Implants for mechanical testing (n = 5) were placed in Ringer's solution immediately after excision for uniaxial tensile testing.

### **2.1.5 Histologic and immunolabeling analysis**

The tissue was embedded in paraffin, cut into 5-um thick sections, and mounted onto glass slides before being stained with Masson's trichome. The primary antibodies used for the immunolabeling studies were: (1) monoclonal anti-myosin (skeletal, slow, clone NOQ7.5.4D; Sigma Aldrich, St. Louis, MO) at 1:4000 dilution for identification of slow (type I) skeletal muscle fibers; (2) monoclonal anti-myosin (skeletal, fast, alkaline phosphatase conjugate, clone MY-32, Sigma Aldrich) at 1:200 dilution for identification of fast (type II) skeletal muscle fibers; (3) rabbit polyclonal CD31 (Abcam, Cambridge, MA) at 1:100 dilution for identification of endothelial cells; (4) anti Beta-III Tubulin (Dako USA, Carpinteria, CA) at 1:200 dilution for identification of neurons; (5) goat polyclonal CD206 (Santa Cruz Biotech, Santa Cruz, CA) at 1:100 for identification of M2 macrophages; (6) rabbit monoclonal CCR7 (Epitomics, Burlingame, CA) at 1:100 for identification of M1 macrophages; and (7) mouse-anti rat CD68 (Serotec, Raleigh, NC) at 1:50, as a pan macrophage marker. Table 2 shows the details of the specific staining performed at each time point.

To identify fast and slow muscle fibers, unstained sections were deparaffinized and heat-mediated epitope retrieval was performed with 0.1 mM EDTA buffer at 95-100 °C for 25 min followed by enzyme-mediated antigen retrieval with 0.1% trypsin/0.1% calcium chloride digestion at 37 °C for 10 min. Slides were washed in Tris buffered saline (TBS), pH 7.6, then incubated for 10 min in a blocking solution containing 0.1% Tween 20, 0.1% Triton X, 2%

normal horse serum and 2% normal goat serum at room temperature to prevent non-specific antibody binding. To inhibit endogenous peroxidase activity, the slides were incubated with 3% hydrogen peroxide (Spectrum, New Brunswick, NJ) in methanol for 10 min at room temperature. The slow anti-myosin antibody was applied and incubated for 30 min at room temperature. The slides were then incubated with the secondary antibody (biotinylated anti-rabbit; Vector) at 1:200 for 30 min at room temperature, followed by horseradish peroxidase solution (Vector) for 30 min at 37 °C. Diaminobenzidine (DAB) (Vector) was applied to detect positive staining cells. The blocking solution was then applied again for 10 min at room temperature, followed by the fast anti-myosin antibody for 60 min at room temperature. Red alkaline phosphatase substrate was applied to detect positive staining (Vector).

For Beta-III Tubulin immunolabeling, slides were deparaffinized, and heat-mediated epitope retrieval was performed as described above. The slides were washed in phosphate buffered saline (PBS) then incubated for 30 min with 2% normal horse serum (Vector) at 37 °C to prevent non-specific antibody binding. Endogenous peroxidase activity, was inhibited by incubating with 3% hydrogen peroxide (Spectrum) in methanol for 30 min at room temperature. The tissue sections were then incubated in the Beta-III tubulin primary antibody for 1 hour at room temperature, followed by the secondary antibody (biotinylated anti-mouse; Vector) at 1:200 for 30 min at room temperature. Horseradish peroxidase solution (Vector) was applied for 30 min at 37 °C, and diaminobenzidine (DAB) (Vector) was used to detect positive staining cells. The slides were counterstained with hematoxylin.

Similarly, for CD31 immunolabeling the slides were deparaffinized and heat-mediated epitope retrieval was performed with 0.01 M citrate buffer (Spectrum), pH 6.0, at 95-100°C for 20 min. Enzyme-mediated antigen retrieval was then performed using proteinase K in a buffer of

50 mM Tris base and 1 mM EDTA, pH 8.0, at 60°C for 10 min. Following washes in PBS, the slides were incubated for 60 mins with 2% normal horse serum (Vector) at 37°C to prevent non-specific antibody binding, followed by a 30 minute incubation in 3% hydrogen peroxide. The tissue sections were then incubated in the CD31 primary antibody for 1 hour at room temperature, followed by the secondary antibody for 30 min at 37°C. Horseradish peroxidase solution (Vector) was applied for 30 min at 37°C. Diaminobenzidine (DAB) (Vector) was used to detect positive staining cells and the slides were counterstained with hematoxylin.

M1 vs. M2 polarized macrophages were identified by immunolabeling. After deparaffinization, heat-mediated antigen retrieval was performed with 0.01 M citrate buffer (Spectrum), pH 6.0, at 95-100°C for 20 min. Tissue sections were incubated in blocking buffer (1% bovine serum albumin/0.05% Tween-20/0.05% Triton X-100) for 1 hour. The primary antibodies (CD206, CCR7, and CD68), diluted in blocking buffer, were then added to the slides for 16 hours at 4°C in a humidified chamber. The secondary antibodies (also diluted in blocking buffer) were incubated on the slides for 1 hour in a humidified chamber at room temperature. The secondary antibodies used were Alexa Fluor® goat anti-rabbit 568 (Invitrogen), Alexa Fluor® donkey anti-goat 488 (Invitrogen) and Alexa Fluor® donkey anti-mouse 350 (Invitrogen). Draq5 (Cell Signaling Technologies, Danvers MA) was used as a nuclear counterstain.

### **2.1.6 Quantification of histologic and immunolabeling analysis**

All tissue sections were imaged using a Zeiss Axio Observer Z1 or Nikon E600 microscope with Nuance multispectral imaging system (CRI Inc, Cambridge MA) with appropriate brightfield and fluorescent filter sets. Three random Masson stained images of the device implant site at the

interface with native tissue were taken at 100x magnification. A quantitative analysis of the trichrome staining was conducted by determining the percent of blue stained tissue within the surgical site using the Nuance software. Collagen or connective tissue (blue) and nuclei or muscle fibers (red) were isolated by spectral filtration and subsequent thresholding. High percent blue staining indicates the predominant presence of collagenous connective tissue.

Quantification of M1/M2 polarization was achieved using a custom image analysis pipeline developed using the cell profiler image analysis package (299, 300). This custom pipeline identified and quantified the number of CD68+CCR7+ (M1 macrophage phenotype) and CD68+CD206+ (M2 macrophage phenotype) cells present within scaffold implantation sites. Any cells that co-expressed the CCR7 and CD206 markers were excluded. These values were then expressed as a ratio of M1:M2.

Quantification of CD31 positive blood vessels was done by immunolabeling and counting the number of blood vessels per 400x field of view (FOV). Six images of each surgical site were quantified by two blinded independent investigators. Only positively labeled cells that were associated with a visible lumen were counted.

### **2.1.7 Mechanical testing**

Tissue explants were trimmed to dog-bone geometry (midsubstance width  $5.7 \pm 1.6$  mm, length  $20.4 \pm 6.6$  mm) with exact specimen dimensions dependent on animal and explant size. All specimens were subjected to 10 pre-load cycles (25.4 mm/min, 0.1-0.5 N) immediately prior to testing to failure (25.4 mm/min). Ultimate tensile stress was calculated from the peak load, width, and thickness ( $2.3 \pm 0.5$  mm):  $\sigma = F/(w*t)$ . Strain at failure was calculated by dividing the change in length by the original length:  $\epsilon = \Delta L/L_0$ . Elastic modulus was taken as the slope of the

stress-strain curve in the range of 20-60% of the ultimate tensile stress:  $E=0.4*\sigma/(\epsilon_{60\%}\sigma-\epsilon_{20\%}\sigma)$ . Five specimens were tested from each control and experimental group with the following exceptions: native tissue = 9; SIS-ECM implant from >52 week aged animal (sow) = 4.

### **2.1.8 Statistical analysis**

A one-way analysis of variance (ANOVA) was used in conjunction with a Tukey's post-hoc test to compare results between groups. Differences were considered significant at  $p < 0.05$ . Statistical analysis was completed using SPSS Statistical Analysis Software (IBM, Chicago, IL, USA).

## **2.2 RESULTS**

### **2.2.1 Histomorphologic and immunolabeling findings**

All treatment groups elicited a robust cellular infiltrate consisting mostly of mononuclear cells after 14 days (Figure 4A). Angiogenesis was also observed in all groups at day 14 and remained a feature of the remodeling process throughout the entire study (Figure 5). All of the ECM scaffold materials degraded completely based upon morphologic analysis and were replaced with host tissue by 180 days. However, there were notable differences in the remodeling responses to the different aged ECM materials which are detailed below.

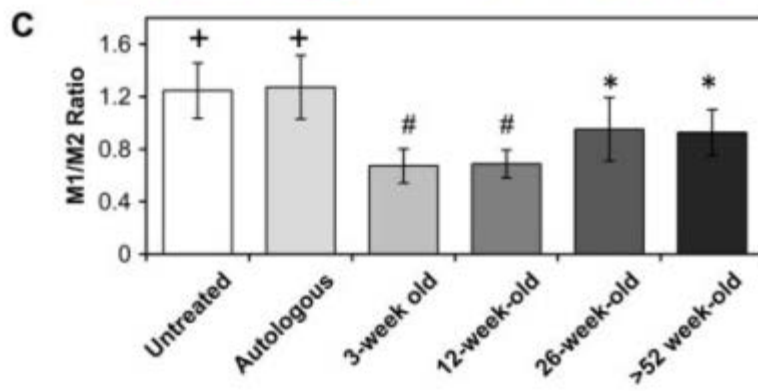
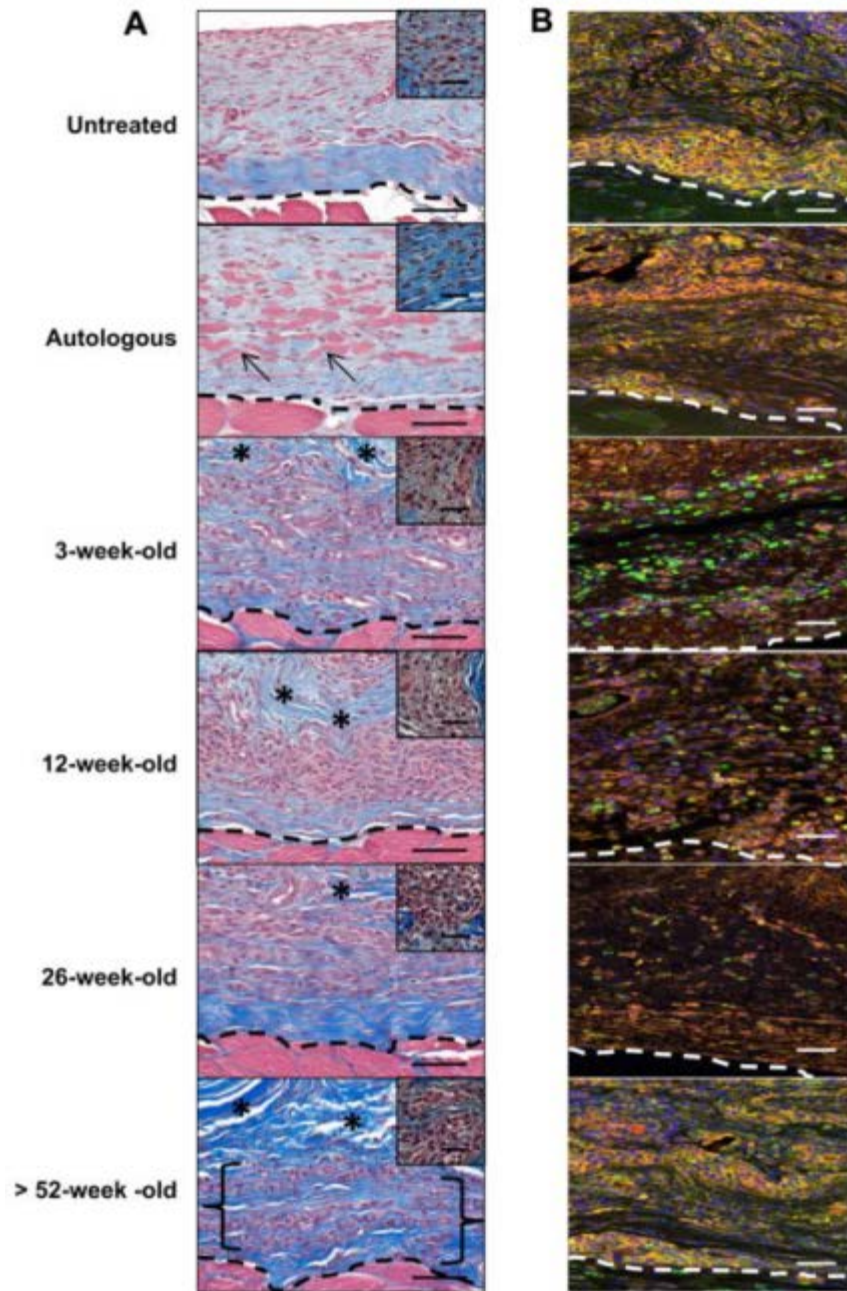


**Figure 4: Host cellular response at the surgical site at 14 days post-surgery.** The *in vivo* host response to untreated injury, autologous tissue graft, or scaffolds derived from differently aged source ECMs was assessed by histologic methods with Masson's Trichrome staining (A) and by the immunolabeling of macrophages (B & C). Necrotic islands of skeletal muscle could be identified within the implantation site of the autologous tissue graft (arrows). A mononuclear cell infiltrate (morphology depicted in high power inset) was identified throughout the 3, 12, and 26-week-old scaffolds, while the >52-week-old scaffold was only partially infiltrated (bracket) (A). All treatment groups showed the presence of macrophages (CD68; Red). The untreated and autologous implant surgical sites displayed a predominant M1 macrophage (CCR7; Orange) phenotype (+,  $P < 0.001$  for both when compared to all other treatment groups). The >52 and 26-week-old implant sites were populated by a balanced M1 to M2 macrophage (CD206; Green) ratio (#,  $p < 0.004$  for both when compared to all other treatment groups). The 3 and 12-week-old scaffolds displayed a predominant M2 macrophage response (B & C; \*,  $p < 0.004$  for both when compared to all other treatment groups). Scale bars = 50  $\mu\text{m}$  (inset scale bars = 20  $\mu\text{m}$ ), \* = scaffold. Error bars = standard deviation.

#### 2.2.1.1 Untreated defect

Untreated defect sites were characterized by a loose collagenous connective tissue after 14 days. A mononuclear cell infiltrate was localized to the defect margins (Figure 4A) Immunolabeling studies showed an M1:M2 macrophage ratio of  $1.24 \pm 0.21$  indicating a predominant M1 macrophage response (Figure 4B,C). After 180 days untreated defects formed dense collagenous tissue consistent with scar tissue (Figure 6). Quantitative analysis of the trichrome staining over time showed an increase in the amount of collagenous connective tissue within the defect site after 180 days when compared to the 14 day time point ( $p < 0.005$ ) (Figure 8). After 180 days the defect site showed no evidence of new skeletal muscle or nerve (Figure 9, Figure 10).

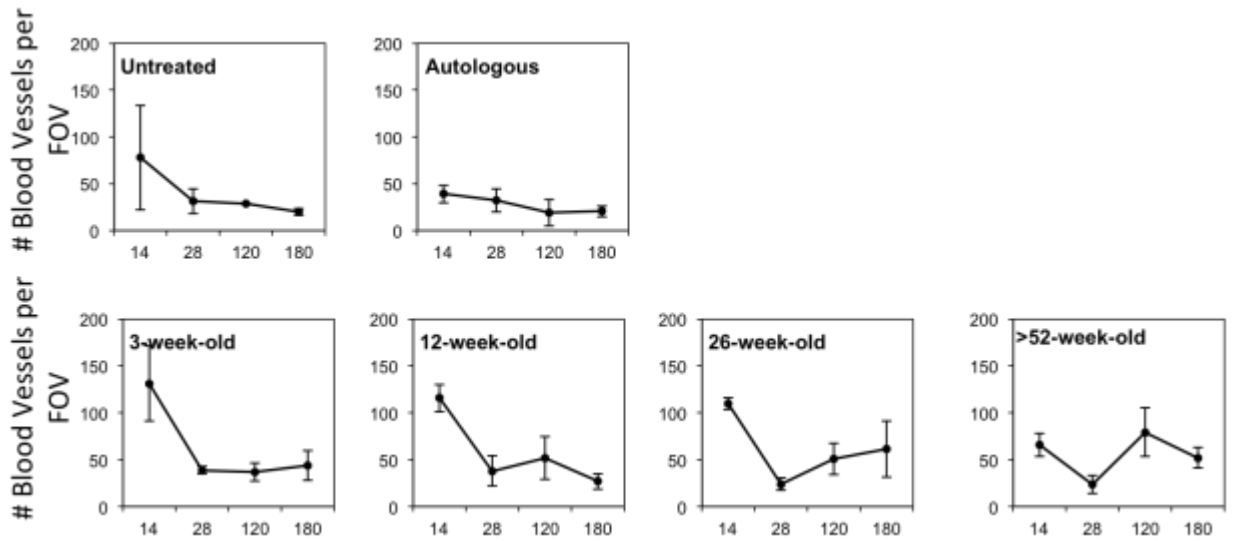


**Figure 5: Quantitative immunohistochemical analysis of vascularity.** CD31 Immunopositive blood vessels were counted per 400x field of view (FOV) by two independent investigators. 6 fields per surgical site were examined at the interface with underlying host tissue. Untreated, 3, 12, and 26-week-old treated defects showed significant vascularity after 14 days that decreased over time. Autologous and >52-week-old treated defects showed a balanced level of vascularity throughout the study period.

### **2.2.1.2 Autologous tissue graft**

Treatment of the defect site with autologous tissue elicited a mononuclear infiltrate that was localized around the remnants of necrotic skeletal muscle within the autograft after 14 days. Similar to untreated defects, immunolabeling studies showed an M1:M2 macrophage ratio of  $1.27 \pm 0.24$  indicating a predominant M1 macrophage response (Figure 4B,C). Between 28 and 120 days there was a decreased cellular infiltrate and loss of skeletal muscle within the autograft although small islands of necrotic skeletal muscle could still be identified (Figure 7). After 180 days the autologous tissue graft had remodeled into dense and relatively acellular collagenous tissue (Figure 6). The surgical site showed no evidence of new skeletal muscle tissue (Figure 9) or signs of innervation (Figure 10). Quantitative analysis of the Masson's trichrome staining over time revealed an increase in the amount of collagenous connective tissue at 180 days when compared to the 14 ( $p < 0.01$ ) and 28 ( $p < 0.09$ ) days (Figure 8).

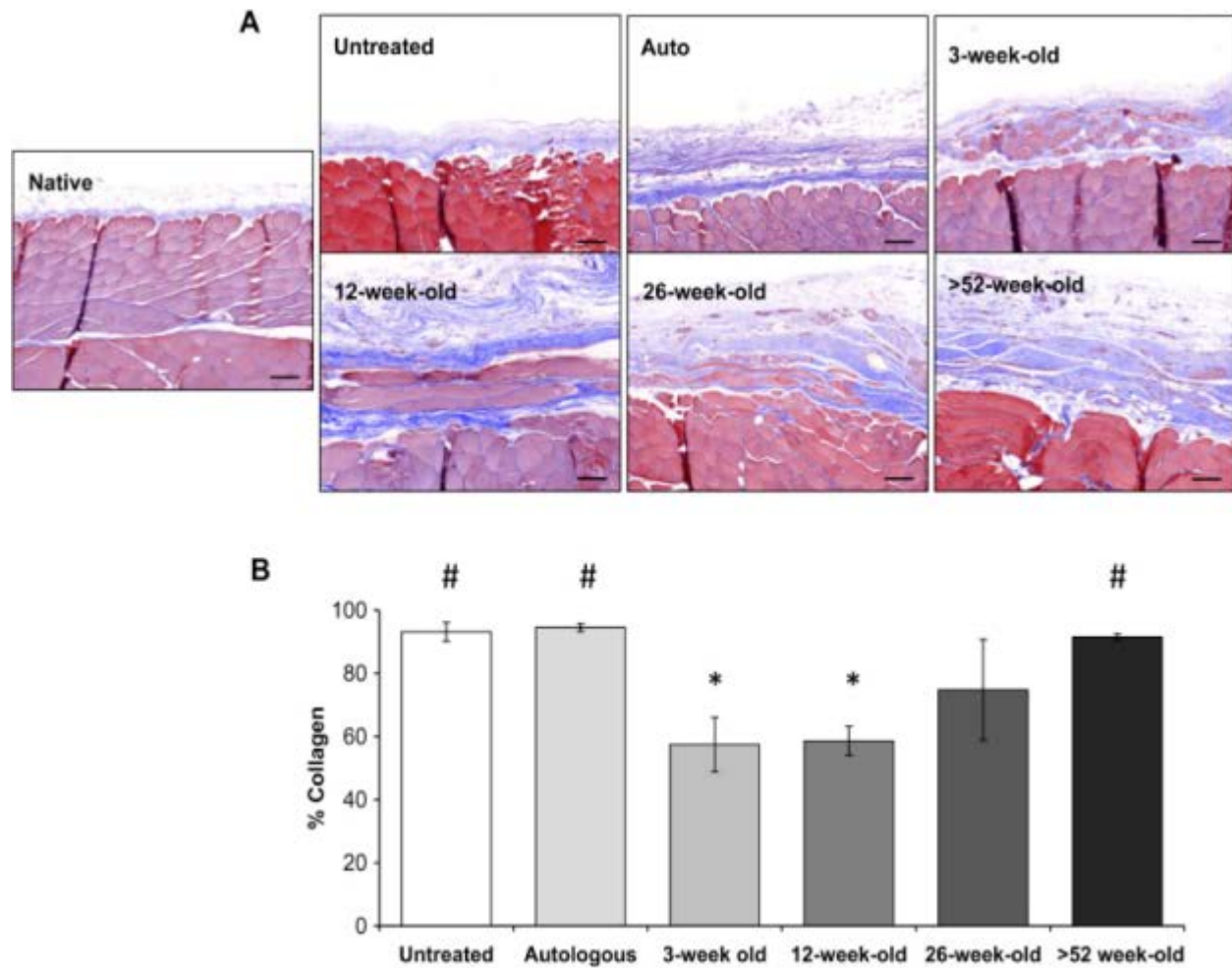


**Figure 6: Trichrome staining (A) and collagen content quantified (blue staining) using spectral unmixing (B).** 3-week-old and 12-week-old scaffolds showed a constructive remodeling response after 180 days when compared to the untreated, autologous, or >52-week-old treated surgical sites as indicated by the formation of site appropriate skeletal muscle myofibers within the implant site (A & B). Collagen content showed 3 ( $p < 0.007$ ) and 12-week-old ( $p < 0.003$ ) scaffolds had significantly less collagenous tissue than the untreated, autologous, or >52-week-old treatment groups (B). Means with different symbols are significantly different. Scale bars = 50  $\mu$ m. Error bars = standard deviation

### **2.2.1.3 Neonate aged SIS-ECM scaffold**

The neonate aged SIS-ECM graft showed a mononuclear cell infiltrate throughout the entire scaffold at 14 days (Figure 4A). Small remnants of the original ECM implant and a large amount of host derived neomatrix were present within the defect site. Immunolabeling studies showed an M1:M2 macrophage ratio of  $0.67 \pm 0.13$  indicating a predominant M2 macrophage response after 14 days. At 28 days neonate aged SIS-ECM scaffolds showed a decreased cellularity and were replaced with host derived matrix (Figure 7). Small Islands of skeletal muscle could be seen scattered throughout the defect site after 120 days. At 180 days the implant site contained new host tissue that contained organized bundles of new skeletal muscle myofibers surrounded by partially organized collagenous connective tissue (Figure 6). In addition, like native tissue and feeder treated defects described below, the majority of the muscle fibers within the defect site stained positive for fast type II myosin with slow type I myosin fibers dispersed throughout the remodeled scaffold placement site (Figure 9). Nerve fibers were present adjacent to the myofibers throughout the defect site (Figure 10). Quantitative analysis of the Masson's trichrome stained neonate treated defects showed an increase in collagenous connective tissue between 14 and 120 ( $p < .018$ ) (Figure 8). The surgical site further remodeled and became partially replaced with skeletal muscle tissue, resulting in a decreased collagen percentage at 180 days when compared to the 120 day time point ( $p < 0.03$ ). This collagen percentage at 180 days was not significantly different from that at 14 days (Figure 8).

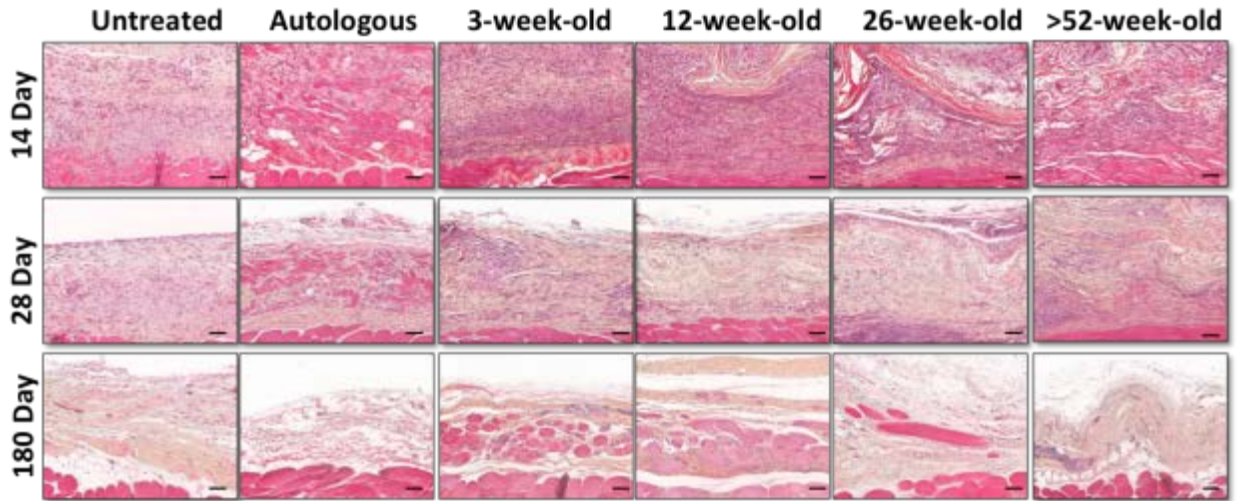


**Figure 7: Scaffold composition at 14, 28, and 180 days post-surgery.** The remodeled tissue was assessed histologically with Movats Pentachrome staining. Even at 14 days post-surgery all treatment groups showed no observable GAG's. 3, 12, and 26-week-old scaffolds showed signs of myofiber formation at 180 days post-surgery. Scale bars = 50µm.

#### 2.2.1.4 Feeder aged SIS-ECM graft

The feeder aged SIS-ECM treated defect sites showed a mononuclear cell infiltrate throughout the scaffold at 14 days (Figure 4A). In addition at 14 days, small remnants of the original ECM implant were present within the defect site. Immunolabeling studies showed an M1:M2 macrophage ratio of  $0.69 \pm 0.11$  indicating a predominant M2 macrophage response. After 28 days the SIS-ECM grafts showed decreased cellularity and at 120 days small islands of skeletal muscle were present (Figure 7). Feeder aged SIS-ECM scaffolds remodeled in a similar fashion to that of the neonate aged SIS-ECM scaffolds. At 180 days the implant site contained new host tissue that consisted of organized bundles of skeletal muscle myofibers surrounded by partially organized collagenous connective tissue (Figure 6). Similar to native tissue, the majority of the

muscle fibers within the defect site stained positive for fast type II myosin with a smaller number of widely dispersed slow type I myosin fibers (Figure 9). Nerve fibers were present adjacent to the myofibers throughout the defect site (Figure 10). Quantitative analysis of the Masson's trichrome stained feeder treated defect site tissues showed a slight increase in collagenous connective tissue between 14 and 120 days ( $p < .001$ ) (Figure 8). The surgical site further remodeled and became partially replaced with skeletal muscle tissue, resulting in a decreased collagen percentage at 180 days when compared to the 120 day time point ( $p < 0.004$ ). This collagen percentage at 180 days was not significantly different from that at 14 days (Figure 8).

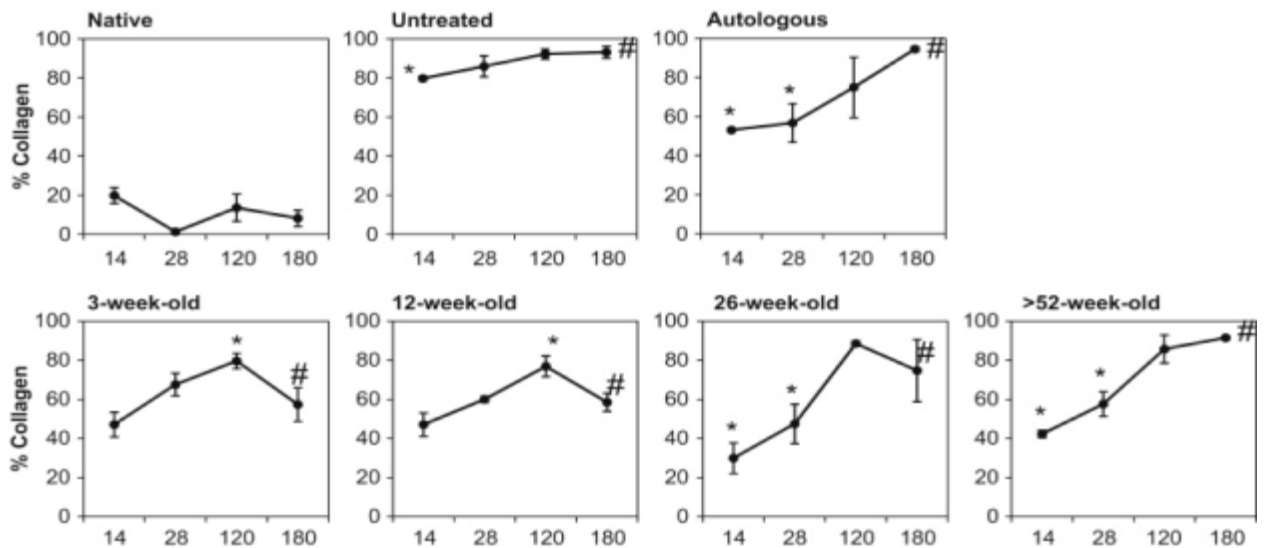


**Figure 8: Connective tissue deposition within each surgical site over time.** Quantification of Masson's trichrome, in terms of % collagen (blue staining), using spectral unmixing. Untreated defects as well as the autograft and sow aged scaffolds induced a steady increase in connective tissue deposition from 14 to 180 days post-surgery. Whereas, the feeder and neonate aged scaffolds were associated with a lower collagen presence more similar to that seen in native tissue. Means with different symbols are significantly different within each age group. Error bars = standard deviation.

### **2.2.1.5 Market aged SIS-ECM graft**

The market aged SIS-ECM treated defect sites showed a mononuclear cell infiltrate throughout the scaffold at 14 days (Figure 4A). Original ECM scaffold material could be identified along with host derived neomatrix. Immunolabeling studies showed an M1:M2 macrophage ratio of  $0.95 \pm 0.24$  indicating a balanced macrophage phenotype response (Figure 4B,C). At 28 days the surgical site showed a decreased cellularity and increased amount of neomatrix. At 120 days no evidence of the original implanted scaffold was observed and small islands of skeletal muscle could be identified within the defect site (Figure 7). At 180 days isolated skeletal muscle myofibers were dispersed between collagenous connective tissue throughout the defect site (Figure 6). These individual myofibers stained positive for fast type II myosin (Figure 9) and were adjacent to nerve fibers (Figure 10). Quantitative analysis of the Masson's trichrome staining over time revealed an increase in the amount of collagenous connective tissue at 180 days when compared to the 14 ( $p < .001$ ) and 28 ( $p < .046$ ) day time points (Figure 8).

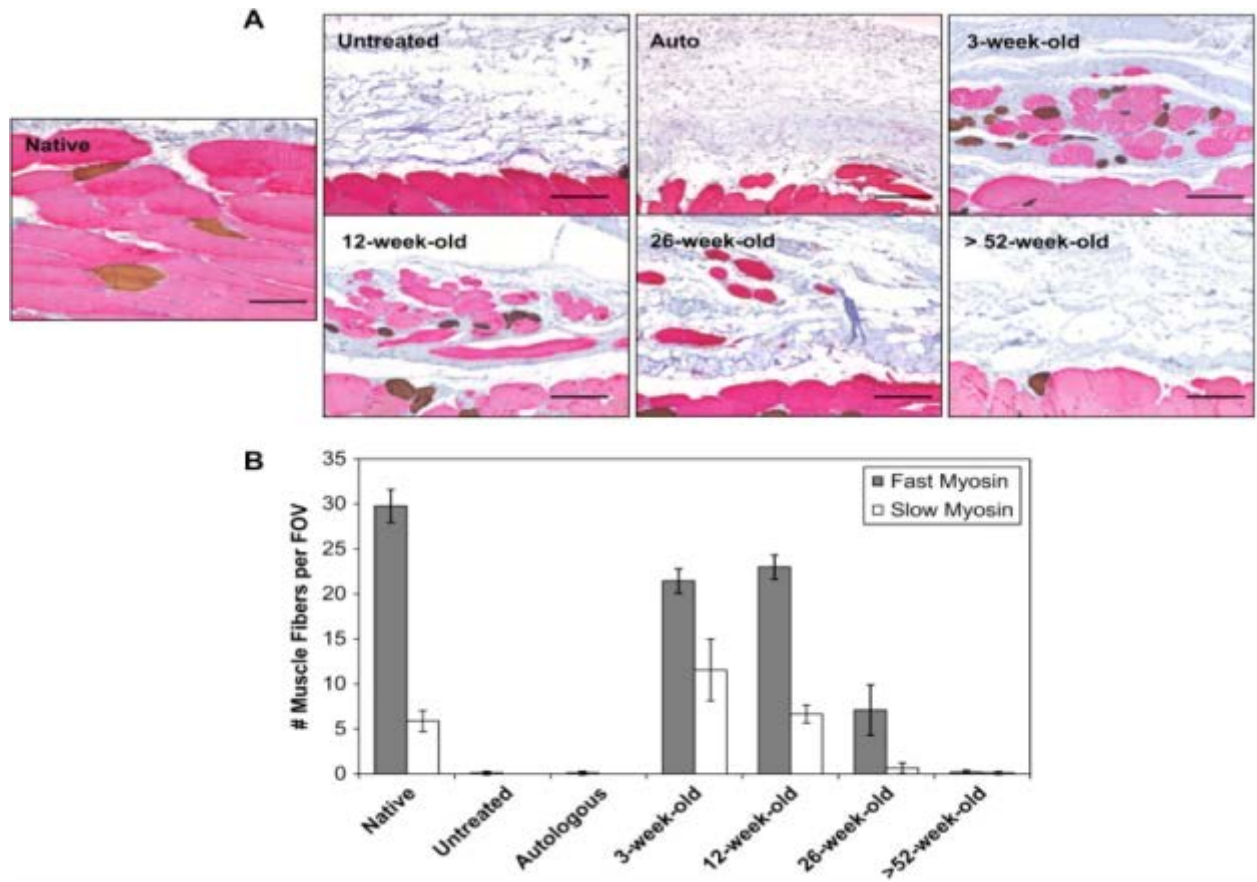


**Figure 9: Distribution of slow and fast skeletal muscle fibers within the remodeled tissue at 180 days post-surgery.** Tissue sections were double-labeled for anti-myosin slow (type I) skeletal muscle (brown stain) and anti-myosin fast (type II) skeletal muscle (red stain) to assess myofiber phenotype in the native and remodeled tissue (A). The native tissue showed that the slow muscle fibers were uniformly distributed between the fast muscle fibers. The remodeled 3 and 12-week-old scaffolds showed a similar distribution. 26-Week-old scaffolds showed predominantly fast muscle fibers, whereas the untreated defects, autograft, and >52-week-old scaffolds showed no signs of myofiber expression. Quantification of fast vs. slow muscle fibers per field of view (FOV) showed 3-week-old scaffolds displayed an increased number of slow muscle fibers when compared to all other surgical sites (B). Scale bars = 50  $\mu$ m. Error bars = standard deviation.

### **2.2.1.6 Sow aged SIS-ECM scaffold**

The sow aged SIS-ECM graft elicited a cellular infiltrate which was localized around the suture lines and did not completely penetrate the full thickness of the scaffold at 14 days (Figure 4A). In addition at 14 days, much of the original ECM scaffold could be identified along with a small amount of host derived neomatrix. Immunolabeling studies showed an M1:M2 macrophage ratio of  $0.93 \pm 0.18$  indicating a balanced macrophage phenotype response (Figure 4B,C). After 28 and 120 days the sow treated defects showed decreased cellularity with remnants of the ECM implant (Figure 7). At 180 days the sow treated defect sites contained pockets of cellularity surrounded by collagenous connective tissue (Figure 6). No evidence of the originally implanted scaffold was observed and there were no signs of new skeletal muscle or innervation (Figure 9, Figure 10). Quantitative analysis of the Masson's trichrome staining over time revealed an increase in the amount of collagenous connective tissue at 180 days when compared to the 14 ( $p < .001$ ) and 28 ( $p < .001$ ) day time points (Figure 8).

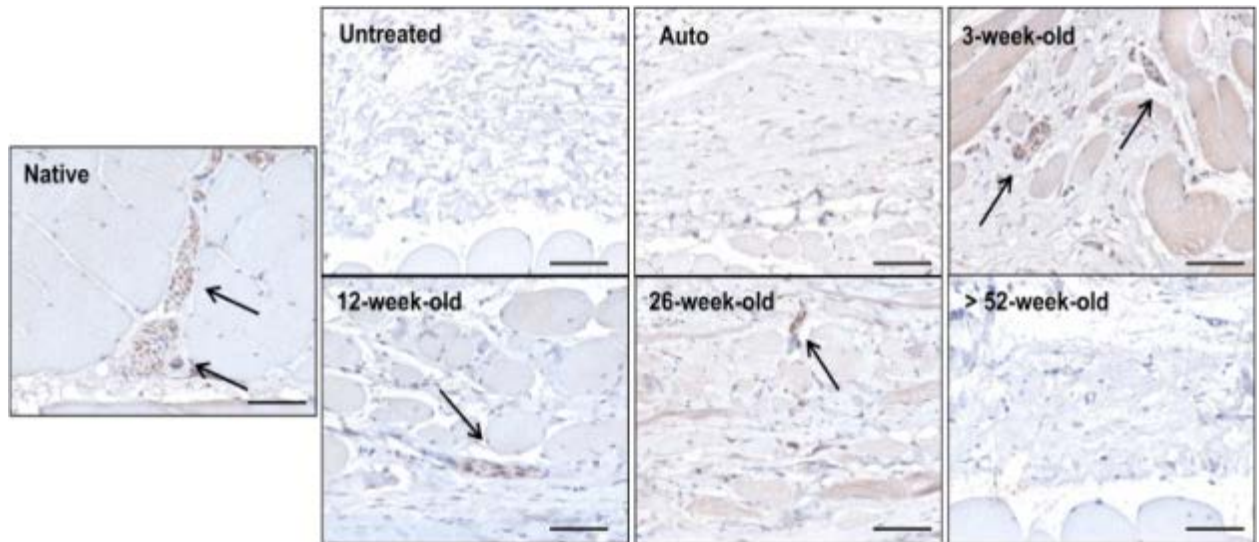


**Figure 10: Innervation of remodeled tissue at 180 days post-surgery.** Tissue sections were immunolabeled for anti-beta-III Tubulin (arrows; brown stain) to identify neurons in the native and remodeled tissue sections. Neurons were located adjacent to the myofiber bundles within the native tissue. Similar nerve structures were found around myofibers within the remodeled 26, 12, and 3-week-old scaffolds. The remodeled untreated defect site along with the >52-week-old scaffold and autograft treated sites showed no signs of innervation. Scale bars = 50  $\mu$ m.

### 2.2.2 Mechanical testing

Rat abdominal body wall containing remodeled neonate aged SIS-ECM grafts withstood greater uniaxial tensile stress compared to all other control and experimental groups as determined by ANOVA and Tukey-Kramer post-hoc evaluation (Figure 11A). Strain at failure and modulus did not differ significantly for control and experimental groups, including native body wall, body wall with a defect site that remained untreated, body wall treated with autologous tissue, or body wall treated with SIS-ECM from neonate, feeder, market, or sow aged animals (Figure 11B-C).

## 2.3 DISCUSSION AND CONCLUSIONS

The present chapter represents a systematic comparison of the *in vivo* host response to xenogeneic biologic scaffold materials that differ by a single variable; specifically, age of the animal from which the source tissue was harvested. There are two outcomes of note. First, source animal age is an important variable and ECM harvested from neonatal and feeder age pigs promotes the formation of greater amounts of site-appropriate skeletal muscle tissue than ECM harvested from older pigs. Secondly, the constructive site-appropriate remodeling response is associated with a predominant M2 macrophage response.

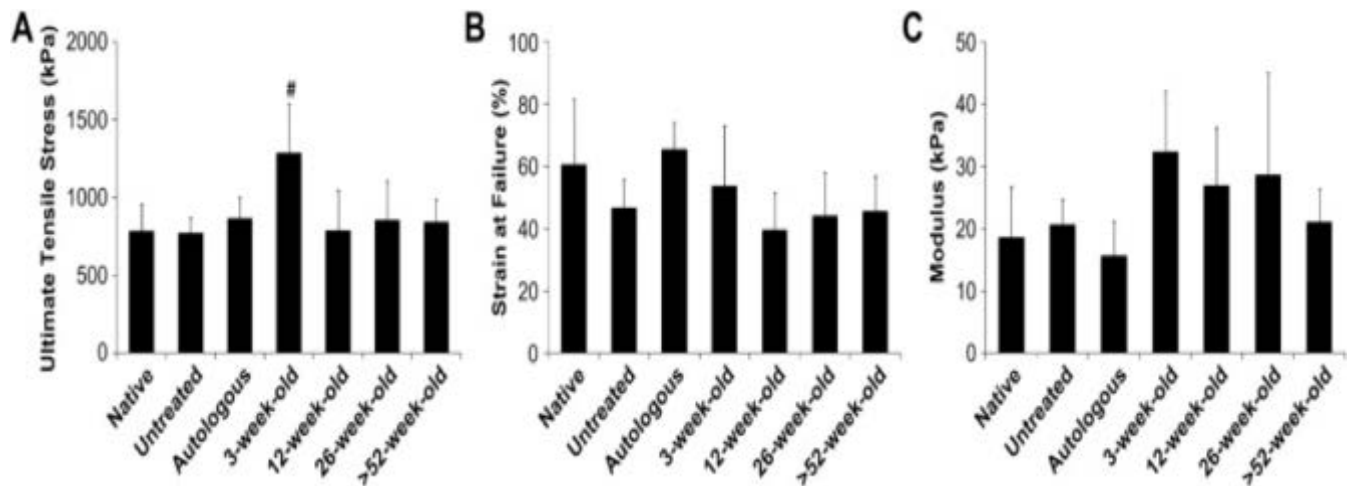


**Figure 11. Mechanical properties of explanted surgical sites at 180 days post-surgery.** Uniaxial tensile testing of explants (full thickness of the body wall including underlying and remodeled tissue) was used to characterize tissue mechanical properties for comparison to native tissue with respect to strength, distensibility, and stiffness. Body wall with remodeled 3-week-old aged SIS-ECM grafts withstood greater stress compared to native body wall and all other treatment groups (A). No differences were detected in strain at failure (B) or modulus (C) between native body wall and any other treatment group (<sup>#</sup>,  $p < 0.05$ ). Error bars = standard deviation. Error bars = standard deviation.

It is well known that fetal and neonatal mammals have greater wound healing and regenerative potential than adult mammals. The composition of fetal and neonatal ECM is distinctly different from that of adults and plays an important role in tissue development (301, 302). Fetal wounds have increased amounts of glycosaminoglycans (GAGs) such as hyaluronic acid and chondroitin sulfate (287, 290) which facilitate cell migration, mitosis, and differentiation (291). Compared to ECM in mature mammals, the ECM of fetal tissue is composed of more immature collagen containing fewer molecular cross links; a feature which promotes rapid degradation and remodeling (303). Therefore it is logical and plausible that bioscaffolds composed of ECM derived from fetal or neonatal tissues would induce a more robust and constructive tissue remodeling response than ECM derived from adult tissues. The results of the present chapter are consistent with this hypothesis.

The mechanisms by which scaffolds composed of ECM mediate a favorable remodeling process are not fully understood but include ECM scaffold degradation with the generation of bioactive cryptic peptides (8) release of bound growth factors (16), recruitment of endogenous stem and progenitor cells (5, 32), and modulation of the innate immune response (21, 22), among others. Of these potential mechanisms, only a component of the innate immune response was investigated in the present study; specifically, macrophage phenotype. A previous study compared the *in vitro* structural, mechanical, compositional, and bioactive properties of the same differently aged SIS-ECM materials (208). Scaffolds composed of neonatal and feeder aged ECM elicited increased progenitor cell chemotaxis and showed greater glycosaminoglycan (GAG) content than ECM scaffolds derived from older tissues. The purpose of the present study was not to determine cause-effect relationships between these variables, but rather to determine

the association of source tissue age within downstream remodeling events in an animal model of body wall reconstruction.

The response of skeletal muscle, which is a prominent natural component of the abdominal body wall, to injury is dependent on the temporal participation of different macrophage phenotypes (57). These macrophage phenotypes are characterized by distinct functional properties, effector molecule production, and surface marker expression (47, 304). Macrophage phenotypes range from classically activated (M1) macrophages which are pro-inflammatory at one end of a spectrum to alternatively activated (M2) macrophages which facilitate constructive tissue remodeling and repair at the opposite end of the spectrum (47, 49). Following an initial M1 macrophage response which stimulates muscle progenitor cell recruitment and mitosis, a subsequent predominant M2 macrophage response promotes the differentiation of skeletal muscle precursor cells (57). Inhibition of the M2 phenotype results in a severe lack of muscle regeneration and an accentuation of inflammation and necrosis (217). Dominant M1 or M2 macrophage populations at the *in-situ* interface of host tissue with ECM scaffolds are associated with either chronic inflammation with fibrotic tissue deposition or site appropriate tissue restoration, respectively (305). In the present chapter, scaffolds derived from younger animals were associated with a predominant M2 macrophage response after 14 days and showed the greatest amount of skeletal muscle at 180 days; a finding consistent with the predictive association of the M2 phenotype with favorable remodeling of surgical mesh products composed of biologic materials (305). It has previously been shown that surgically implanted ECM scaffolds enhance a host M2 macrophage response (22). The specific cause of the robust M2 response found within ECM scaffolds manufactured from neonatal or feeder pig tissues is unknown.

Repair of rat abdominal body wall with SIS-ECM from distinctly different aged animals resulted in remodeled tissue with similar mechanical properties to those of native body wall (Fig. 6). However, SIS-ECM from neonate aged animals remodeled into stronger tissue compared to native body wall (Fig. 6A). Based on a previous study (208), it is likely that biologic cues from degradation products of neonate SIS-ECM vary from those of degrading SIS-ECM from older animals and lead to different downstream remodeling outcomes. It is possible that because the neonate scaffolds degraded more rapidly and promoted greater cell migration (208), the skeletal muscle tissue that formed within the neonate SIS-ECM treated surgical sites had more time to mature, and this in combination with the increased amount of connective tissue, compared to native tissue, resulted in stronger tissue. In addition, passive mechanical testing may not have been sensitive enough to detect discernable differences in such a small defect site. Furthermore, biologic variability between animals may also have masked subtle differences between experimental groups. However, mechanical data in this study clearly showed that donor age can impact functional outcomes.

In conclusion, the present chapter examines an important variable that should be considered in the design and manufacturing of biologic devices composed of mammalian ECM; specifically, the age of the source animal. Biologic scaffold materials derived from younger (feeder and neonate) aged animals are associated with a host innate immune response consisting predominantly of M2 macrophages and a more robust constructive remodeling response when compared to scaffolds prepared from market weight or sow aged pigs. The remaining chapters of this dissertation will examine market weight and young (feeder) aged SIS-ECM.

## 2.4 LIMITATIONS AND FUTURE DIRECTIONS

The present chapter compared xenogeneic biologic scaffold materials differing only in source animal age. However, there are limitations that must be noted in the interpretation of the data. First, the results represent the findings from a single source tissue of ECM material; specifically porcine SIS-ECM. These results cannot necessarily be generalized to ECM prepared from other tissue sources such as dermis, urinary bladder, and others. Secondly, ECM materials are prepared by decellularization of various tissues, and the decellularization procedures utilized can vary significantly. Results of the present study may not apply to materials prepared by other methods that affect surface epitopes, biochemical composition, and rate of degradation of various scaffold materials. Finally, the association of the M1/M2 macrophage phenotype ratio with constructive remodeling does not prove cause-effect.

### **3.0 THE ABILITY OF ECM TO ENHANCE THE POLARIZATION OF MACROPHAGES ISOLATED FROM YOUNG AND AGED SUBJECTS AND THE EFFECT OF ECM AND POLARIZED MACROPHAGES UPON SKELETAL MUSCLE PROGENITOR CELLS**

#### **3.1 BACKGROUND**

Macrophages are recognized as phagocytic and antigen presenting cells responsible for propagating the pro-inflammatory response of the mammalian innate immune system (43, 306). It is now accepted that macrophages also play a larger role as regulators of tissue homeostasis during the host response to disease and tissue injury (45-49). Macrophages, like other myeloid cells, are a heterogeneous population of cells capable of assuming different phenotypes. These phenotypes are defined by select surface markers, diverse functional properties, and patterns of gene expression. Macrophages assume phenotypes that are context dependent and responsive to signals from their local microenvironment. Thus, the phenotype of circulating or migratory macrophages exists along a spectrum of differentiation (30, 50). Cells on the opposite ends of this spectrum, similar to the Th1/Th2 paradigm, are broadly categorized as M1 or M2 macrophages (307). M1 macrophages are pro-inflammatory or “classically activated” cells stimulated by pro-inflammatory factors (e.g., IFN $\gamma$ , LPS). M1 activated macrophages secrete toxic reactive oxygen and nitric oxygen intermediates and inflammatory cytokines such as IL-1 $\beta$ ,

IL-6, and TNF $\alpha$  and produce high levels of inducible nitric oxide synthase (iNOS). These cells are responsible for microbicidal activity, debris clearance, and the propagation of a pro-inflammatory and Th1 response. Conversely, “alternatively activated” and constructive M2 macrophages are stimulated by immunomodulatory and anti-inflammatory factors (e.g., IL-4, IL-10). M2 activated macrophages express IL-10 and Fizz1; have high levels of scavenger and mannose receptors (e.g., CD206); and produce arginase in the place of iNOS, subsequently producing ornithine and polyamines. These cells are responsible for propagation of a constructive immunomodulatory or Th2 response, matrix deposition, and tissue repair and reconstruction (46, 47). Most macrophages likely express a phenotype somewhere between the extremes dependent upon microenvironmental cues and temporal factors; however, the factors that modulate this macrophage phenotypic profile are only partially understood.

Adult skeletal muscle tissue retains inherent regenerative potential following minor tissue injury (55, 61) that is dependent upon activated skeletal muscle progenitor cells and a temporal transition of M1 to M2 macrophages (57). Satellite cell derived myoblasts are the primary stem / progenitor cell type responsible for the skeletal muscle regenerative response to injury. However, myogenic perivascular stem cells (PVSC) have been shown to occupy the satellite cell niche and give rise to myoblasts as well (33, 35, 36). These skeletal muscle progenitor cells become activated when effector molecules secreted by M1 macrophages promote their mitogenesis and expansion. A transition in macrophage phenotype is necessary for efficient differentiation of myoblasts. Specifically, M2 macrophage associated effector molecules promote the fusion, myotube formation, and myogenic differentiation of these progenitor cells (57, 215). The factors which contribute to the M1 to M2 transition have not yet been identified.

Biologic scaffolds derived from mammalian tissues are composed of naturally occurring extracellular matrix (ECM) and are referred to as ECM bioscaffolds. ECM bioscaffolds are manufactured by tissue decellularization methods which remove pro-inflammatory immunogenic cellular material while preserving ECM constituents such as growth factors and the ECM ultrastructure. ECM bioscaffolds have been used, both in pre-clinical animal studies and in human clinical applications, to successfully promote constructive tissue remodeling in a variety of tissues including skin, bladder, heart, tendon, and skeletal muscle (2, 200-202, 214, 236, 295, 308). The mechanisms responsible for this constructive remodeling response include the release of bioactive degradation products (i.e., cryptic peptides) with the potential for endogenous stem and progenitor cell recruitment (5-8, 10, 27, 28, 33) and immunomodulation (21, 22, 29, 30), among others. Furthermore, surgically placed ECM bioscaffolds have been associated with a predominant M2 macrophage phenotype. The effect of bioactive ECM degradation products upon macrophage has not been investigated.

The objectives of the present chapter were: (1) To determine the effect of ECM degradation products upon macrophage phenotype; (2) To determine the effect of young vs. aged ECM upon skeletal muscle progenitor cells; and (3) To determine the effect of ECM-treated macrophages upon skeletal muscle progenitor cells.

## **3.2 MATERIALS AND METHODS**

### **3.2.1 Overview of Experimental Design**

Macrophages were derived from bone marrow of C57bl/6 female mice at 6-8 weeks and 20-24 months of age and treated with pro-inflammatory cytokines to derive M1 macrophages, immunomodulatory cytokines to derive M2 macrophages, or degradation products from market weight (26 week old) and young (<12 week old) aged small intestinal submucosa (SIS)-ECM. Macrophage phenotype was determined by immunolabeling and western blotting for markers of M1 and M2 macrophages. In addition, macrophage supernatants and ECMs were investigated as potential chemoattractants in a Boyden Chamber cell migration assay to study the recruitment of perivascular stem cells (PVSC) and C<sub>2</sub>C<sub>12</sub> skeletal muscle myoblasts (ATCC). To examine the effect of macrophages on proliferation of these progenitor cells, mitogenic effects of macrophage supernatants and ECMs were evaluated using 5-bromo-2'-deoxyuridine (BrdU) incorporation. The influence of macrophages and ECMs on myogenic differentiation was also determined by examining the PVSC and myoblast fusion index and sarcomeric myosin-heavy chain expression.

### **3.2.2 Preparation of ECM degradation products**

Small intestinal submucosa (SIS)-ECM was prepared from porcine jejunum (298). The SIS-ECM was prepared from the market weight (26 week old) and feeder aged (<12 week old) animals as described in Chapter 2 of the present dissertation. The resultant SIS-ECMs were lyophilized, powdered, and digested at 10mg/ml dry weight with 1 mg/ml pepsin as previously described (26).

### **3.2.3 Isolation and culture of murine bone marrow derived macrophages**

Adult, female 6 to 8-week and 20-24 month old C57bl/6 mice obtained from Jackson Laboratories (Bar Harbor, ME) were euthanized via cervical dislocation. Using aseptic technique, the skin from the top of each hind leg to the foot was removed, the ankle joint was disarticulated and the tibia isolated. Similarly, the hip joint was disarticulated for isolation of the femur. Excess tissue was removed using forceps and a scalpel blade. Bones were kept on ice and rinsed in a sterile dish containing macrophage complete medium consisting of DMEM (Gibco, Grand Island, NY), 10% fetal bovine serum (FBS) (Invitrogen, Carlsbad, CA), 10% L929 supernatant, 0.1% beta-mercaptoethanol (Gibco), 100 U/ml penicillin, 100 ug/ml streptomycin, 10 mM non-essential amino acids (Gibco), and 10 mM hepes buffer. In a sterile environment, the ends of each bone were transected and the marrow cavity flushed with complete medium using a 30-gauge needle attached to a 10 ml syringe. Harvested cells were spun, filtered, plated, and allowed to differentiate into macrophages for 7 days at 37°C, 5% CO<sub>2</sub> with complete media changes every 48 hours.

### **3.2.4 Polarization and immunolabeling of bone marrow derived macrophages**

After 7 days, resulting naïve macrophages were treated with basal media consisting of DMEM, 10% FBS, 100 ug/ml streptomycin, 100 U/ml penicillin and one of the following treatments: (1) 20 ng/ml IFN- $\gamma$  and 100 ng/ml LPS to derive M1 macrophages, (2) 20 ng/ml IL-4 to derive M2 macrophages, (3) 200 ug/ml of SIS-ECM degradation products. After 18 hours of incubation at 37°C, 5% CO<sub>2</sub> cells were washed with sterile PBS, and fixed with 2% paraformaldehyde for immunolabeling. The primary antibodies used for immunofluorescent staining were: (1)

monoclonal F4/80 (Abcam) at 1:200 dilution for a pan-macrophage marker, (2) polyclonal iNOS (Abcam) at 1:100 dilution for an M1 marker, and (3) polyclonal Fizz1 (Peprtech) for an M2 marker. Cells were incubated in blocking solution consisting of PBS, 0.1% Triton-X , 0.1% Tween-20, 4% goat serum, and 2% bovine-serum albumin to prevent non-specific binding for 1 hour at room temperature. Blocking solution was removed and cells were incubated in primary antibodies for 16 hours at 4°C. After washing in PBS, cells were incubated in fluorophore-conjugated secondary antibodies (Alexa Fluor donkey anti-rat 488 or donkey anti-rabbit 488, Invitrogen) for 1 hour at room temperature. After washing again with PBS, nuclei were counterstained with 4'6-diamidino-2-phenylindole (DAPI) prior to imaging. Representative images of three 20x fields were taken for each well using a Zeiss Axiovert inverted fluorescence microscope. Light exposure times for ECM-treated macrophages were standardized based on exposure times set for cytokine-treated internal controls. Images were quantified using a CellProfiler pipeline for relative expression of F4/80, iNOS, and Fizz.

### **3.2.5 Validation of Macrophage Phenotype with Western Blots**

Western blots were performed on treated macrophage cell lysates. Cell lysates were boiled at 100°C for 5 minutes and electrophoresed on 15% acrylamide gels. One-hundred micrograms of protein was loaded into each well. Separated proteins were transferred to PVDF membranes using a standard wet transfer procedure. Following transfer, membranes were blocked for 18 hours at 4°C in TBS-T with 3% milk to prevent non-specific antibody binding. Membranes were incubated in the following primary antibodies for 18 hours in 3% milk at 4°C: (1) polyclonal anti-rabbit mannose receptor (Abcam) at 1:714 dilution for an M2 marker, and (2) polyclonal anti-rabbit IL-6 (Abcam) at 1:500, and (3) monoclonal anti-mouse B-actin (Santa Cruz) at a

dilution of 1:1000 as a loading control. Blots were visualized using a Li-Cor Odyssey western blot detection system. Densitometry of protein expression was standardized to the housekeeping loading control.

### **3.2.6 Progenitor Cell Culture**

Perivascular stem cells isolated from human skeletal muscle as previously described (33) and murine C<sub>2</sub>C<sub>12</sub> myoblasts were purchased from ATCC and cultured in DMEM containing 20% FBS and 10% FBS, respectively, and 100 ug/ml streptomycin and 100 U/ml penicillin. Cells were grown at 37°C, 5% CO<sub>2</sub> and were assayed for a chemotactic response in a Boyden chamber chemotaxis assay when they reached approximately 80% confluence.

### **3.2.7 Preparation of Boyden Chamber Test Articles**

For examination of the chemotactic properties associated with market vs. young SIS-ECM bioscaffolds, degradation products were generated as described above (26). For examination of the chemotactic properties associated with polarized macrophage conditioned media, macrophages were polarized or treated with ECM as described above (section 3.2.4). Following 18 hours of treatment, the media was removed and cells were washed with PBS. Media was then replaced with growth factor and ECM free media. Cells were allowed to condition media for 5 hours at 37°C, 5% CO<sub>2</sub>. After 5 hours, supernatants were collected for use as potential chemoattractant test articles in a Boyden chamber assay. Following supernatant harvest, cells were fixed with 2% paraformaldehyde and stained according to the previously described protocol (section 3.2.4) to verify phenotype maintenance following growth-factor withdrawal.

### **3.2.8 Chemotaxis Assay**

Migration of progenitor cells towards ECM degradation products and macrophage-conditioned media was investigated using a Boyden chamber assay. C<sub>2</sub>C<sub>12</sub> myoblasts and perivascular stem cells were cultured in starvation media (DMEM, 0.5% FBS, 1% pen/strep) for 18 hours prior to assay. Cells were then trypsinized, re-suspended in growth factor and serum free DMEM, and transferred to a 15 ml conical tube for 1 hour incubation at 37°C, 5% CO<sub>2</sub>. Polycarbonate chemotaxis membranes with a pore size of 8µm were coated with 0.05 mg/ml collagen type I. ECM degradation products (market weight vs. young), macrophage conditioned media (M1, M2, SIS-ECM treated), as well as positive (DMEM with 20% FBS) and negative (growth factor and serum-free DMEM) controls were added to the lower wells of a Neuro Probe 48-well micro chemotaxis chamber. Collagen-coated membranes were placed over the chemoattractants and 6x10<sup>5</sup> cells were added to each of the upper wells of the chamber. Cells were allowed to migrate across the chamber for 3 hours at 37°C, 5% CO<sub>2</sub>. Following the migration period, non-migrating cells were scraped from the upper side of the membrane using a rubber scraper and migrated cells on the bottom of the membrane were fixed with 95% methanol and stained with DAPI prior to imaging. Membranes were imaged using Zeiss Axiovert inverted fluorescence microscope. The number of migrated cells was quantified using a custom CellProfiler, image analysis software pipeline.

### **3.2.9 Mitogenesis Assay**

C<sub>2</sub>C<sub>12</sub> skeletal muscle myoblasts and PVSCs were seeded in normal growth media at 1x10<sup>3</sup> cells per well in a 96 well plate. Media was switched to starvation media (DMEM, 0.5% FBS, 1%

penn/strep) for 18 hours. Following the starvation period, cells were treated with ECM conditioned media or macrophage supernatants, as well as positive (DMEM with 20% FBS) and negative controls (serum free DMEM). Treatments were supplemented with 10 mg/ml 5-bromo-2'-deoxyuridine (BrdU) for 18 hours for PVSCs and 4 hours for C<sub>2</sub>C<sub>12</sub> skeletal muscle myoblasts. Following treatment pulse, cells were fixed with 95% methanol for 10 minutes, and washed with PBS. Cells were then treated with 2 N HCl for 30 minutes at 37°C. Following HCl treatment, cells were blocked using the previously described blocking solution for 1 hour at room temperature. Following the blocking period, cells were incubated in G3G4 (Anti-BrdU) antibody (Developmental Studies Hybridoma Bank) at a dilution of 1:1000 for 16 hours at 4°C. Following primary incubation, cells were washed 3 times with PBS, incubated in Alexa Fluor donkey anti-mouse 488 at a dilution of 1:300 for 1 hour at room temperature, and counterstained with DAPI solution. BrdU incorporation was imaged using a Zeiss Axiovert inverted fluorescence microscope and quantified using an ImageJ macro.

### **3.2.10 Myogenesis Assay**

Myogenic differentiation potential was determined by examining myotube formation by PVSCs and skeletal muscle myoblasts. PVSCs and myoblasts were cultured in normal growth media with high serum until they reached approximately 80% confluence. Media was then changed to treatment media consisting of (market vs. young) ECM degradation products, macrophage supernatants, or high and low serum controls (High serum media retains cells proliferating within the cell cycle providing a negative control for differentiation; conversely, low serum induces cell-cycle exit and myotube formation providing a positive control) (309). Following 5-7 days, or when low serum controls showed myotube formation, cells were fixed for immunolabeling with

2% paraformaldehyde, or harvested for western blot analysis. PFA fixed cells were blocked for 1 hour at room temperature, and incubated in MF20 (anti-sarcomeric myosin) primary antibody (Developmental Studies Hybridoma Bank) at a dilution of 1:500 for 16 hours at 4°C. Following primary incubation, cells were washed with PBS and incubated in Alexa Fluor donkey anti-mouse 488 secondary antibody at a dilution of 1:200 for 1 hour at room temperature and counterstained with DAPI. Myotube formation was imaged on an Olympus Axiovert inverted fluorescence microscope.

### **3.2.11 Statistical analysis**

A one-way analysis of variance (ANOVA) was used in conjunction with a Tukey's post-hoc test to compare results between groups. Differences were considered significant at  $p < 0.05$ . Statistical analysis was completed using SPSS Statistical Analysis Software (IBM, Chicago, IL, USA).

## **3.3 RESULTS**

### **3.3.1 Degradation Products from ECM Bioscaffolds Promote the M2 Macrophage Phenotype**

Macrophages were derived from the bone marrow of young (6-8 week) and aged (20-24 months) C57bl/6 mice and subsequently exposed to IFN $\gamma$ /LPS, IL-4, or ECM degradation products. After 18 hours, degradation products from ECM bioscaffolds promoted M2 macrophage

activation similar to IL-4 exposure in macrophages derived from young mice (Figure 12). The M2 macrophage phenotype was confirmed using Fizz 1 immunolabeling (Figure 12A), quantified using the Cellprofiler image analysis software (Figure 12B) and corroborated using CD206 western blotting (Figure 12C). Degradation products from ECM also promoted M2 macrophage activation in macrophages derived from age-impaired mice (Figure 13).

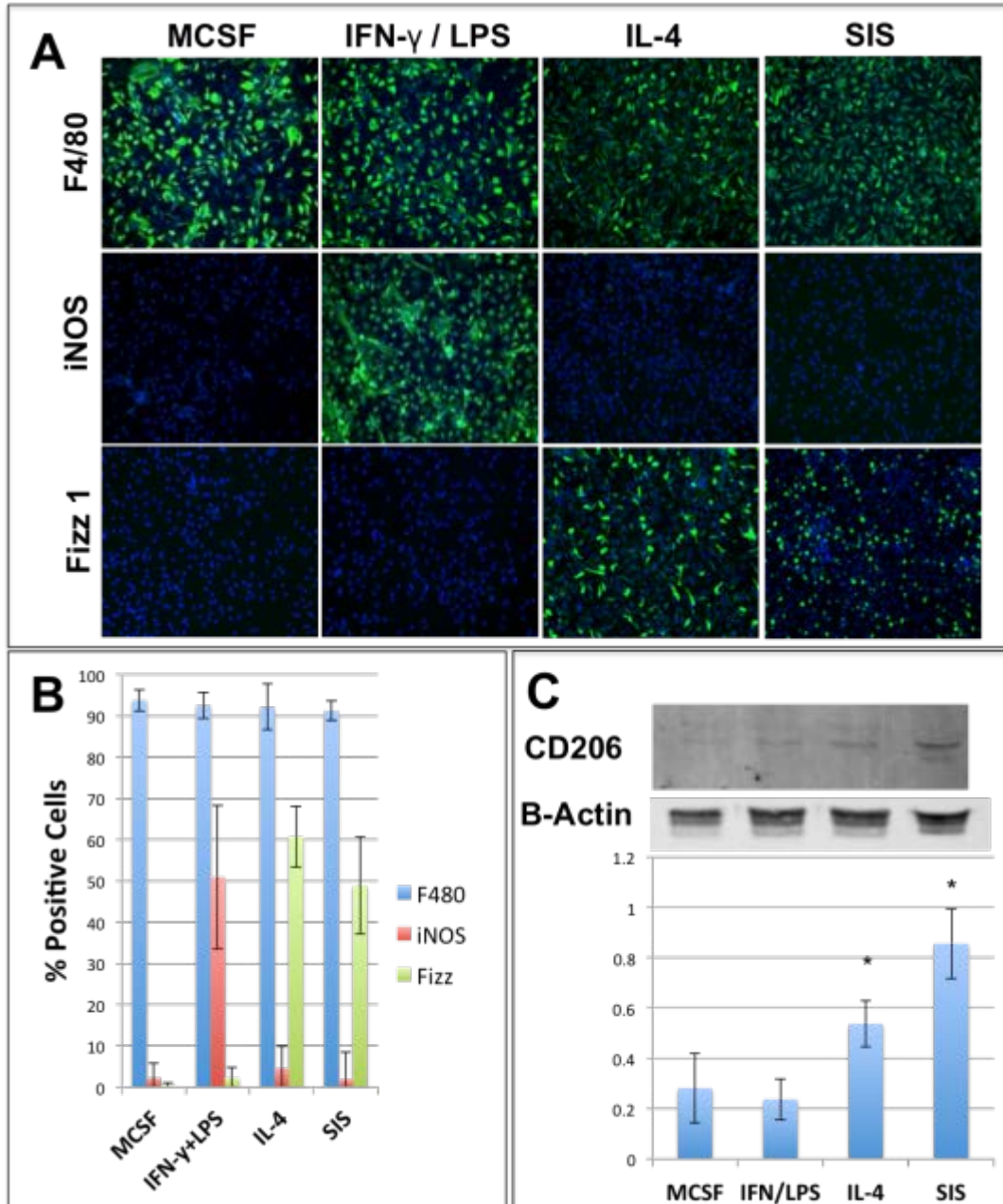


**Figure 12: Mammalian ECM promotes the M2 macrophage phenotype.** Murine bone-marrow-derived macrophages were treated with: 100 ng/ml monocyte colony stimulating factor (MCSF) for derivation of naïve M0 macrophages, 20 ng/ml IFN- $\gamma$  & 100 ng/ml LPS for derivation of pro-inflammatory M1 macrophages, 20 ng/ml IL-4 for immunomodulatory / constructive M2 macrophages, or with 200  $\mu$ g/ml SIS-ECM degradation products for 18 hours. Cells were then fixed and immunolabeled for the pan-macrophage marker (F4/80) and for indicators of M1 (iNOS) and M2 (Fizz1) macrophages (A). Degradation products from SIS-ECM were able to promote the constructive M2 macrophage phenotype similar to IL-4 treatment. Quantification of immunolabeling using Cell Profiler image analysis software (B). Western blot analysis of the CD206 M2 macrophage marker and the associated densitometry normalized to the  $\beta$ -actin housekeeping control (\*  $p < 0.05$  for both when compared to all other groups).

### **3.3.2 ECM-Treated and IL-4 induced M2 Macrophages are Chemotactic and Myogenic for Skeletal Muscle Progenitor Cells.**

Macrophages were polarized as above, allowed to condition media, and retained their phenotype following growth factor and ECM withdrawal (Figure 14). The effect of media conditioned by M1, M2, and ECM-treated macrophages upon human PVSCs and C<sub>2</sub>C<sub>12</sub> myoblasts was examined (Figure 15). Trends showed that products secreted by IL-4 derived M2 and ECM-treated macrophages were chemotactic for PVSCs (Figure 15A) and myoblasts (Figure 15B) when compared to products secreted by M1 macrophages. Medium conditioned by M1 macrophages, but not IL-4 induced M2 or ECM treated macrophages was mitogenic for PVSCs and (Figure 16). Furthermore, media conditioned by both IL-4 induced M2 and ECM-treated macrophages promoted myogenesis of skeletal muscle myoblasts (Figure 17) when compared to media conditioned by M1 macrophages.

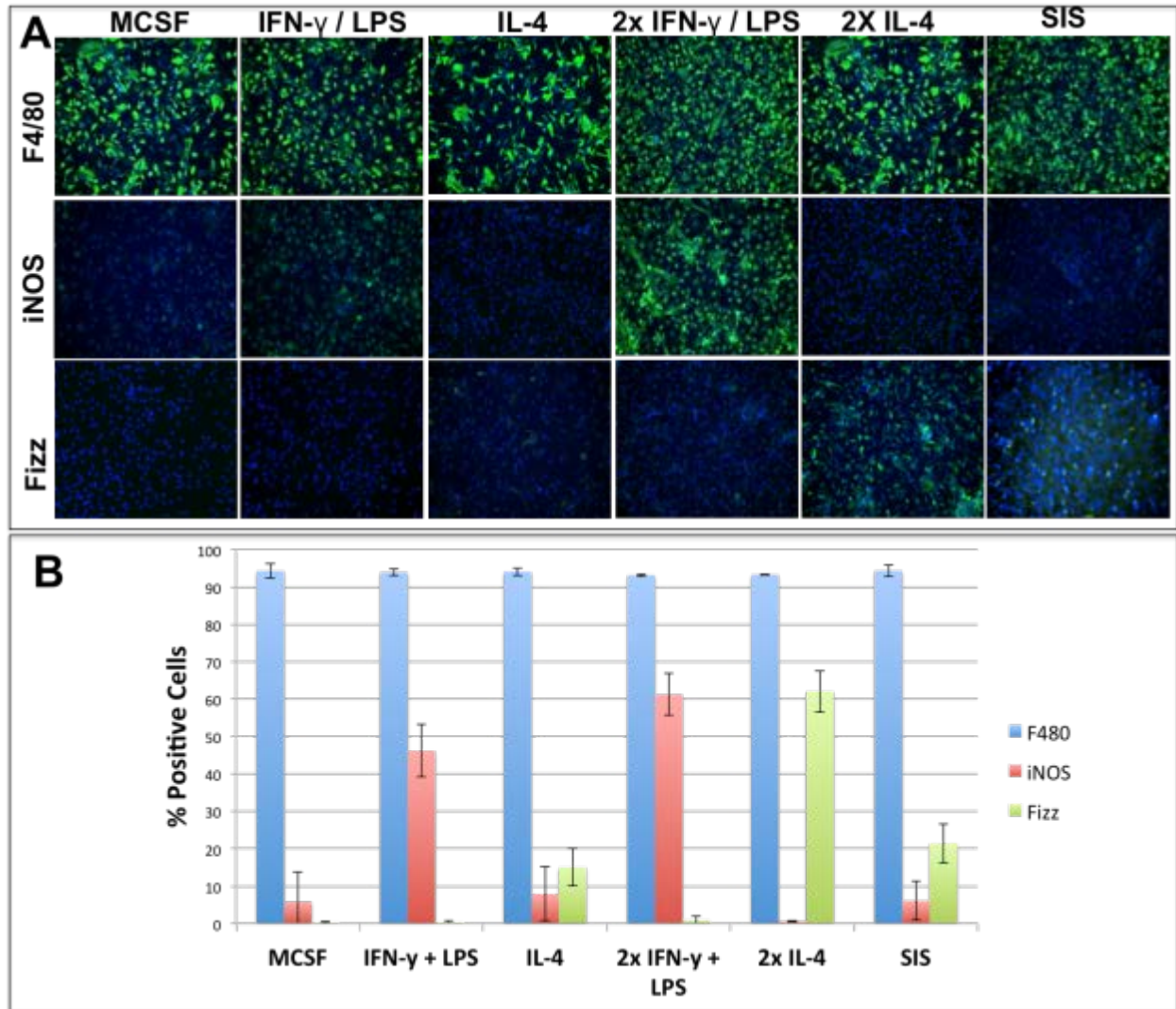


**Figure 13: Mammalian ECM promotes the M2 macrophage phenotype in aged macrophages.** Murine bone-marrow-derived macrophages from 20-24 month old mice were treated with the same factors as in Fig 12, but required twice the concentrations to achieve polarization. Specifically: 40 ng/ml IFN- $\gamma$  & 200 ng/ml LPS for derivation of pro-inflammatory M1 macrophages, and 40 ng/ml IL-4 for immunomodulatory / constructive M2 macrophages. 200  $\mu$ g/ml SIS-ECM degradation products was able to promote the M2 phenotype similar to that of 20 ng/ml IL-4. Cells were then fixed and immunolabeled for the pan-macrophage marker (F4/80) and for indicators of M1 (iNOS) and M2 (Fizz1) macrophages (A). Quantification of immunolabeling using Cellprofiler image analysis software (B).

### **3.3.3 Degradation Products from Market Weight and Young ECM are Chemotactic and Myogenic for Skeletal Muscle Progenitor Cells**

The effect of degradation products from market weight (26 week old) and young aged (<12 week old) SIS-ECM upon PVSCs and skeletal muscle myoblasts was examined. ECM derived from both aged pigs was chemotactic for PVSCs (Figure 18A) and C2C12 myoblasts (Figure 18B) in a Boyden Chamber chemotaxis assay when compared to controls. No differences in chemotactic activity between market weight vs. young SIS-ECM were identified. Degradation products from market weight vs. young SIS-ECM scaffolds were not mitogenic for PVSCs (Figure 19). No difference in mitogenic activity between market weight vs. young SIS-ECM was identified. Furthermore, degradation products from both market weight and young SIS-ECM were myogenic for PVSCs (Figure 20) and C2C12 skeletal muscle myoblasts (Figure 21). Myosin heavy chain (MHC) expressing myofibers were more abundant in media conditioned with degradation products from both market weight and young SIS-ECM (Figure 20 B,C).

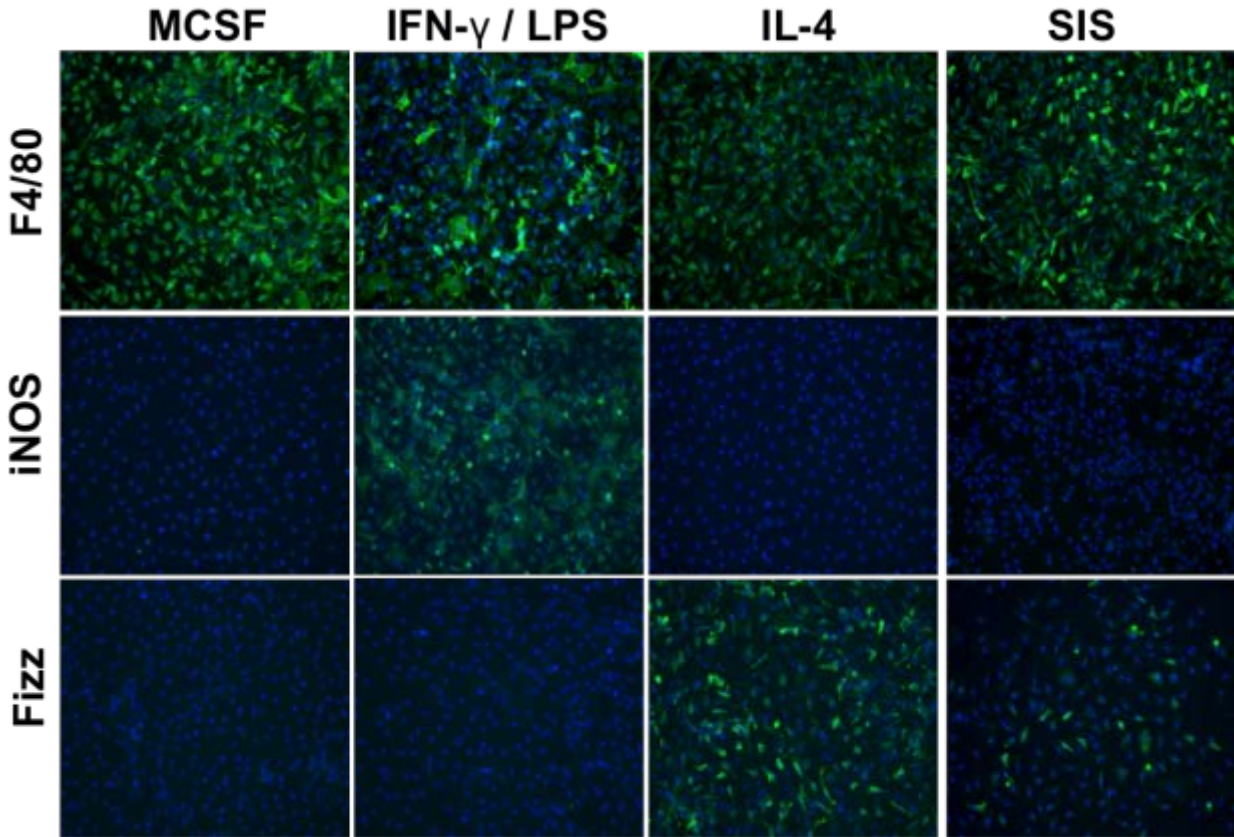


**Figure 14: Polarized macrophages retain phenotype after growth-factor withdrawal.** Murine bone-marrow-derived macrophages were derived as in Figure 12 & 13. Following polarization or ECM-treatment, the cells were washed and replaced with growth factor free media. After 5 hours the supernatants were collected and used in the following chemotactic and differentiation assays. Macrophages retained their phenotype at the time of supernatant collection.

### 3.4 DISCUSSION AND CONCLUSIONS

The present chapter represents a systematic examination of the effect of mammalian ECM upon macrophage phenotype and how ECM-treated macrophages influence the activity of skeletal muscle progenitor cells. Furthermore, ECM harvested from different aged animals (market

weight [26 weeks old] vs. young [12 week old]) was compared in their ability to affect the same skeletal muscle progenitor cells.

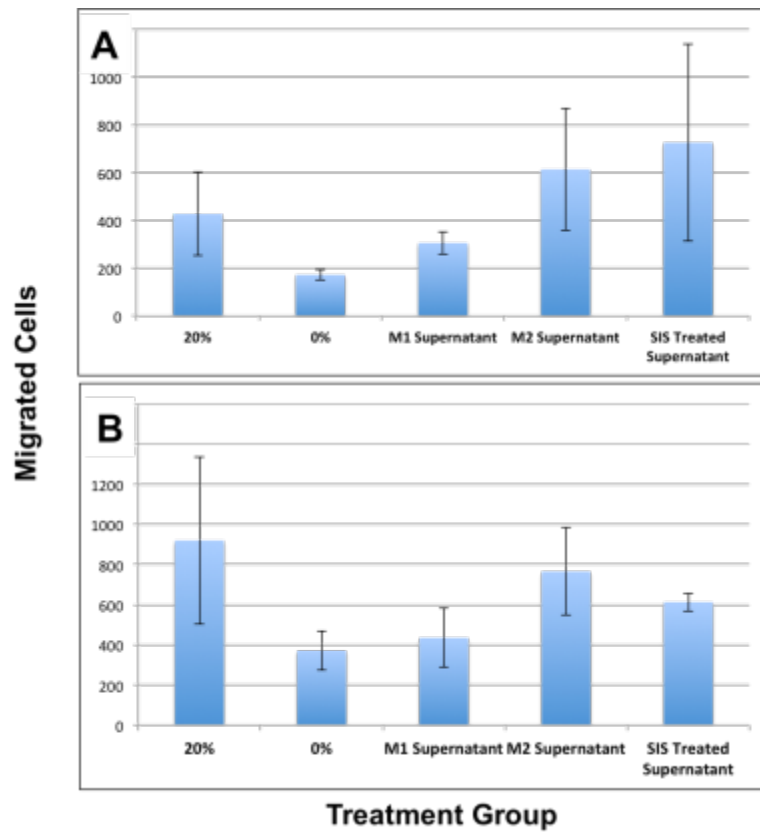


**Figure 15: M2 and ECM-treated macrophages are chemotactic for progenitor cells.** Polarized and ECM-treated macrophage conditioned media were used as chemoattractants for PVSCs (A) and myoblasts (B).

The results of this chapter showed that degradation products of mammalian ECM were directly able to promote the constructive M2 macrophage phenotype, similar to IL-4 exposure, in bone marrow derived macrophages from young and old mice. Furthermore, ECM-treated macrophage conditioned media was chemotactic for PVSCs and skeletal muscle myoblasts and myogenic for skeletal muscle myoblasts. Degradation products from market weight and young ECM were chemotactic and myogenic for PVSCs and skeletal muscle myoblasts. Quantitative

analysis showed no differences in the chemotactic potential of market weight vs. young ECM. However, qualitative analysis suggests a difference in the myogenic potential of these ECMs derived from differently aged source material. Specifically, degradation products from young SIS-ECM showed an increase in the size of myosin heavy chain positive PVSC derived myotubes when compared to market weight SIS-ECM (Figure 20 C). This difference may partially contribute to the increased constructive remodeling associated with young SIS-ECM from Chapter 2 of the present dissertation.

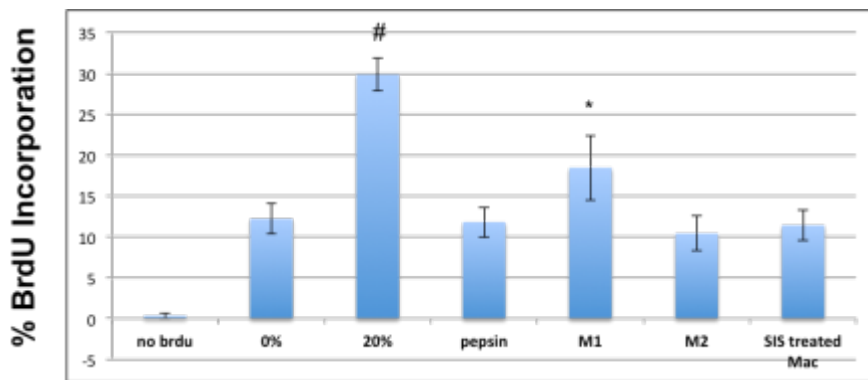


**Figure 16: M1 macrophages are mitogenic for progenitor cells.** Media conditioned by M1 macrophages induced greater BrdU incorporation when compared to media conditioned by M2 or ECM-treated macrophages (\*, #  $p < 0.05$  when compared to each other and all other groups).

Biologic scaffolds composed of mammalian ECM have been associated with a predominant M2 macrophage phenotype when surgically placed at sites of tissue injury (21, 22, 222). The mechanisms behind this M2 response remain largely unknown. The present chapter shows that degradation products from SIS-ECM bioscaffold materials directly affect macrophage phenotype and promote M2 expression. Furthermore, the study shows that ECM-treated macrophages not only express M2 markers (e.g., Fizz1, CD206), they also function as bona fide

IL-4 generated M2 macrophages with respect to progenitor cell chemoattraction, proliferation, and differentiation.

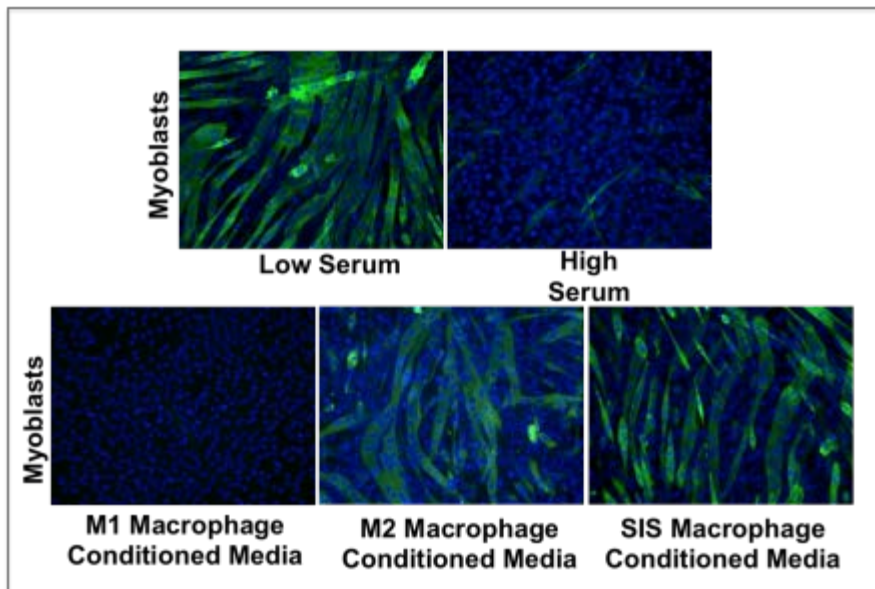


**Figure 17: Media conditioned by polarized M2 and ECM-treated macrophages are myogenic for myoblasts.**

*C<sub>2</sub>C<sub>12</sub>* myoblasts were cultured in fusion media (low serum), proliferation media (high serum), or proliferation media conditioned with supernatants from M1, M2, and SIS-ECM-treated macrophages. Cells were then fixed and immunolabeled for sarcomeric myosin heavy chain (MHC) (green).

It has been shown that a heterogeneous transition of M1 to M2 macrophages is required for an efficient host derived regenerative response following skeletal muscle injury (57, 250, 310). M1 macrophages comprise the predominant cellular response to skeletal muscle injury at 48 hours post-injury. Conversely, at 3-8 days post-injury, M2 macrophages predominate the host cellular response (57). Second only to short-lived neutrophils, classically activated M1 macrophages represent the next cell-type to invade the wound site, kill pathogens and phagocytose myofiber and other necrotic or injured cellular debris, and propagate a type-1 pro-inflammatory response (215). In addition to these cytotoxic responses, M1 macrophages, through effector molecule production, promote skeletal muscle myoblasts to enter the cell cycle and

expand (216, 311). During the resolution of inflammation at the injury site, there is a phenotypic switch of macrophages towards the M2 or constructive phenotype. M2 macrophages, through effector molecule production, promote immunomodulation and the myogenic differentiation of the expanded skeletal muscle myoblasts (217, 312). The present chapter confirms these phenomena, showing that M1 macrophage conditioned media promote the proliferation of skeletal muscle progenitors, while M2 macrophage conditioned media promotes chemotaxis and myogenesis of skeletal muscle progenitor cells. Moreover, the chapter shows that ECM-treated M2 macrophages promote chemotaxis myogenesis similar to IL-4 activation.

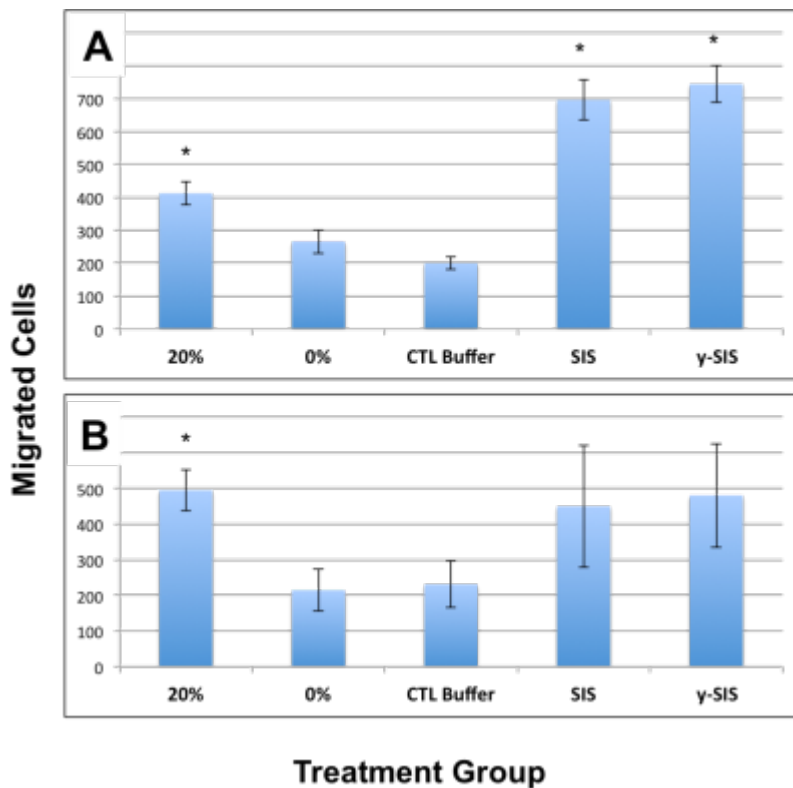


**Figure 18: Degradation Products from ECM are chemotactic for progenitor cells.** Skeletal muscle progenitor cells were seeded at 30,000 cells/well in a chemotaxis chamber and allowed to migrate for 3 hours at 37°C. Migrated cells were fixed, stained with Dapi nuclear stain, and imaged using a Zeiss Axiovert fluorescence microscope. Images were quantified using Cell Profiler image analysis software. Degradation products of SIS-ECM, at a

concentration of 200 ug/ml, were chemotactic for Perivascular stem cells (PVSCs) (A) and C2C12 skeletal muscle myoblasts (B) (\*p < 0.05 when compared to all other groups).

### 3.5 LIMITATIONS AND FUTURE DIRECTIONS

The present chapter showed that ECM promotes the M2 macrophage phenotype, and compared market weight vs. young source aged ECM. However, there are limitations that must be noted in the interpretation of the data. First, although the study shows that degradation products directly promote differentiation of the M2 macrophage phenotype, it remains unknown which factor(s) are responsible for this effect. Similarly, it is unknown which pathway is activated within naïve macrophages, following ECM exposure, driving M2 gene expression. The *in vitro* studies from this chapter were completed using the mouse C<sub>2</sub>C<sub>12</sub> skeletal muscle myoblast cell line and corroborated using human PVSC primary cells. Although no direct comparison between cell types is made, this species difference must be acknowledged. The mitogenic effects of ECM degradation products and polarized macrophages was only examined in PVSCs. Future studies will test the mitogenic effects of these treatment groups against myoblasts. PVSC myogenesis was only tested in response to market weight vs. young ECM, studies are ongoing examining the myogenic effects of polarized and ECM-treated macrophages upon this cell-type. Finally, myoblast fusion and myotube formation was only qualitatively analyzed, future studies will provide quantitative analysis of this phenomenon.

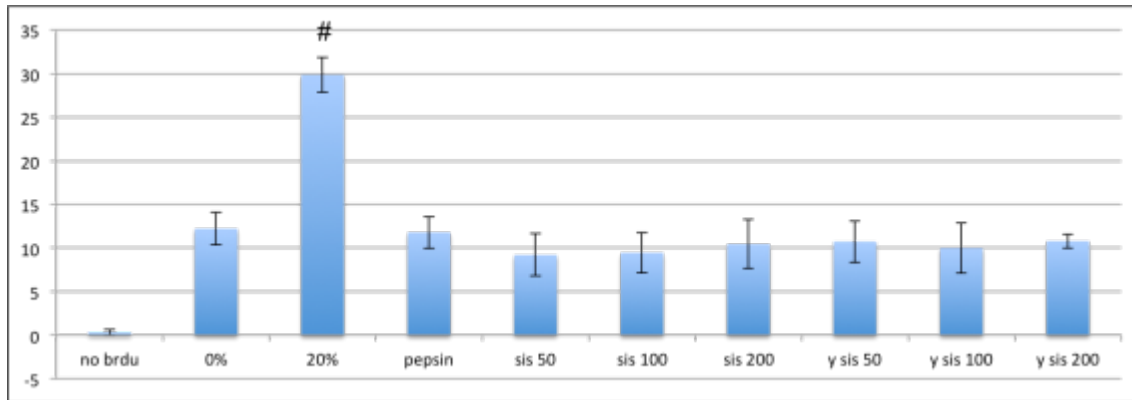


**Figure 19: Degradation Products from ECM are not mitogenic for PVSCs.** Media conditioned with market weight SIS-ECM (SIS) and young SIS-ECM (y SIS) did not induce BrdU incorporation at 50, 100, or 200 ug/ml concentrations (#  $p < 0.05$  when compared to all other groups).

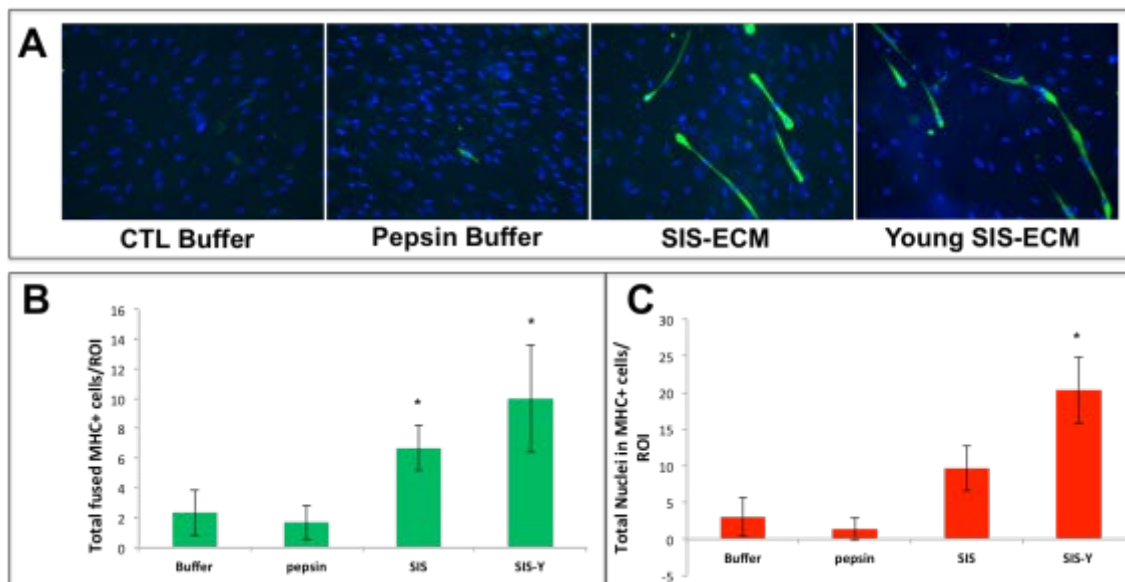


**Figure 20: Degradation products from ECM are myogenic for PVSCs.** PVSCs were cultured in fusion media (low serum), proliferation media (high serum), or proliferation media conditioned with 100 ug/ml market weight SIS-ECM (SIS) and young SIS-ECM (SIS-Y). Cells were then fixed and immunolabeled for sarcomeric myosin heavy chain (MHC) (green) (A). Images were quantified by counting the number of fused MHC cells / region of

interest (ROI) (B), and the number of nuclei in MHC+ cells / ROI (C) (\*  $p < 0.05$  when compared to all other groups).  $n=3$ .

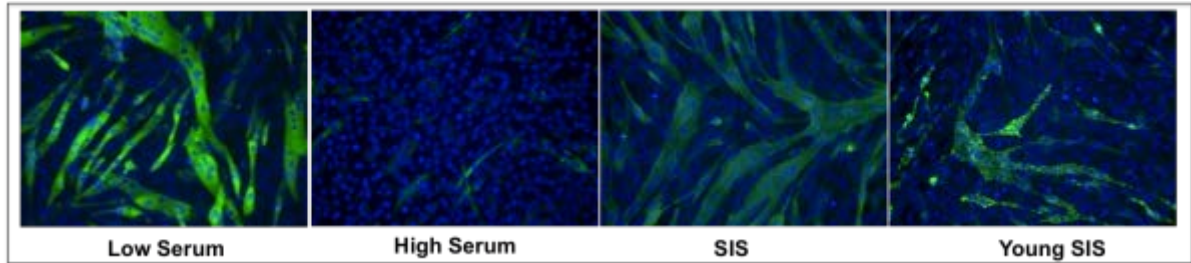


**Figure 21: Degradation products from ECM are myogenic for C2C12 skeletal muscle myoblasts.** Myoblasts were cultured in fusion media (low serum), proliferation media (high serum), or proliferation media conditioned with 100 ug/ml market weight SIS-ECM (SIS) and young SIS-ECM (Young SIS). Cells were then fixed and immunolabeled for sarcomeric myosin heavy chain (green).

## **4.0 ECM MEDIATED CONSTRUCTIVE REMODELING IN A MOUSE MODEL OF VOLUMETRIC MUSCLE LOSS**

### **4.1 BACKGROUND**

Adult skeletal muscle has robust inherent ability to regenerate in response to injury (55, 61, 62). Skeletal muscle damage associated with crush injury or blunt trauma is typically associated with a host response that relies in large part upon the presence and activation of a myogenic stem cell population called satellite cells. Satellite cells possess the ability to exit quiescence, divide, migrate and differentiate into myoblasts and then fuse into multinucleate muscle fibers (313). The regenerative process has been described as occurring in 3 stages: a proliferative phase, the early differentiation stage, and the terminal differentiation stage. Each stage is regulated in part by the temporal expression of well-recognized muscle transcription factors of the basic helix-loop-helix family (314). However, this regenerative response is critically dependent upon the type and severity of muscle insult (313). When skeletal muscle injury is more severe and cannot be compensated via inherent regenerative mechanisms, the resulting irrecoverable loss of tissue is referred to as volumetric muscle loss (VML) (74).

Common causes of VML include military battlefield injuries (315-317), civilian traumatic accidents, tumor ablation, or degenerative disease, and are associated with cosmetic and functional impairment. In the military setting, muscle trauma now accounts for between 50%

and 70% of total war injuries with 80% of the surgical amputations performed on military casualties directly related to this missing tissue (318, 319). Therapeutic options for VML are very limited and include autologous tissue transfer, muscle transposition, or amputation with the implementation of prosthetic devices. These procedures however, have yielded minimal success (67-69) and are associated with extensive donor site morbidity (320, 321). The lack of a reliable and easily reproducible animal model of VML has delayed the development of more effective treatment strategies.

Surgically placed biologic scaffolds composed of naturally occurring extracellular matrix (ECM) have been used to promote the site appropriate constructive remodeling of soft tissue defects within the abdominal wall musculature (21, 202, 203, 206), musculotendinous junction (200), esophagus (194, 278) and heart (322). ECM mediated constructive remodeling has been associated with enhanced functional myogenesis (202), innervation (205) and vascularization (202, 203, 206) within the remodeling scaffold. Therefore, scaffolds composed of ECM may provide a viable therapeutic approach for the clinical treatment of VML.

In the present study, a preclinical rodent model of VML that involved a unilateral excisional defect of the mouse quadriceps muscle was developed and evaluated. After 56 days, histologic examination revealed the defect to be of critical size and healed with dense collagenous scar tissue. Using this model, a bioscaffold-based regenerative medicine approach to VML treatment and the role of polarized macrophages and multipotent perivascular stem cells (PVSC)s in the remodeling process was evaluated.

## **4.2 MATERIALS AND METHODS**

### **4.2.1 Overview of Experimental Design**

Approval was obtained from the University of Pittsburgh Institutional Animal Care and Use Committee. Thirty-two female C57BL/6 mice were randomly assigned into either treated or untreated experimental groups. Both groups were subjected to a muscle defect consisting of unilateral resection of the tensor fascia latae quadriceps muscle. The defects within the treated group were filled with a biologic scaffold composed of porcine derived small intestinal submucosa (SIS)-ECM. Non-resorbable marker sutures were placed at the corners of the defect in both groups and were used to identify the defect margins. The time points for evaluation were 7, 14, 28, and 56 days (n=4 per time point / group). Microscopic analysis included histochemistry and immunolabeling to examine macrophage phenotype, progenitor cell activity, skeletal muscle regeneration, vascularization, and innervation.

### **4.2.2 Scaffold Preparation**

The SIS-ECM material was prepared by decellularization of porcine jejunum using a combination of mechanical and chemical methods as previously described (323). This material was then lyophilized and milled to produce particulate SIS with dimensions of 850 mm<sup>2</sup>, and 250 mm<sup>2</sup>. This particulate SIS was combined in a ratio of 2:1, respectively, and vacuum pressed to form a “powder pillow” construct 25x12.5x3mm. This construct was cut into smaller pillows 4x4x3mm weighing approximately 27.6 ± 04.5 mg to be used as implants. Lyophilized SIS sheets (1 cm<sup>2</sup>) were used to secure the pillows within the defect.

### 4.2.3 Surgical Procedure

Female C57BL/6 mice, age 6-8 weeks, were purchased from Jackson Laboratories (Bar Harbor, ME). Mice were anesthetized and maintained at a surgical plane of anesthesia with 1.5-2.5% isoflurane in oxygen and positioned in ventral recumbency. The surgical site was prepared in sterile fashion using a commercially available hair remover and 70% isopropyl alcohol followed by the placement of sterile drapes. A unilateral longitudinal incision measuring approximately 1.5 cm in length was made in the epidermis, dermis, and fascia to expose the underlying quadriceps compartment (Figure 12A). Following resection of a 4mm x 3mm full thickness segment of the tensor fasciae latae muscle along with a partial resection of the underlying rectus femoris, marker sutures (7-0 prolene, Ethicon Inc.) were placed along the deep corners of the defect and anchored through the rectus femoris muscle (Figure 12B). Sutures were placed to clearly identify the injury and / or implantation site at the time of tissue harvest. In the untreated group the most superficial edge of each defect was also marked by a simple interrupted suture. A minimal amount of suture material was placed only at the defect corners to avoid eliciting a host response to the suture that would obscure the host response to the injury alone. Defects in the treated group were filled with SIS-ECM powder pillows (Figure 12C) and covered by a cubic centimeter of SIS-ECM sheet. The sheet was then sutured to the top edges of the defect in an interrupted fashion similar to the control (Figure 12D). The entire sheet-pillow implant was hydrated using normal saline prior to dermal closure with 7-0 prolene in a continuous pattern. The wound was covered in betadine ointment after closure and assessed for signs of infection for 2 days post-surgery. Each mouse received Buprenex (buprenorphine hydrochloride, 0.25 mg/kg)

for analgesia, and Baytril (enrofloxacin, 20mg) an antibiotic, for three days post-operatively. All animals survived the surgical procedure and their predetermined study period without complications.

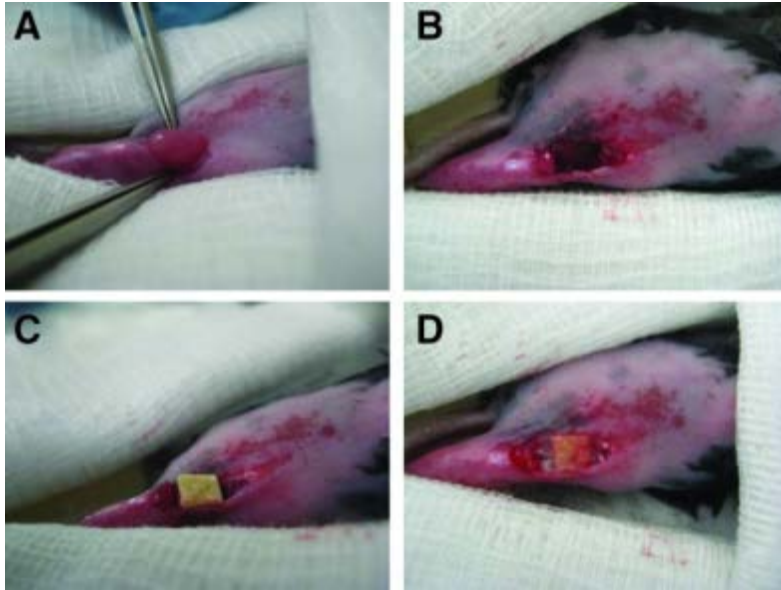


**Figure 22: Induction of VML injury.** The exposed quadriceps muscle compartment after skin incision and blunt dissection of the surrounding fascia (A). Volumetric defect consisting of a 4×3 mm full-thickness resection of the tensor fasciae latae quadriceps muscle (B). Treated defect filled with a size-matched piece of vacuum-pressed SIS-ECM (C). Single-layer SIS-ECM sheet overlay sutured to adjacent native muscle before dermal closure (D). VML, volumetric muscle loss; SIS, small intestinal submucosa; ECM, extracellular matrix.

#### 4.2.4 Specimen Harvest and Histology

Animals were sacrificed at 7, 14, 28, and 56 days. Each mouse was euthanized with 5% isoflurane in oxygen followed by an intracardiac injection of potassium chloride to induce cardiac arrest. The defect site and associated proximal and distal segment of the quadriceps

muscles were isolated and surgically removed. The isolated tissue was either (1) flash frozen in liquid nitrogen cooled 2-methyl butane or (2) fixed in 10% neutral buffered formalin (NBF). Frozen tissues were embedded in OCT compound and cryosectioned into 8- $\mu$ m thick sagittal sections. NBF fixed tissue was embedded in paraffin and cut into 5- $\mu$ m thick sagittal sections. All tissue sections were mounted onto glass slides for histologic staining (i.e: Masson's Trichrome) or for immunolabeling analysis.

#### **4.2.5 Immunolabeling Studies**

Frozen tissue sections were fixed in ice cold 50:50 methanol:acetone for 5 mins at room temperature and washed in PBS. Tissue sections were blocked in blocking buffer (1% (w/v) bovine serum albumin / 2% (v/v) normal horse serum / 0.05% (v/v) Tween-20 / 0.05% (v/v) Triton X-100 in PBS) for 1 hour to reduce non-specific antibody binding. Tissue sections were then incubated in primary antibodies diluted in blocking buffer at 4 °C for 16 hours. The primary antibodies used for the immunolabeling studies were: (1) rabbit polyclonal CD31 (Abcam, Cambridge, MA) or von-Willebrand factor (vWF) on NBF fixed tissues at 1:200 dilution for identification of endothelial cells; (2) rabbit polyclonal Gap-43 (Abcam, Cambridge, MA) on NBF fixed tissues at 1:200 for identification of neurons; (3) monoclonal anti-desmin (Abcam, Cambridge, MA) on frozen fixed tissues at 1:200 dilution for identification of muscle cells; (4) monoclonal anti-iNOS and Fizz1 on NBF fixed tissues for identification of M1 and M2 polarized macrophages respectively; (5) monoclonal anti-CD146 for identification of perivascular stem cells (PVSC). After washing in PBS, tissue sections were incubated in fluorophore conjugated secondary antibodies (Alexa Fluor® donkey anti-mouse or donkey anti-rabbit 488 or 594,

Invitrogen). After washing again with PBS, nuclei were counterstained with DAPI and slides were coated with anti-fade mounting media (Dako).

NBF fixed tissues were deparaffinized with xylene and rehydrated through a graded ethanol series. Heat-mediated antigen retrieval was performed with 0.1 mM EDTA buffer at 95-100 °C for 25 min. After cooling for 15 min, enzyme-mediated antigen retrieval was performed with 0.1% (v/v) trypsin / 0.1% (w/v) calcium chloride digestion at 37 °C for 10 min. After washing in PBS tissue sections were blocked in blocking buffer for 1 hour and incubated in primary antibodies at 4 °C for 16 hours. After additional PBS washing tissue sections were incubated in secondary antibodies for 1 hour at room temperature, followed by DAPI nuclear stain before coverslipping. All tissue sections were imaged using a Zeiss Axio Observer Z1 or Nikon E600 microscope with Nuance multispectral imaging system (CRI Inc, Cambridge MA) with appropriate brightfield and fluorescent filter sets. Quantification of CD31 positive blood vessels was done by immunolabeling and counting the number of blood vessels per 400x field of view (FOV). Three images of each surgical site were quantified by two blinded independent investigators. Only positively labeled cells that were associated with a visible lumen were counted.

#### **4.2.6 Statistical Analysis**

An independent Student's t-test was used to determine the differences in vascularity between SIS-ECM and no treatment at 7, 14, 28, and 56 days post-injury. All statistical analysis used SPSS Statistical Analysis Software (SPSS, IBM, Chicago, IL, USA).

## 4.3 RESULTS

### 4.3.1 Surgical Procedures

All mice recovered from the surgical procedure without complications. The behavior and appetite of all subjects were unchanged following the procedure. No macroscopic abnormalities were noted at the time of removal of skin sutures (10-14 days after the procedure) or throughout the duration of the study.

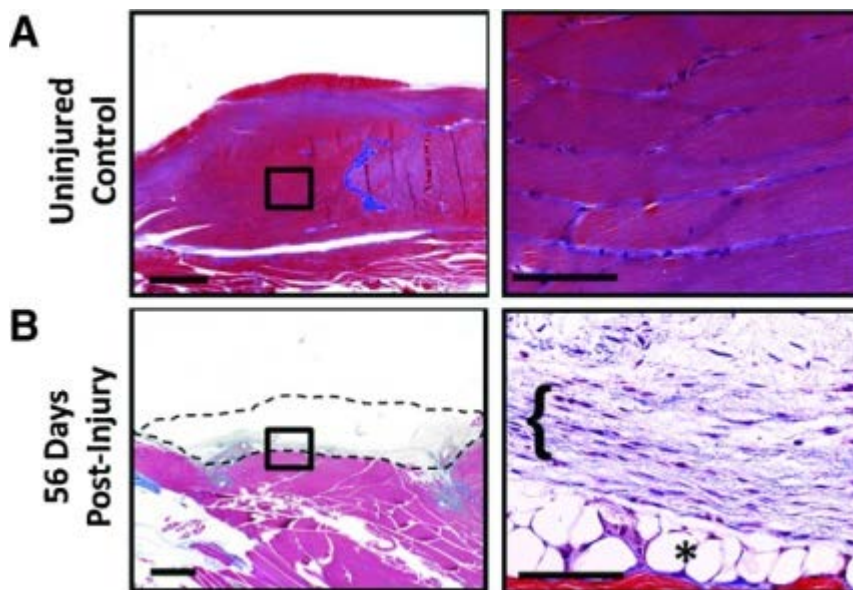


**Figure 23: VML injury is of critical size.** Histological analysis of uninjured (A) and injured (B) muscle at 56 days post-surgery. After 56 days low-power magnification (left panels) reveals an obvious volumetric defect (dotted line). Higher magnification (right panels) shows the defect partially remodeled with a collagenous connective tissue consistent with scar formation ({} and some adipose (\*). No signs of new skeletal muscle formation are seen in untreated injured muscle. The black boxes on the left represent the area of the high-power images on the right (scale bar=1 mm).

## **4.3.2 Macroscopic and Microscopic Findings**

### **4.3.2.1 Control Group**

Mice were allowed to heal for 56 days following surgical excision of a 4mm x 3mm full thickness resection of the tensor fasciae latae and rectus femoris muscles in mouse quadriceps muscle. After 56 days post-surgery the volumetric defect remained and was easily identifiable by histologic methods (Figure 13B, left panel, dotted line). The defect only experienced a mild flattening and associated deposition of a thin layer of disorganized, collagenous scar tissue (Figure 13B, Right Panel). The persistence of a volumetric defect and deposition of collagenous connective tissue was consistent with a critical size defect, irrecoverable by the inherent endogenous regenerative potential of skeletal muscle. These results show that the VML injury model is of critical size and does not spontaneously heal.

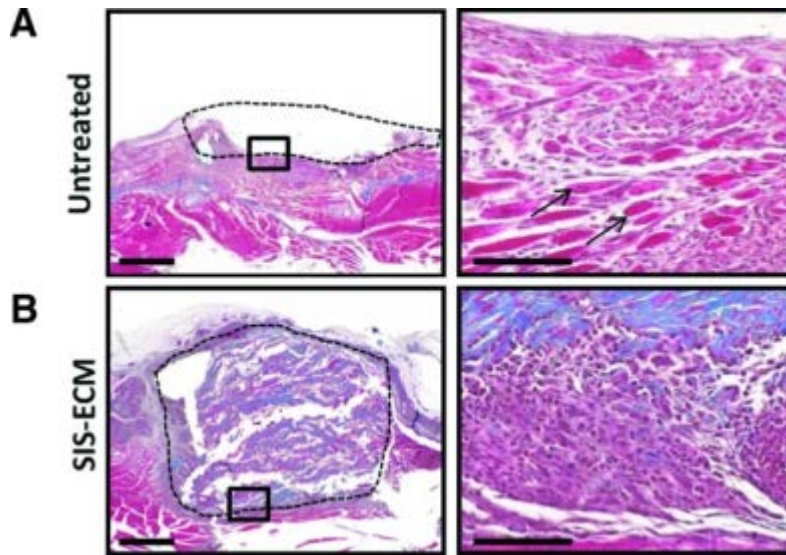


**Figure 24: Defect site at 7 days post-surgery.** Low magnification (left panels) shows the defect site (dotted lines). Untreated defects (A) show a VML injury characterized by necrotic skeletal muscles (arrows), while treated defects (B) are filled with the SIS-ECM scaffold. High magnification (right panels) shows a robust mononuclear cell infiltrate in both untreated and treated defects. The black boxes on the left represent the area of the high magnification images on the right (scale bar=1 mm).

The host response to untreated VML defects showed necrosis of skeletal muscle immediately surrounding the defect margins after 7 days (Figure 14A, arrows). Neutrophils and mononuclear cells were present within the wound site at day 7. New blood vessels were present at day 7 and persisted through 28 days post-surgery (Figure 19A & C). CD146+ Multipotent perivascular stem cells (PVSC) remained in their normal anatomic location, around vWF+ vasculature after 7 days (Figure 17). Gap-43+ nerve fibers were also observed around the defect margins at the interface with native muscle from days 7-28 post-surgery but did not extend into the defect site itself (Figure 20A). By day 14, the defect site became partially filled with granulation tissue and the cells populating the defect site were predominantly mononuclear in morphology (Figure 15A). This mononuclear cell infiltrate was characterized by the predominant

expression of the pro-inflammatory M1 marker iNOS (Figure 16). After 14 days, CD146+ PVSCs remained in their normal anatomic location. By day 28 the cell population showed a marked decrease in number and host derived neomatrix could be identified along the margins of the defect site (Figure 18A). After 56 days the untreated defects were characterized by dense partially organized connective tissue consistent with scar tissue formation within the injury site (Figure 13B,Right Panel).

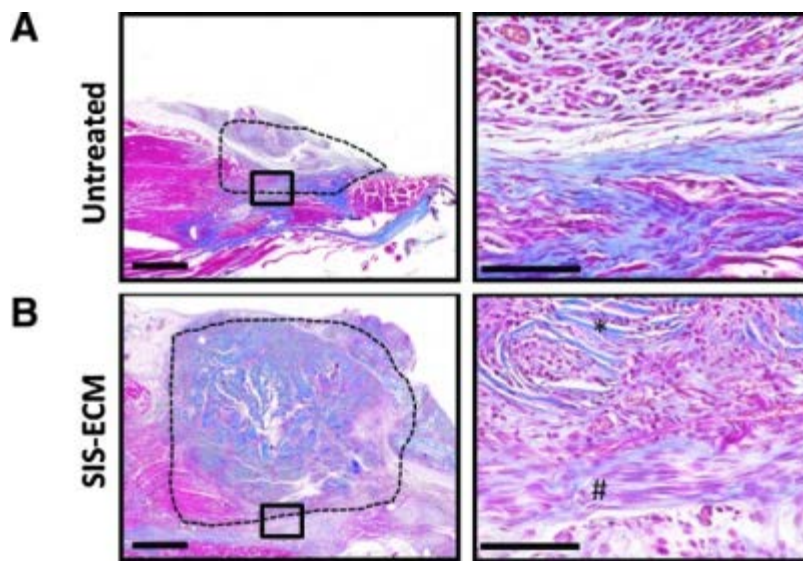


**Figure 25: Defect site at 14 days post-surgery.** Low magnification (left panels) shows the defect site (dotted lines). Untreated defects are filling with granulation tissue, while the ECM scaffold is becoming infiltrated with cells. The black boxes on the left represent the area of the high magnification images on the right. (#, host derived neomatrix; \*, scaffold) (scale bar=1 mm).

#### 4.3.2.2 SIS-ECM Treated Group

The host response to VML defects treated with an SIS-ECM scaffold was characterized by a dense infiltration of both neutrophils and mononuclear cells that surrounded the defect site and populated the outer edges of the scaffold at 7 days post-surgery, similar to untreated control

groups (Figure 14B). CD146+ PVSCs were found in their normal anatomic location (Figure 17) Angiogenesis was prominent at day 7 and remained a feature of the ECM treated defect throughout the 56 day study period (Figure 19B) Nerve fibers were present within the remodeling scaffold after 7 days and for the duration of the study period (Figure 20B). After 14 days a uniformly distributed population of mononuclear cells populated the majority of the ECM scaffold (Figure 15B). Unlike untreated defects, this cell infiltrate was characterized as predominantly M2 macrophages by the expression of Fizz1 (Figure 16). In further contrast to the untreated group, CD146+ PVSCs were identified outside their normal anatomic location (Figure 17), suggesting that they participate in the remodeling of the ECM scaffold. Host derived neomatrix was intermingled with remnants of the ECM scaffold within the defect site. After 28 days, the majority of the ECM implant was cellularized, with the exception of a few areas within the center of the scaffold (Figure 18A). Abundant neomatrix along with native skeletal muscle ingrowth could be identified along the scaffold margins. At 56 days post-surgery, the ECM scaffold was almost completely cellularized (Figure 21A), showed islands of desmin+ cells along the interface with the underlying native muscle (Figure 21B, Left Panel) and was populated by islands of desmin+ striated skeletal muscle cells throughout (Figure 21B, Right Panel).

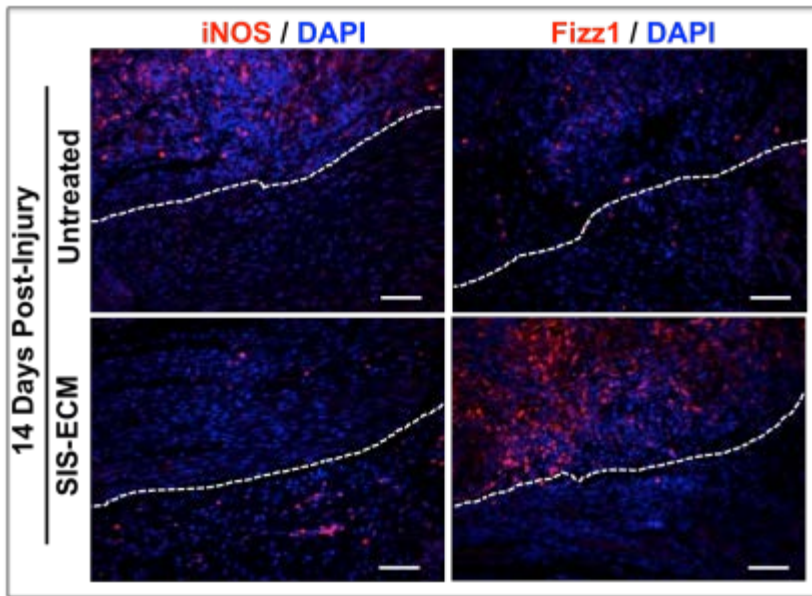


**Figure 26: Macrophage Phenotype.** After 14 days, untreated VML defects are associated with a predominant M1 macrophage phenotype (iNOS staining), while ECM scaffold treated VML defects are associated predominantly with M2 constructive macrophages (Fizz1 staining).

#### 4.4 DISCUSSION AND CONCLUSIONS

The present chapter describes a murine model of volumetric skeletal muscle injury that does not spontaneously heal. In addition, the findings of the present study showed that implantation of a biologic scaffold composed of extracellular matrix at the site of injury alters the default wound healing response from scar tissue deposition toward constructive remodeling, including the presence of new innervated and vascularized skeletal muscle.

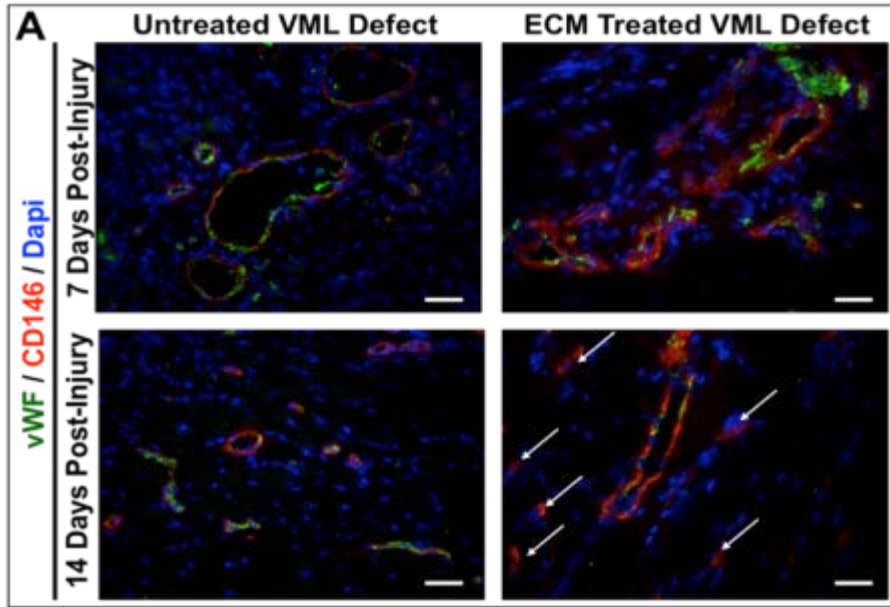


**Figure 27. Perivascular Stem Cell Activation.** After 14 days, without ECM intervention, CD146+ PVSCs remain in their normal anatomic location (B, top panels). In contrast, SIS-ECM treated defects are populated with vessel-unassociated PVSCs outside their normal anatomic location (B, bottom panels, arrows), suggesting that they participate in the remodeling of the ECM scaffold.

Skeletal muscle has a robust capacity for regeneration following injury. The accepted paradigm of skeletal muscle regeneration is that quiescent satellite cells located beneath the basement membrane become activated and differentiate into new myotubes (60, 324-328). However, although debated, it is increasingly being recognized that there are additional progenitor cell populations that have the ability to form new muscle tissue (121, 329-332). Common rodent models used to experimentally induce skeletal muscle injury include cardiotoxin injection (333), freezing (257, 334), and eccentric contraction-induced injury (335, 336) among others. Although these skeletal muscle injury models induce a significant amount of localized injury acutely, the tissue is typically able to be restored to native structure and function by the

inherent regenerative capacity of skeletal muscle. Therefore, these canonical skeletal muscle injury models would be ineffective in studying potential VML therapies because of this spontaneous recovery. The present study describes a critical size volumetric muscle defect within an extremity, specifically within the quadriceps muscle compartment.

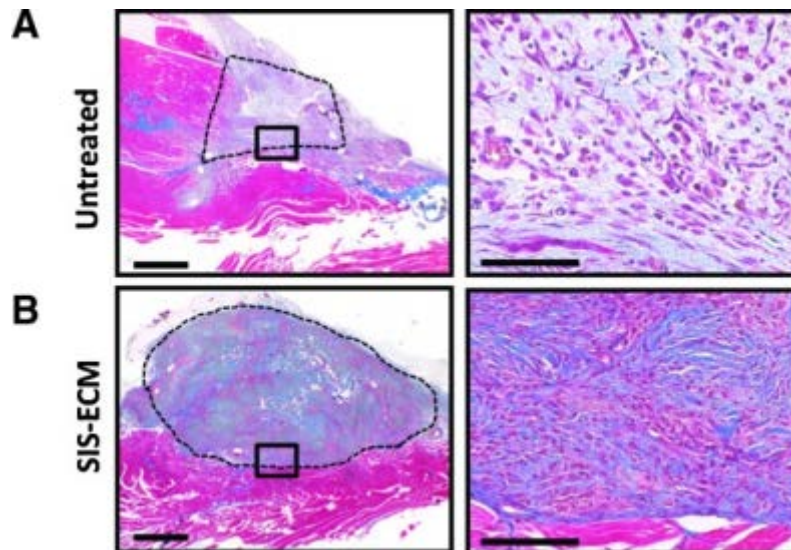


**Figure 28. Defect site at 28 days post-surgery.** Low magnification (left panels) shows the defect site (dotted lines). High magnification (right panels) shows predominantly spindle-shaped cells populating the untreated defect site (A), while treated defects are comprised of cells with varying morphologies (B). The black boxes on the left represent the area of the high-magnification images on the right (scale bar=1 mm).

There are very limited therapeutic options for massive and overt loss of skeletal muscle tissue subsequent to trauma. Autologous muscle grafts or muscle transposition represent possible salvage procedures for restoration of absent muscle tissue but these approaches have limited success and are plagued by the associated morbidity at the donor site. Cell based therapies are in their infancy and to date have been focused largely upon hereditary muscle disease such as Duchenne Muscular Dystrophy. There is an unequivocal need for regenerative medicine

strategies that can enhance the innate regenerative ability of skeletal muscle following traumatic injury and/or induce de novo formation of functional muscle tissue due to congenital absence of such tissue. Development of a therapy that avoids the collection, isolation and/or expansion and purification of autologous stem cells with subsequent re-introduction to the patient would almost certainly reduce the regulatory hurdles for clinical translation, reduce the cost of treatment, and avoid the risks associated with cell-based approaches.

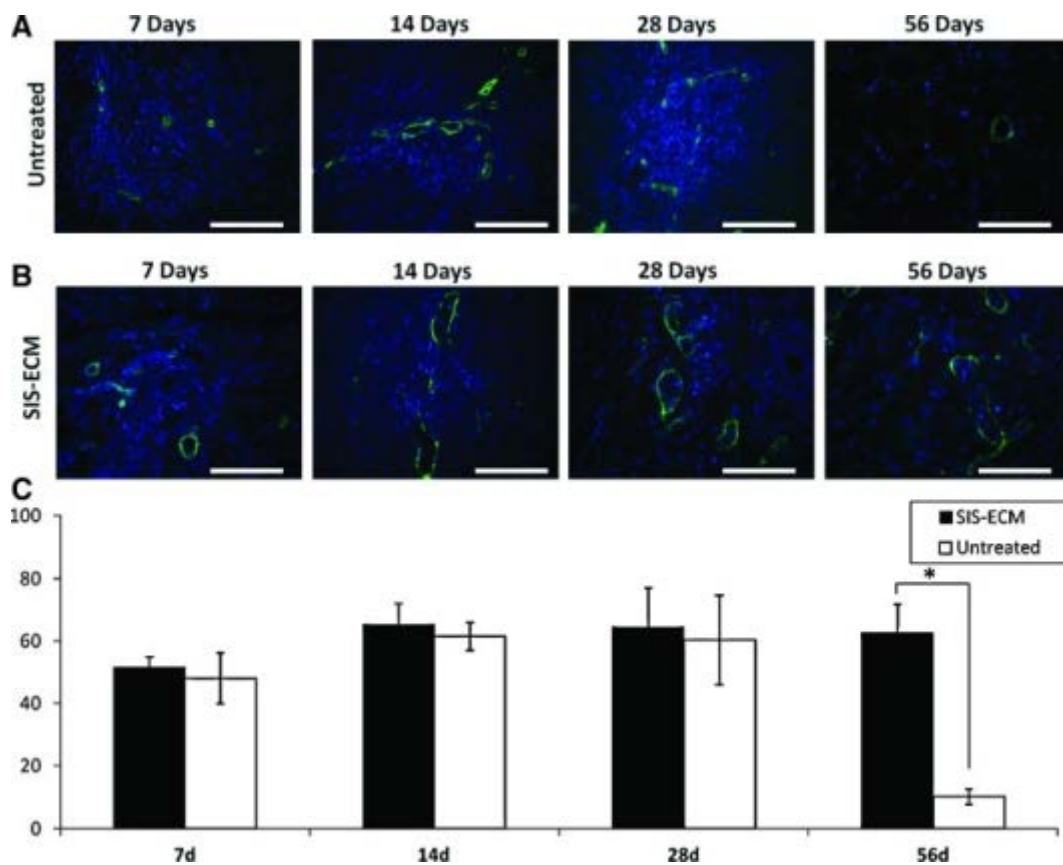


**Figure 29. Vascularity of treated versus untreated VML defects.** CD31 staining (green) of endothelial cells at 7, 14, 28, and 56 days after VML in untreated defects (A) or defects treated with an SIS-ECM scaffold (B). CD31 immunopositive blood vessels were counted per 400 $\times$  field of view (C). Three fields per surgical site were examined at the interface with underlying host tissue (\* $p$ <0.01) (scale bar=1 mm). (Error bars=standard deviation).

Surgically placed biologic scaffolds composed of naturally occurring ECM have been used previously in pre-clinical studies to promote constructive remodeling of soft tissue defects (200, 337). Although such studies have not evaluated the ability of ECM scaffolds to promote constructive remodeling of volumetric muscle injuries, implantation of an ECM scaffold at a site of muscular injury resulted in deposition of site appropriate, functional muscle within 6 months post-implantation (202). The mechanisms underlying this process are not well understood, however rapid angiogenesis, degradation of the ECM scaffold, recruitment of differentiated and progenitor cells, and local modulation of the immune response are all logical and plausible factors that contribute to ECM-mediated remodeling of muscular tissue (205, 294, 337, 338).

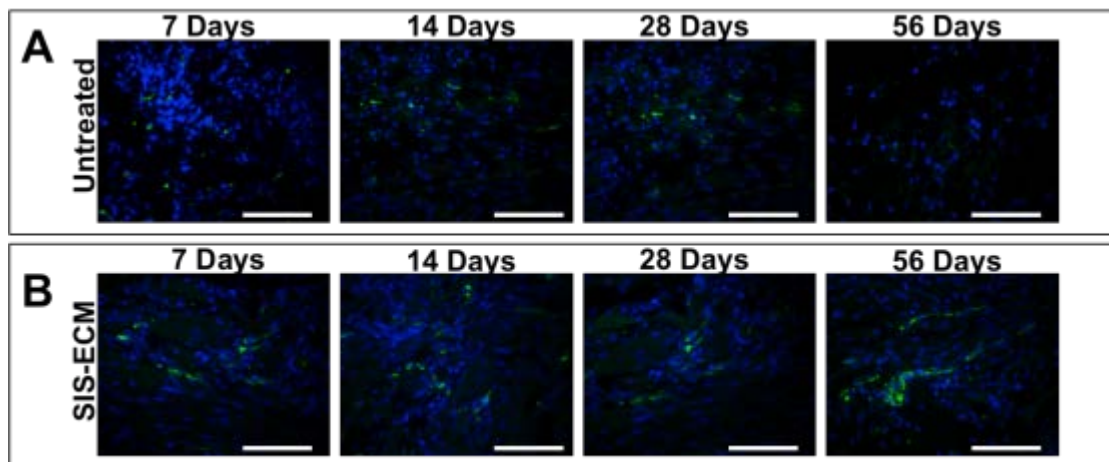


**Figure 30. Evidence of innervation within treated versus untreated VML defects.** Representative images of Gap-43+ (green) neurons at 7, 14, 28, and 56 days after VML in untreated defects (A) or defects treated with an SIS-ECM scaffold (B) (scale bar=1 mm).

Previous studies have shown that cells which accumulate at a site of ECM implantation include macrophages (21, 22), multipotential stem/progenitor cells (5, 7), endothelial cells (186, 339), nerves (205), and muscle cells (202). The temporal appearance of these cell phenotypes is likely dependent upon anatomic site (294), microenvironmental niche factors (160), and epigenetic factors such as mechanical forces (295). Degradation products of ECM scaffolds have been shown to include chemotactic factors for myogenic progenitor cells (5, 11, 33). Thus it is possible that a subset of the dense mononuclear cells includes progenitor cells with myogenic potential. Future studies will further investigate the spatial and temporal pattern of accumulation of various myogenic progenitor cells following implantation of an ECM scaffold at a site of volumetric muscular injury.

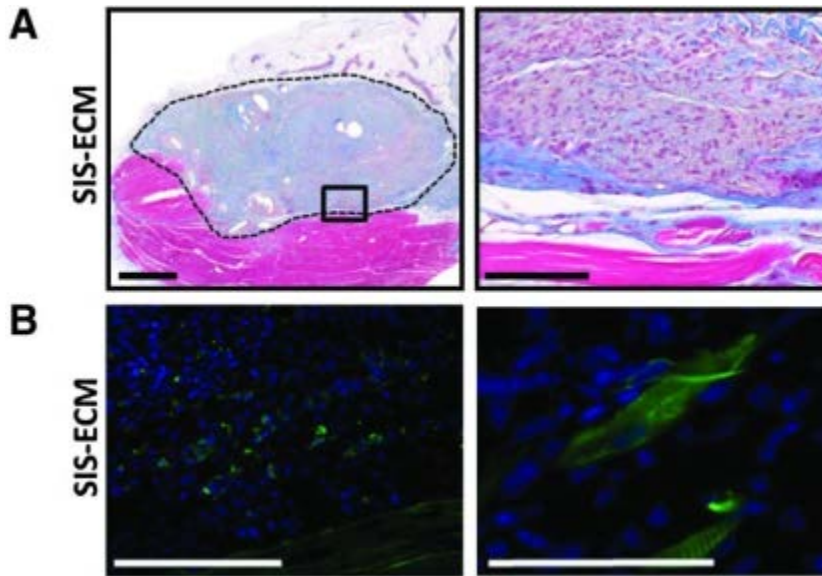


**Figure 31. Site-appropriate remodeling by ECM scaffolds.** Defect sites treated with SIS-ECM (dotted line) maintain robust high cellularity after 56 days (A). Immunolabeling shows desmin+ cells (green staining) populating the area of ECM implantation along the interface of the underlying native muscle [(B), left panel]. Desmin+-striated skeletal muscle cells were also observed throughout the SIS-ECM scaffold [(B), right panel]. The black box on the left represents the area of the high magnification image on the right.

Site appropriate and constructive remodeling following a traumatic VML injury would intuitively be associated with a robust cellular response including prolonged angiogenesis and neurogenesis. The present study shows that following injury, ECM treated and untreated VML defects are both characterized by a robust mononuclear response consisting of many different cell types including endothelial and nerve cells at 7 – 28 days post-injury. However, these treated vs. untreated injury responses are dissimilar at 56 days post-injury. After 56 days the ECM treated defects continue to show angiogenesis, the presence of nerves, and a diffuse cellular infiltrate that includes desmin+ striated skeletal muscle cells. In contrast, at 56 days post-injury, untreated defects show a response consistent with default wound healing and scar formation

including a decreased cellular infiltrate and no signs of angiogenesis, innervation, or skeletal muscle. This murine model represents a useful tool for studying potential VML therapies.

In conclusion, the present chapter describes a model of volumetric muscle injury that does not spontaneously heal. The placement of an ECM scaffold at the site of injury results in a significant deviation from the default response of scar tissue deposition toward a more constructive remodeling outcome including the formation of desmin<sup>+</sup> islands of muscle within the ECM construct. Although the mechanisms underlying this process are not yet fully understood, the development of a murine model allows for a more sophisticated and in-depth investigation of potential mechanisms by which ECM scaffolds promote constructive remodeling.

#### **4.5 LIMITATIONS AND FUTURE DIRECTIONS**

The present chapter developed a mouse model of VML and evaluated a bio-scaffold based regenerative medicine approach for site-specific tissue replacement. However, there are limitations that must be noted in the interpretation of the data. First, the results represent remodeling outcomes up to 56 days post-injury. Although desmin<sup>+</sup> striated skeletal muscle cells were populating the scaffold implantation site, future studies of longer duration will prove if these cells have the capability to fuse and span the length of the defect. Secondly, the present study uses iNOS and Fizz immunolabeling to identify and distinguish between M1 and M2 macrophages respectively. Because macrophage phenotypes evolve along a spectrum of differentiation, more than a single M1 vs. M2 marker is desirable for effective identification of phenotype. Therefore, although iNOS and Fizz are strong indicators of M1 vs. M2 macrophages,

future studies will corroborate these findings with other markers of macrophage as well as pan macrophages. The present study is lacking functional testing. Future studies examining the extent of functional recovery after a longer study period are warranted and in progress. Finally, the study shows perivascular stem cells (PVSC) found outside their normal perivascular niche and participating in the remodeling of the ECM scaffold. Although this phenomenon correlates with downstream islands of desmin<sup>+</sup> skeletal muscle cells, future studies employing transgenic technologies and lineage tracing are necessary to determine if the PVSCs give rise to the de novo skeletal muscle cells.

## **5.0 CLINICAL TRANSLATION OF EXTRACELLULAR MATRIX BIOSCAFFOLDS**

### **5.1 BACKGROUND**

Skeletal muscle accounts for more than 40% of the body's mass (54, 340) and, unlike most other tissues in the adult mammal, possesses the inherent ability to regenerate following injury (53, 55, 341-344). However, the regenerative response fails when a large volume of muscle is lost as a result of trauma; i.e., volumetric muscle loss (VML) (74), and the default outcome is scar tissue formation (10-14). Treatment options for VML are limited and include scar tissue debridement and/or muscle transposition, both of which are typically associated with morbidity and unfavorable outcomes (67, 320, 321, 345, 346).

Skeletal muscle regeneration relies in large part upon the activation, proliferation, migration and differentiation of the canonical muscle stem cell, termed the satellite cell, within a conducive and permissive microenvironmental niche (55, 60-62, 313, 347). Other stem/progenitor cell populations, such as perivascular stem cells (PVSC; CD146+, NG2+) have been shown to play important roles in skeletal muscle regeneration (33, 100, 348-351). The response of skeletal muscle to injury is critically dependent upon the innate immune response; particularly the recruitment, accumulation, activation, and temporal polarization of macrophages (i.e., M1/ M2 phenotype) (57, 352). Finally, the extracellular matrix (ECM) of all tissues largely defines the microenvironmental niche and modulates the migration, behavior, and phenotype of resident

cells during development, homeostasis, and in response to injury (161, 353-355). While most strategies to address the loss of muscle mass have been cell-centric, the present study describes an acellular approach that is based upon use of an ECM biologic scaffold to provide a supportive microenvironmental niche that influences endogenous cell behavior at the site of interest.

Surgical placement of acellular biologic scaffold materials composed of mammalian ECM promotes a constructive, functional skeletal muscle response following experimentally-induced skeletal muscle injury in small (21, 179, 181, 182, 202, 210, 356-358) and large (200, 204) animal models. There is also an anecdotal report of the use of an ECM bioscaffold in a human patient following extremity trauma with VML (201). This ECM-mediated response occurs by mechanisms thought to include the recruitment of stem/progenitor cells via the formation of chemotactic cryptic peptides (5, 7, 8, 10, 186, 359) and modulation of macrophage phenotype (21, 22, 24, 29, 222, 338).

Herein, we report the use of a recently described rodent model of VML to evaluate the effect of an ECM biologic scaffold upon the healing response (357). Results show the presence of PVSC both surrounding neovasculature and spatially distinct from vascular structures during the process of ECM scaffold remodeling, and the associated *de novo* formation of skeletal muscle fibers. In a parallel human clinical study, five patients suffering from extremity VML were treated with an ECM biologic scaffold and showed not only a similar presence and distribution of PVSCs with associated *de novo* formation of skeletal muscle as observed in the rodent model, but also a functional improvement in three of the five patients.

## **5.2 MATERIALS AND METHODS**

### **5.2.1 Mouse Model of Volumetric Muscle Loss**

Experimental design, scaffold preparation, surgical procedure, and tissue harvest were performed as previously described (357). Briefly, approval was obtained from the University of Pittsburgh Institutional Animal Care and Use Committee. Twenty-four female C57BL/6 mice were randomly assigned into either treated or untreated experimental groups. Both groups were subjected to a muscle defect consisting of unilateral resection of the tensor fascia latae quadriceps muscle. The VML defect accounts for a loss of approximately 90% of the fascia latae and 60% of the rectus femoris. In total, the defect represents a volumetric loss of approximately 75% of the quadriceps skeletal muscle compartment. This 75% loss is analogous to the VML injuries treated in the translational portion of the present manuscript. The defects within the treated group were filled with a biologic scaffold composed of ECM. Non-resorbable marker sutures were placed at the corners of the defect in both groups and were used to identify the defect margins. The time points for evaluation were 7, 14, and 56-72 days (n=4 per time point / group). Microscopic analysis included histochemistry and immunolabeling to examine PVSCs and skeletal muscle tissue.

### **5.2.2 Patient Selection and Screening Examination**

A minimum of 6 months from time of injury and age between 18-70 years were inclusion criteria for experimental surgical intervention with the ECM scaffold approach. In addition, a minimum of 25% loss of muscle mass as determined by MRI or CT and a documented minimum loss of

25% function, compared to the contralateral muscle group, were required. Innervation to existing musculature within the injured compartment was considered to be necessary for a positive outcome and was confirmed prior to surgical procedure based upon electromyography (EMG) testing. Exclusion criteria included open wounds or active infection at the site of injury, bleeding disorders, medical comorbidities that would impair wound healing, and inability to comply with physical therapy. Informed consent was obtained after the nature and possible consequences of the study were explained. The criteria for patient selection are summarized in Table 3.

**Table 3: Patient exclusion and inclusion criteria.** Patients were screened against a priori established exclusion and inclusion criteria.

<b>Exclusion Criteria</b>	<b>Inclusion Criteria</b>
Inability to provide informed consent	Age: 18 to 60 years and able to provide informed consent
Poor nutrition	Subjects: military & civilian
Cancer diagnosis within last 12 months	Time since injury: within last 18 months. Target of 18 months or less but subject's may be enrolled with injury outside this range if the PI determines there is viable muscle in the injured compartment by clinical exam and imaging studies.
Complete muscle/tendon gaps greater than 5 cm	Structural deficit: 25% (of muscle mass)
Infection	Functional Deficit: 25%
Known coagulopathy	Injuries may encompass a single muscle belly or compartment. Whether an area is expected to be repaired by sutures will be determined from imaging studies and physical examination.
Diagnosis of schizophrenia or bipolar disorder	Eligible for study procedures 3 months post injury
Chronic disease such as congestive heart failure, liver disease, renal disease, or diabetes	Willing and able to comply with follow up exams, radiographic studies, physical therapy, muscle biopsy and lab tests.
Active and unstable disease state or infection anywhere in the body per MD's evaluation and determination	
Pregnancy	
Hypersensitivity to bovine serum or porcine products	

### 5.2.3 Physical Therapy Screening

The screening evaluation included a clinical examination performed by a licensed physical therapist. A medical history was obtained and the subject goals for participation in the study were documented. The greatest perceived functional limitations were identified. Active and

passive ranges of motion were assessed using a goniometer, and strength of the affected region was assessed using a hand-held dynamometer. Functional assessments were established on a patient-by-patient basis and were aligned with the subject's self-reported greatest deficits and the clinical examination.

#### **5.2.4 Pre-Surgical Physical Therapy**

Functional outcome variables were established *a priori* immediately following completion of the screening visit. Since each subject was unique in their clinical presentation, outcome variables that isolated tissue and functional deficits across specific joints were identified through a study team consensus. Outcome variables previously shown to be valid and reliable, and when possible aligned with the participants self-reported deficits were selected. This custom-designed pre-surgical rehabilitation protocol lasted 6-8 weeks, and only subjects who reached maximum strength and functional capacity upon completion of the pre-surgical physical therapy program, as determined by the treating physical therapist, proceeded to surgery.

#### **5.2.5 Surgical Procedure**

Procedures were performed under general anesthesia in a tertiary care medical center. Through an open incision, sharp debridement of scar tissue was performed, along with selective tenolysis. The injured muscle compartment was reconstructed with the ECM device (Matristem<sup>TM</sup>, ACell, Inc. Columbia, MD). The scaffold material consisted of 8 layers of urinary bladder ECM laminated by vacuum pressing into a sheet configuration and measuring approximately 4 mm in thickness. The ECM scaffold was implanted within the VML injury site, with maximal surface

contact adjacent to native healthy tissue, and secured under moderate tension with either permanent or slowly absorbing sutures. Range of motion was then evaluated to ensure that the graft was secure. Care was taken to avoid contact of the scaffold with bone, and all empty space was obliterated prior to closure of the surgical site to ensure maximal contact of the scaffold with host soft tissue on all surfaces. Closed suction drains were placed in most cases prior to closure of the subcutis with absorbable sutures.

### **5.2.6 Post-Surgical Physical Therapy**

Physical therapy that mimicked the pre-operative program was initiated within 24-48 hours post-surgery. Pain level, range of motion, strength and functional capacity were evaluated at each visit. Strength measures were assessed with a hand held dynamometer. Targeted exercises were performed within the subject's pain tolerance as early as the first post-operative day with the goal of stimulating muscle contraction and weight bearing across the scaffold implantation site. Subjects were instructed in a home exercise program, which they were encouraged to perform multiple times each day. Physical therapy visits were completed 3 times per week for the first 6 weeks post-surgery. The customized physical therapy program was then adjusted in frequency based upon the patients' functional improvement.

#### **5.2.6.1 Imaging**

The MR imaging protocols included a variety of sequences in sagittal, coronal, and axial planes using T1-weighted spin echo, T2-weighted fast spin echo with or without fat suppression, and short tau inversion recovery (STIR) sequences. The CT imaging protocol included unenhanced axial image acquisition at a slice thickness of 1.25 mm and 2.5 mm with both soft tissue and

bone kernels. The kVp and mA were optimized at 120 and 240, respectively. The images were volumetrically reformatted into coronal and soft tissue planes.

Imaging was reviewed by a musculoskeletal-trained radiologist. Pre-surgical MR imaging was assessed for: degree of loss of normal muscle bulk, muscle signal abnormality including presence or absence of fatty infiltration and denervation edema, integrity of the musculotendinous units (when possible), presence of concomitant fascial injury and characterization of prior post-surgical and/or post-traumatic changes. Pre-surgical CT imaging was assessed for similar features, with characterization of muscular attenuation replacing characterization of muscle signal abnormality. Characterization of the location and appearance of the ECM scaffold as well as a change in volume or appearance of the surrounding musculature was performed on the post-surgical imaging.

### **5.2.7 Tissue Biopsy**

Ultrasound guided needle biopsies were taken from the scaffold implantation site on two separate occasions: 5-8 weeks post-surgery and again at 24-32 weeks post-surgery. The biopsies spanned the full length (i.e., proximal to distal) and width (i.e., medial to lateral) of the scaffold implantation site and ranged in number from 6-9. The specimens were snap frozen with liquid nitrogen and stored at -80°C for subsequent processing.

### **5.2.8 Immunolabeling Studies**

Frozen tissue sections from the rodent study were fixed in ice cold 50:50 methanol: acetone for 5 minutes at room temperature and washed in phosphate buffered saline (PBS). To reduce non-

specific antibody binding, tissue sections were blocked in blocking buffer (1% (w/v) bovine serum albumin / 2% (v/v) normal horse serum / 0.05% (v/v) Tween-20 / 0.05% (v/v) Triton X-100 in PBS) for 1 hour. Tissue sections were then incubated in primary antibodies diluted in blocking buffer with mouse on mouse blocking reagent (Vector Labs, Burlingame, CA) according to manufacturer's protocol at 4°C for 16 hours. The primary antibodies used for the immunolabeling studies were: (1) mouse monoclonal CD146 (Abcam, Cambridge, MA) at a 1:350 dilution for identification of perivascular cells; (2) rabbit polyclonal Neurogenin-2 (NG2, Millipore, Billerica, MA) at a 1:200 dilution for identification of perivascular cells and; (3) monoclonal anti-desmin (Abcam, Cambridge, MA) on frozen fixed tissues at 1:200 dilution for identification of muscle cells. After washing in PBS, tissue sections were incubated in fluorophore conjugated secondary antibodies (Alexa Fluor® donkey anti-mouse 488 or 594 or donkey anti-rabbit 488, Invitrogen). After washing again with PBS, nuclei were counterstained with DAPI and slides were coated with anti-fade mounting media (Dako).

The human tissue biopsy samples were embedded in optimal cutting temperature compound (OCT, Sakura Finetek, Torrance, CA) and snap frozen in liquid nitrogen. Frozen tissue sections (5µm) were fixed in ice cold 50:50 methanol:acetone for 5 minutes at room temperature and washed in PBS.

Tissue sections were blocked in blocking buffer (1% (w/v) bovine serum albumin, 2% (v/v) normal horse serum, 0.05% (v/v) Tween-20 & 0.05% (v/v) Triton X-100 in PBS) for 1 hour. The primary antibodies were applied, diluted in blocking buffer, at 4°C for 16 hours. The primary antibodies used for the immunolabeling studies were: (1) 1:350 mouse monoclonal anti-CD146 (Abcam, Cambridge, MA); (2) 1:200 rabbit polyclonal anti-Neurogenin-2 (NG2; Millipore, Billerica, MA); (3) 1:200 488 conjugated goat polyclonal anti-von Willebrand Factor (vWF)

(USBiological, Salem, MA) and; (4) 1:200 mouse monoclonal anti-desmin (Abcam, Cambridge, MA). After washing in PBS, the secondary antibodies were applied (Alexa Fluor® donkey anti-mouse 488 or 594 or donkey anti-rabbit 488, Invitrogen). After washing again with PBS, nuclei were counterstained with DAPI and slides were coated with anti-fade mounting media (Dako).

Tissue sections were evaluated using a Zeiss Axio-observer Z1 microscope using an x20, 0.4 NA objective with a x1.6 Optovar magnification changer (Carl Zeiss, Thornwood, NY). A minimum of three fields of view from each of the surgical sites or biopsy samples were examined from each preclinical model (n=4) and human patient (n=5) respectively.

**Table 4: Quantification of Histological Findings from the Mouse Model of VML.** Semi-quantitative findings of PVSCs and muscle cells from the preclinical portion of the study.

	Animal Number	7 Days After Injury			14 Days After Injury			56-72 Days After Injury		
		Angiogenesis	CD146+ NG2+ cells independent of vessels	Desmin+ cells present	Angiogenesis	CD146+ NG2+ cells independent of vessels	Desmin+ cells present	Angiogenesis	CD146+ NG2+ cells independent of vessels	Desmin+ cells present
Untreated VML Defects	1	+++	-	-	++	-	-	-	-	-
	2	+++	+	-	+	-	-	-	-	-
	3	++	-	-	+++	+	-	+	+	-
	4	+++	-	-	++	-	-	-	-	-
ECM Treated VML Defects	1	++	+	-	++	+++	-	++	+	+++
	2	+++	-	-	+++	++	-	+++	++	++
	3	+++	-	-	++	+++	-	+++	+	+++
	4	+++	-	-	+++	+++	-	++	+	+++

## 5.3 RESULTS

### 5.3.1 Mouse Model of Volumetric Muscle Loss

A murine model of VML (357) was used to evaluate the spatial and temporal presence of endogenous PVSCs and skeletal muscle cells during the remodeling of biologic scaffolds at the site of skeletal muscle injury (Table above, mouse staining semi-quant). In uninjured skeletal muscle, PVSCs were identified within their native peri-vascular anatomic location around von Willebrand Factor (vWF)<sup>+</sup> capillaries and arterioles. PVSCs remained within their normal vascular-associated niche in both untreated VML defects and those implanted with an ECM biologic scaffold at 7 days post-injury and scaffold implantation (Figure 22A, Top). However, at 14 days post-injury, untreated defects showed vascular-associated PVSCs while defects treated with ECM showed PVSCs outside their normal peri-vascular niche and in the midst of the degrading ECM scaffold material (Figure 22A, Bottom). At 56-72 days post-injury, the untreated VML defects showed scar tissue formation and no sign of new skeletal muscle formation, whereas defects treated with ECM showed the formation of islands of desmin<sup>+</sup> striated skeletal muscle throughout the area of scaffold placement, consistent with an ECM mediated constructive remodeling effect (Figure 22 B).

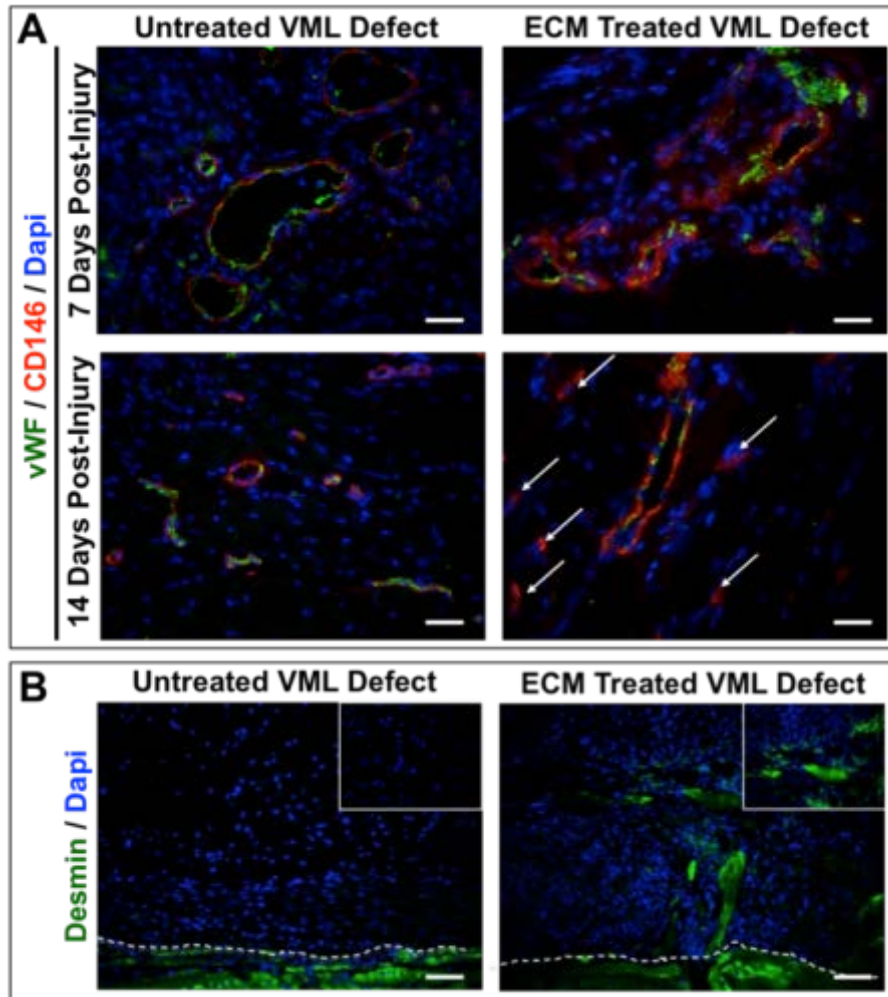


**Figure 32: Progenitor cells are present at the site of constructive remodeling by ECM scaffolds surgically placed within sites of VML injury.** CD146+ PVSCs (red) remained in their normal anatomic location, surrounding vascular structures (von Willebrand Factor (vWF), green) at 7 days post-injury in both untreated and ECM treated defects in a mouse model of VML (A, top panels). After 14 days, untreated VML defects showed perivascular cells maintained their vascular association; conversely, ECM-treated defects were populated with CD146+ PVSCs outside their normal niche (arrows), suggesting that they participate in the remodeling of the ECM scaffold (A, bottom panels). Untreated defects from the mouse model of VML showed no signs of skeletal muscle formation, while ECM scaffold treated defects showed the formation of desmin+ (green) and striated skeletal muscle cells at 56-72 days post-injury (B). ECM treatment showed desmin+ cells near the interface with underlying native muscle (dotted line), as well as throughout the center of the ECM graft (inset). Scale Bar = 50  $\mu$ m.



### 5.3.2 Clinical Cohort Study Design

A clinical trial examining outcomes after reconstruction of VML with ECM was conducted with informed patient consent and approvals from the Institutional Review Board of the University of Pittsburgh and DoD Human Research Protection Office [ClinicalTrials.gov Identifier: NCT01292876]. A schematic of the clinical cohort study design is shown in Figure 23. Briefly, patients were screened against established exclusion & inclusion criteria (Table 3) and those enrolled were first entered into a custom-designed physical therapy program based upon their specific muscle deficit to optimize function. The ability to perform tasks which quantified the function of the injured/missing muscle tissue were tracked during the pre-surgical training period until a plateau was reached and no additional measurable progress could be obtained for a minimum of 2 weeks; i.e., maximum function was reached based upon optimal physical therapy (Figure 23, Blue ramp progression). Imaging studies consisting of MRI or CT scan were conducted in an attempt to quantify the muscle tissue volume deficit relative to the contralateral limb on all patients.

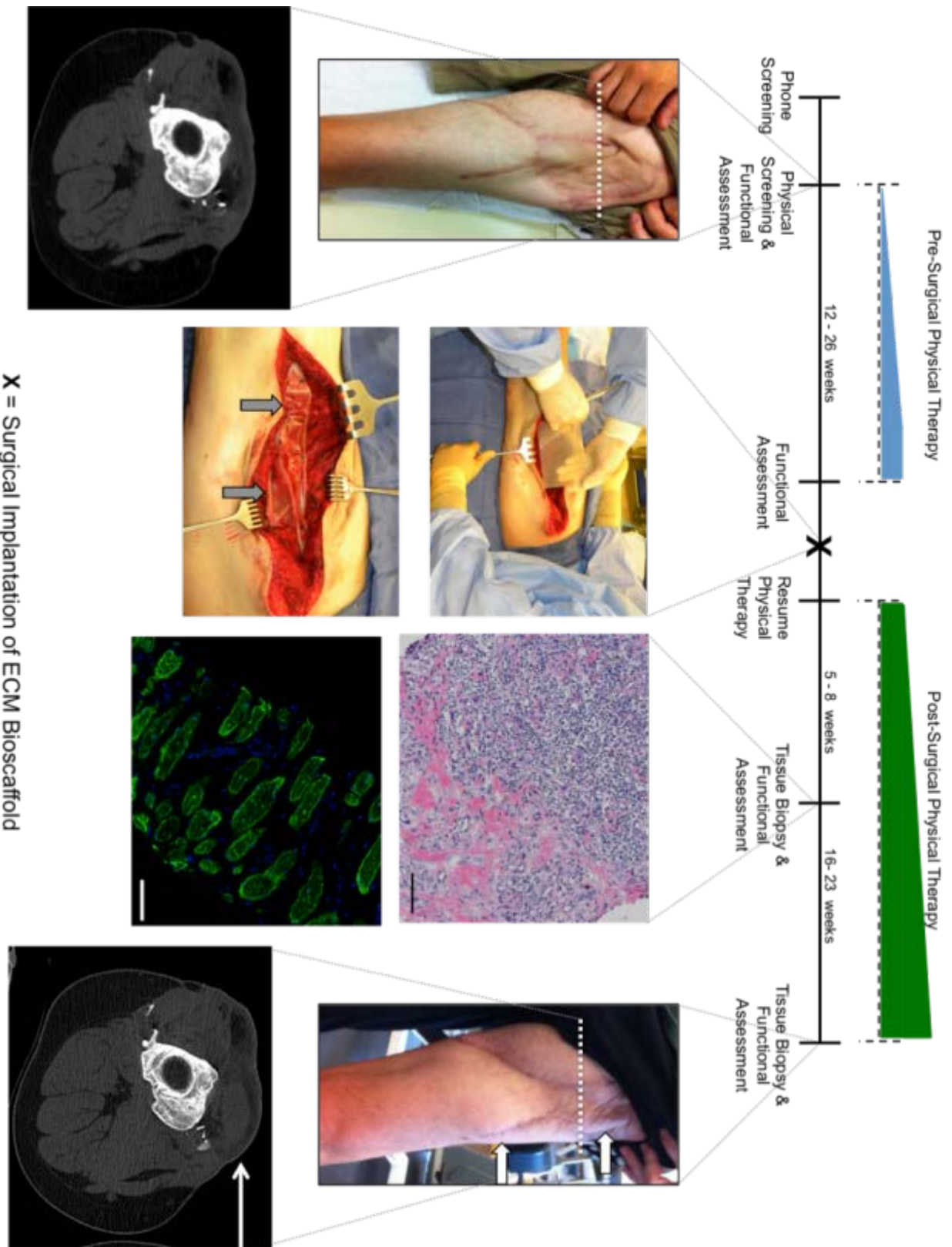


**Figure 33: Schematic of clinical study design.** Potential patients were pre-screened by phone before an initial physical screening and functional assessment. Next, all patients completed a customized pre-surgical physical therapy program that focused specifically upon their individual functional deficits and that was designed to maximize their individual potentials prior to surgical intervention (blue ramp progression). The identification and maximization of functional parameters prior to surgery minimizes the likelihood that any improvement following ECM intervention was solely the result of the physical therapy component of care. Patients then underwent the ECM scaffold surgical placement procedure (grey arrows) and immediately returned to their pre-surgical physical therapy regimen (green ramp progression). Ultrasound guided biopsies taken from the site of scaffold implantation at 5-8 weeks showed robust mononuclear infiltration and the presence of desmin+ (green staining) muscle cells. At 16-23 weeks post-surgery, CT showed dense tissue consistent with skeletal muscle at the surgical site (white arrow) and 3 of 5 patients showed functional improvement.

The surgical procedure involved excision of local scar tissue, identification of adjacent vascularized and innervated muscle tissue, and placement of an acellular biologic scaffold material composed of porcine urinary bladder ECM (Matristem<sup>TM</sup>, ACell, Inc. Columbia, MD) under moderate tension to restore continuity of the injured muscle compartment. Tenolysis was performed if tendon gliding was restricted by scar tissue.

Range of motion, weight bearing of the affected limb, and exercises performed within the subject's pain tolerance were initiated one day post-operatively for all patients. The post-operative rehabilitation program was designed to address the same functional deficits that were identified upon subject inclusion into the study and mimicked the rehabilitation program that was administered pre-operatively (Figure 23, Green ramp progression). Ultrasound-guided biopsy specimens were obtained from the implant site at locations spanning the distance between the proximal and distal borders of interest at both 5-8 weeks post-surgery, and then again at approximately 6 months post-surgery (end of the monitoring period). MRI or CT imaging was repeated at 6 months post-surgery.

**Table 5: Patient information.** Relevant information from each patient included in the present study.

Patient	Sex	Age (years)	Injury Site (Side)	Cause of Injury	Time Since Injury (months)	Previous Surgeries	Tissue Deficit (estimate)	Status
1	M	34	Anterior Tibial Compartment (Left)	Exercise induced	13	5	58%	Military
2	M	37	Anterior Tibial Compartment (Left)	Skiing accident	32	4	67%	Civilian
3	M	28	Quadriceps (Left)	IED blast	18	14	68%	Military
4	M	27	Quadriceps (Right)	IED blast	89	50	83%	Military
5	M	32	Anterior/Lateral Tibial Compartment (Left)	Skiing accident	85	8	90%	Civilian

### 5.3.3 Subjects with Volumetric Muscle Loss

Table 5 describes the characteristics of the first five consecutive subjects enrolled in the clinical study. All subjects were male and at least 6 months removed from the time of injury. In accordance with the established inclusion criterion (Table 3), all subjects exhibited a minimum of 25% functional and structural deficit compared to the contralateral limb. All participants had previously been subjected to multiple surgical procedures and extensive physical therapy, and thus were considered to have exhausted all available standard of care options.

**Table 6: Patient Biopsy Procedure and Findings.** Semi-quantitative findings of PVSCs and muscle cells from the clinical portion of the study.

Patient	1 <sup>st</sup> Biopsy					2 <sup>nd</sup> Biopsy				
	Weeks post surgery	Number of tissue samples collected	Angio-genesis	CD146+ NG2+ cells independent of vessels	Desmin+ cells present	Weeks post surgery	Number of tissue samples collected	Angio-genesis	CD146+ NG2+ cells independent of vessels	Desmin+ cells present
1	5	7	+++	+	-	24	6	+++	+++	++
2	6	6	++	++	-	26	6	++	-	+++
3	6	8	+	+++	++	26	9	+	-	+
4	8	8	+	-	-	32	8	++	+	+++
5	8	5	+++	++	+	27	8	++	+	++

- = Absent
- + = Few isolated cells
- ++ = Moderate number of cells or small clusters
- +++ = Large numbers of cells or large cell clusters

### 5.3.4 Histomorphologic Findings

At 5-8 weeks post-surgical implantation of the ECM scaffold, the histomorphologic characteristics were similar for all 5 patients and showed a mononuclear cell infiltrate of variable density interspersed among fragments of partially degraded ECM scaffold. Neocapillaries and arterioles were present in all specimens (Table 5). Randomly scattered PVSCs were both associated with vWF<sup>+</sup> vascular structures and independent of any vascular structures in all patients except for patient number 4 (Figure 24A, Left). Islands of centrally-nucleated desmin+ cells that were not associated with any vascular structure were present in biopsy specimens from patient numbers 3 & 5 (Figure 24B, Left) but not in biopsy specimens from any of the other patients.

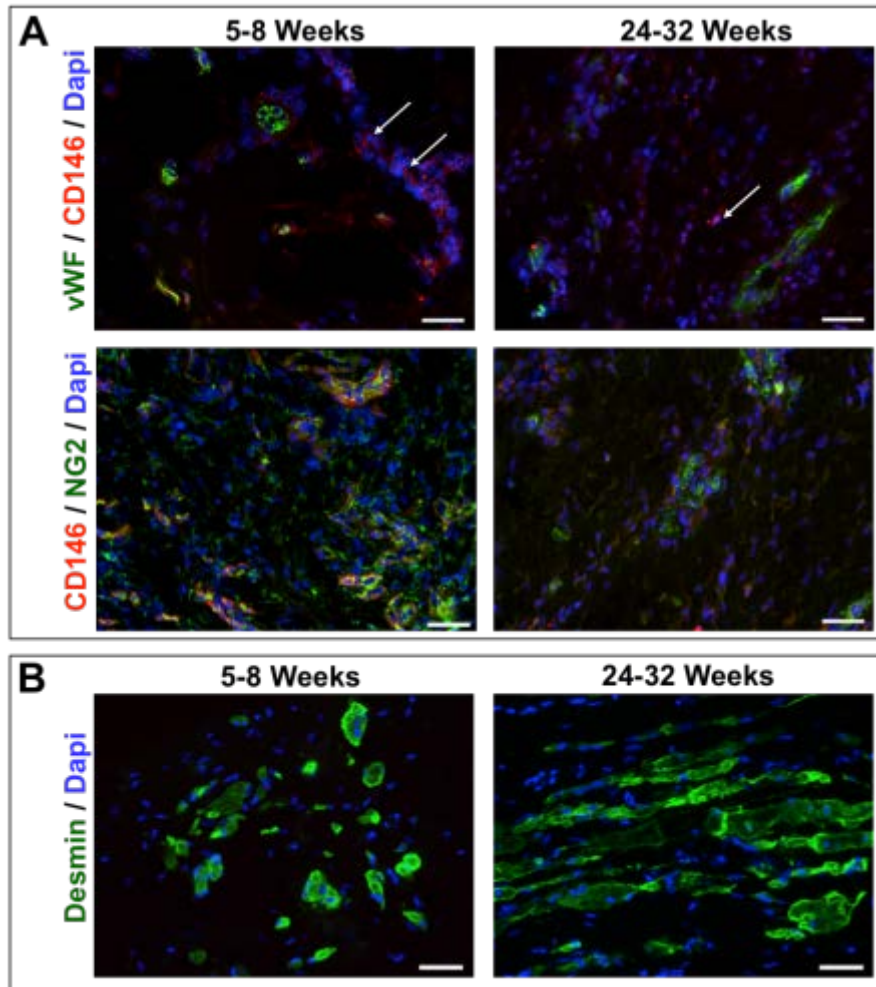


**Figure 34: Constructive tissue remodeling by ECM scaffolds in a human clinical application.** In a human clinical application, CD146+ PVSCs were identified both within and outside of (arrows) their normal perivascular association following representative muscle biopsies from ECM scaffold treated VML defects at both 5-8 and 24-32 weeks post-scaffold implantation (A, top panels). CD146+ cells co-expressed the Neurogenin-2 (NG2) surface marker antigen, identifying them as PVSCs, in human muscle biopsies (A, bottom panels). The identification of PVSCs outside their normal niche suggests that they may participate in the remodeling of ECM scaffolds within human patients, similar to the results of the preclinical study. At both 5-8 and 24-32 weeks post-ECM scaffold treatment, human muscle biopsies from the site of scaffold implantation showed the formation of islands of desmin+ muscle cells (B), similar to the results of the preclinical study. Scale Bar = 50  $\mu$ m.

At 6 months post-surgery, all 5 patients showed similar histologic findings. PVSCs were again identified both associated with vWF<sup>+</sup> vascular structures and independent of any vascular structures (Figure 24A, Right). Desmin<sup>+</sup> cells with central nuclei, indicative of actively regenerating skeletal muscle cells, and new mature skeletal muscle cells were seen in the majority of biopsy samples in all patients either as individual cells or in variably sized clusters of cells (Figure 24B, Right). Areas of mature skeletal muscle cells were present in biopsy samples from patients 2, 4 and 5. Small blood vessels were abundant within the moderately organized connective tissue that represented the original scaffold placement site (Table 5). No recognizable scaffold material was present in any of the biopsy specimens.

### **5.3.5 Pre- & Post-Surgical Imaging**

Initial pre-surgical imaging was performed, and repeated post-surgically at approximately 6 months for each subject. Four of the five subjects were examined using a 1.5 T MRI scanner (Signa HDx, GE Healthcare), whereas one subject was unable to undergo MRI examination as a result of retained shrapnel fragments and indwelling metallic hardware. This subject was examined using a CT scanner (4-slice, LightSpeed, GE Healthcare). The estimated volume of lost muscle ranged from 58% to 90%. Characterization of the location and appearance of the ECM scaffold as well as a change in volume or appearance of the surrounding soft tissue was performed on the post-surgical imaging. When comparing pre- vs. post-scaffold implantation, imaging of the injured limb showed the formation of dense tissue consistent with skeletal muscle at the implantation site at approximately 6 months post-surgery (Figure 25).



**Figure 35: Imaging of affected extremity pre- and post-surgical implantation.** CT images of patient three before and 6 months after surgical placement of an ECM bioscaffold within a site of VML. After 6 months, the site of bioscaffold implantation showed an accumulation of dense tissue consistent with skeletal muscle (arrows).

### 5.3.6 Post-Surgical Function

At 24-28 weeks post-surgery the subjects showed an average increase of approximately 25% and 220% in force production and functional tasks (i.e., activities of daily living), respectively (Figure 26). Three of the five patients showed 20% or greater improvement of strength (range 20%-136%) of the affected limb 6 months after surgery (Figure 27). The two subjects diagnosed with anterior compartment syndrome that were unable to produce any measureable force production before the surgical manipulation, showed no improvement in strength throughout the

duration of the study; yet a third subject with the same diagnosis but who retained some pre-surgical dorsiflexion strength (3.6 lbs as determined by a handheld dynamometer) showed a 33% improvement in strength 6 months post-surgery.

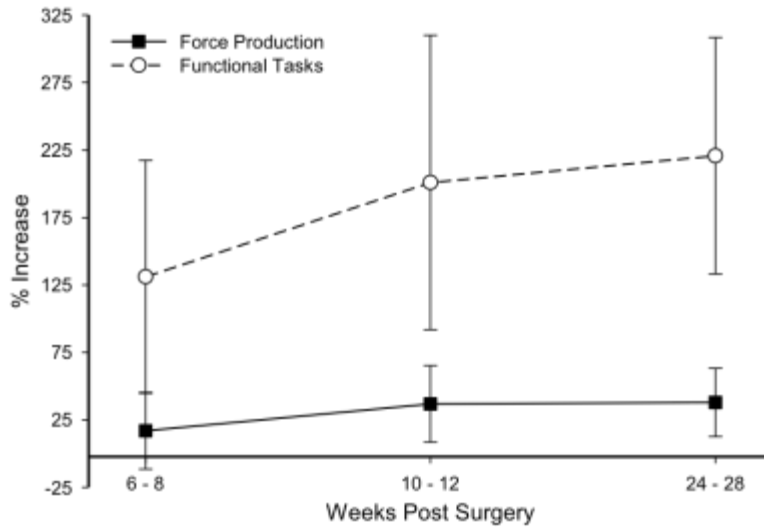
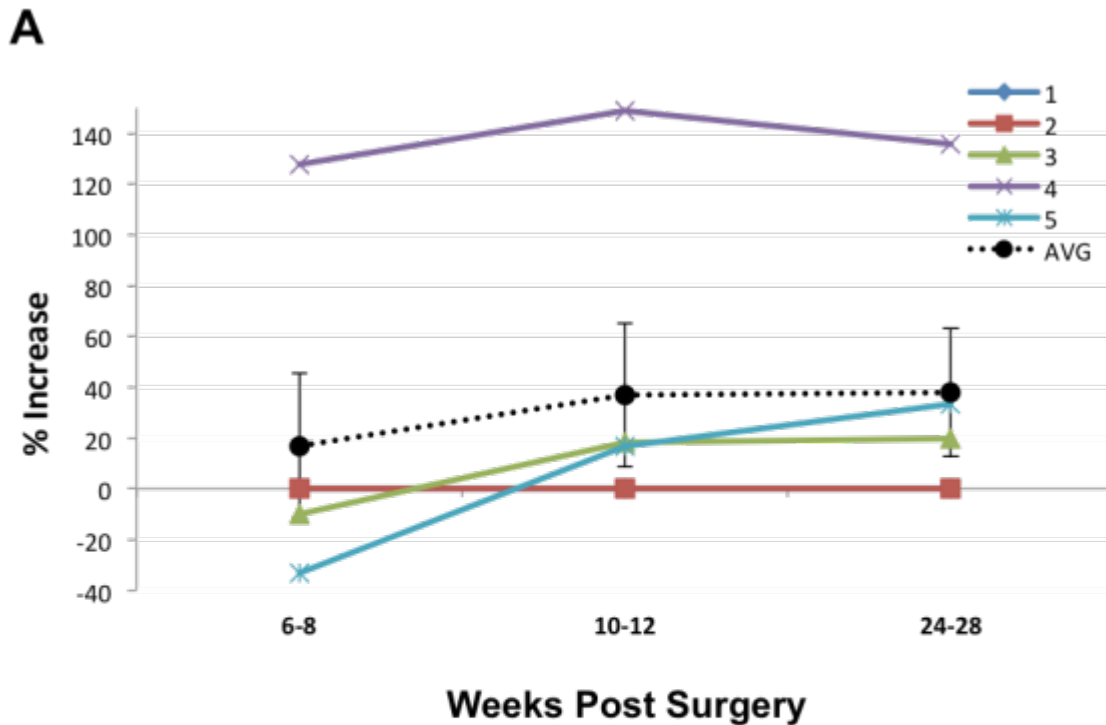


**Figure 36: ECM-mediated constructive remodeling was associated with functional improvements.** Average values of force production (squares) and functional task (circles) measurements from all five patients at 6-8, 10-12, and 24-28 weeks post-scaffold implantation. Force production and function were assessed by dynamometer and task/exercise completion respectively and graphed as percent change from pre-surgical maximum. Average +/- SEM.

Six months after surgery, three of five subjects showed improvement in the functional outcome variables (Figure 7, Supplemental Data). Both individuals receiving ECM transplantation into the quadriceps region showed marked improvements in functional capacity. Subject 3 showed a dramatic improvement (1820%) in Single Hop Test at 6 months after surgery. Subject 4 showed improvements in the Chair Lift Test (324%) and Max Single Leg Squats (417%). Of the individuals receiving ECM transplantation to the anterior compartment,

Subject 1 did not show any functional improvement 6 months after surgery, whereas Subjects 2 and 5 both showed an improvement in balance measures as determined by Single Leg Stance time with eyes closed and the Backward Reach Test (Figure 7, Supplemental Data).



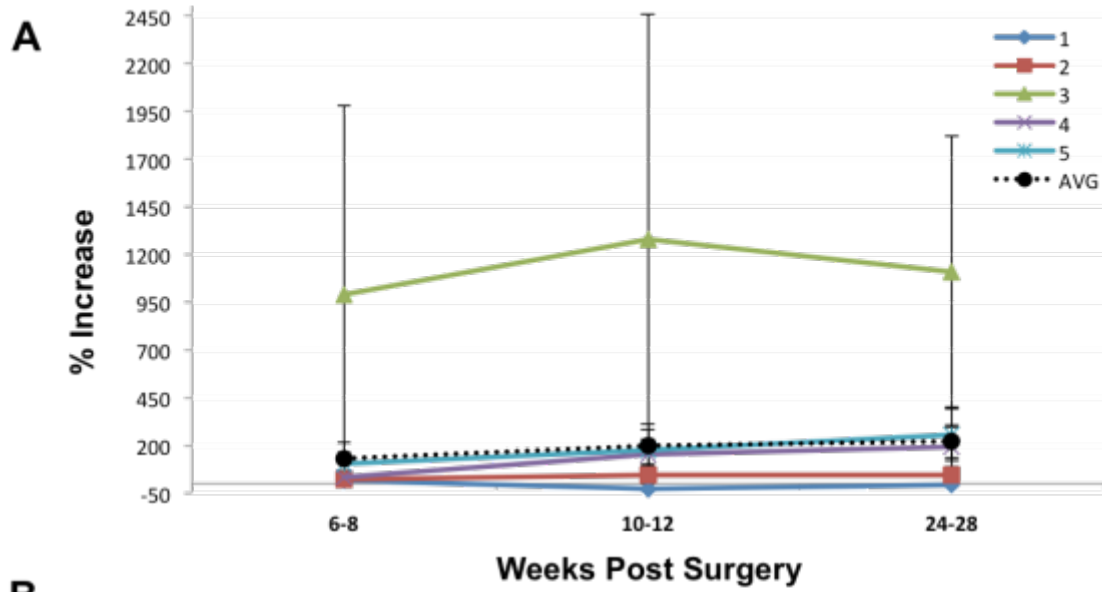
**B**

Patient	Activity	% change from Pre-Surgical Maximum		
		6-8 weeks Post-Surgical	10-12 weeks Post-Surgical	24 -28 weeks Post-Surgical
1	Dorsiflexion	0.0	0.0	0.0
2	Dorsiflexion	0.0	0.0	0.0
3	Knee Extension	-10.0	18.3	20.0
4	Knee Extension	127.9	149.2	136.1
5	Dorsiflexion	-33.3	16.7	33.3

**Figure 37: Force production data from each individual patient.** Strength measures as assessed with a hand held dynamometer from each individual patient and graphed as percent change from pre-surgical maximum (A). Data from each individual patient (B).

## 5.4 DISCUSSION AND CONCLUSIONS

The work described herein shows the remodeling potential of an acellular ECM bioscaffold for restoration of skeletal muscle in both a preclinical rodent model and in patients with VML. The preclinical portion of the study was conducted in an established model of VML (357). The previous study validated the model, showed the excisional defect was of critical size, and examined the presence of myogenic cells after 56 days (1). The present study extends these findings by examining the role of PVSCs and the presence of skeletal muscle cells following injury and ECM implantation after 72 days; and correlates the findings with histomorphologic results from the human study. Implantation of ECM at the site of injury was associated with neovascularization, the mobilization and accumulation of perivascular stem cells, and myogenesis in both the preclinical and clinical studies. Of note, functional improvement surpassing that achieved by physical therapy alone was obtained in 3 of 5 patients.



**B**

Patient	Activity		% change from Pre-Surgical Maximum		
			6-8 weeks Post-Surgical	10-12 weeks Post-Surgical	24 -28 weeks Post-Surgical
1	Single Leg Stance (seconds)	Eyes Open	0.0	0.0	0.0
		Eyes Closed	50.4	-81.2	-6.8
	Get Up & Go (seconds)		-4.0	-2.0	-14.0
2	Single Leg Stance (seconds)	Eyes Open	0.0	0.0	0.0
		Eyes Closed	-20.1	88.7	120.1
	Stork Balance Test (seconds)		33.3	41.7	26.7
	Single Leg Jump Landing (inches)		14.5	18.3	8.5
	Triple Hop Test (inches)		5.1	8.2	6.4
	Functional Reach Test (inches)	Forward	12.0	32.1	56.1
Backward		90.8	108.8	114.1	
3	Single Leg Hop (inches)		1980.0	2460.0	1820.0
	Single Leg Squats (repetitions)		0.0	100.0	400.0
4	Single Leg Hop (inches)		-37.5	25.0	18.8
	Chair Lift Test (repetitions)		84.2	273.7	323.7
	Single Leg Squats (repetitions)		100.0	316.7	416.7
	Triple Hop Test (inches)		-21.2	-8.7	7.7
5	Single Leg Stance (seconds)	Eyes Open	232.1	232.1	232.1
		Eyes Closed	0.0	20.0	85.0
	Stork Balance Test (seconds)		0.0	0.0	180.0
	Single Leg Jump Landing (inches)		400.0	783.3	1050.0
	Triple Hop Test (inches)		49.5	115.4	122.0
	Functional Reach Test (inches)	Forward	12.0	24.0	28.0
Backward		33.3	66.7	83.3	

## = Negative response                      ## = 51 – 75% Increase  
 ## = 0 – 25% Increase                      ## = 76 – 100% Increase  
 ## = 26 – 50% Increase                      ## = ≥101% Increase

**Figure 38: Functional task data from each individual patient.** Functional measures as assessed by task/exercise completion from each individual patient and graphed as percent change from pre-surgical maximum (A) (Average +/- SEM). Data from each individual patient (B).

Most strategies for restoration or *de novo* formation of skeletal muscle tissue are cell centric and typically involve the delivery of exogenous cells to sites of injured or missing tissue (70-73). These cell-based strategies have been largely ineffective for a variety of reasons including immunogenicity of allogeneic cells, inefficient methods of cell delivery, and apoptosis following administration to the site of interest, among others (76, 85). It is now generally accepted that delivered cells most likely exert therapeutic effects via paracrine-mediated mechanisms (137, 138, 140).

The present studies utilize an acellular approach that results in the *de novo* formation of skeletal muscle. ECM implanted bioscaffolds have been shown to provide an inductive niche which facilitates the recruitment and differentiation of endogenous myogenic progenitor cells (5, 7, 200). Directed mobilization of relevant endogenous cell sources obviates the need for exogenous cell administration and removes the associated cell harvesting procedures, regulatory barriers, and any potential cell related immune responses. This translational work shows that ECM scaffolds, when used to treat VML in a manner that entails broad surface contact with adjacent vascularized and innervated muscle, serve as inductive scaffolds that promote remodeling of muscle tissue.

Both the rodent study and the biopsy findings from the five patients showed PVSC's removed from their normal vessel-associated anatomic location, in the midst of partially degraded ECM scaffold material, suggesting that these cells participate in the remodeling of the ECM scaffold. Histologic findings show the appearance of both immature and mature desmin<sup>+</sup>

skeletal muscle cells within the implantation site. The ultrasound-guided biopsies from patients were collected from sites of VML that had been debrided, treated with ECM, and, after 6 months, had formed soft tissue consistent with skeletal muscle as identified by either MRI or CT. In 3 out of 5 subjects, the histologic and imaging findings were concomitant with functional improvement. PVSC's contribute to *de novo* skeletal muscle formation not only during fetal development, but also in adult tissue in response to acute injury (35). Therefore, it is plausible that the PVSC's contribute, either directly through terminal myogenic differentiation or indirectly through paracrine mechanisms, to the formation of skeletal muscle in the present studies. The contribution of alternative sources of precursor cells from the adjacent healthy muscle tissue, and/or resident or circulating mesenchymal stem cells, including satellite cells, cannot be ruled out (76).

PVSCs were originally described following isolation from skeletal muscle tissue, are identified *in vivo* by the expression of the CD146 and NG2 surface marker antigens, and have been shown to be responsive both *in vitro* and *in vivo* to chemotactic cryptic peptides created as a result of ECM degradation (8, 11, 27, 33, 34, 186, 360). The amount of ECM scaffold degradation estimated by morphologic examination in the present studies is consistent with that determined by quantitative <sup>14</sup>C-labelled ECM studies in other anatomic sites (23).

Two aspects of the protocol by which the 5 patients in the present report were treated are of particular note. First, the patients were all well past the acute injury response phase and had been subjected to multiple surgical procedures that included debridement and/or tenolysis as dictated by standard of care. All procedures in these patients proved less than satisfactory and resulted in compromised activities of daily living. It is unlikely that the improvement noted following ECM treatment was part of a delayed natural healing response or the result of debridement and

tenolysis at the time of ECM implantation. Second, all five patients completed a pre-surgical, customized and intense physical therapy program that focused specifically upon their individual functional deficits. The identification and maximization of functional parameters prior to surgery and the use of these optimized parameters as baseline measures for post-operative metrics effectively minimizes the likelihood that any improvement following ECM intervention was solely the result of the physical therapy component of care. Stated differently, since each patient underwent a documented plateau in physical capability prior to ECM implantation, it is unlikely that any increase in muscle mass of the treated compartment or improvement in function was due to hypertrophy of the native muscle.

## **5.5 LIMITATIONS AND FUTURE DIRECTIONS**

The results reported herein show similarities in the cellular remodeling characteristics between a preclinical model and the clinical application of ECM bioscaffolds for the treatment of VML. However, limitations should be noted. First, the preclinical data was limited to 56-72 days post-surgery, and did not evaluate muscle function. However, previous preclinical studies designed to evaluate function have shown significant restoration following ECM scaffold mediated VML repair (200, 202). The preclinical portion of the present study was specifically designed to evaluate the role of host PVSCs after 14 days and the presence of skeletal muscle after 56-72 days and to correlate these findings to tissue biopsies collected from patients suffering from VML. Furthermore, after 56-72 days, untreated VML defects showed the hallmarks of default mammalian wound healing including the formation of scar tissue and the lack of any notable parenchymal cell presence. Conversely, ECM-treated VML defects were

characterized by abundant cellularity, angiogenesis, and the onset of skeletal muscle formation (357). Therefore, although 56-72 days represents a relevant end point for comparing control vs. ECM intervention, longer studies with functional outcomes in the preclinical model are warranted. Secondly, while the pre-clinical model provided for the inclusion of an untreated control group, this was not possible in the clinical study. For example, the impact of the excision of scar tissue and tenolysis, when performed, cannot be assessed as an independent variable. Furthermore, associated placebo effects (i.e., patients may have had more confidence in their treated leg after implantation, which may have affected functional outcomes) were unable to be controlled. Some biologic scaffolds are commonly used in clinical practice to promote host tissue ingrowth, including fibrous tissue formation. A recent study showed functional benefits associated with biologic scaffold induced fibrous tissue remodeling in skeletal muscle (361). However, the present study employed ultrasound guided tissue biopsy, which confirmed tissue formation at the scaffold implantation site was consistent with the presence of non-fibrous skeletal muscle. Nevertheless, it was not possible to characterize the relative relationship between the amount of *de novo* skeletal muscle formation and the degree of functional improvement. The number of subjects was limited and two of our subjects could be considered non-responders. However, given the chronicity of the injury and the preoperative physical therapy the results in 3 subjects are notable. A common finding among the non-responders was lack of active movement across the weakened joint. This finding should be considered in future studies.

Five subjects is insufficient to conduct statistical analysis of the results, which is the reason the data is presented as a series of case studies. The findings described herein represent the interface between the preclinical and clinical application of this therapeutic approach for VML. It

should be recognized that in a human population with a variety of injuries and mechanisms of injury, each patient is unique. No two patients will present with identical or even similar morphometrics, co-morbidities, or anatomic deficits.

The clinical translation of this acellular approach for restoration of skeletal muscle in patients with VML is promising and the concept of providing an inductive niche that can alter the default scar tissue response to injury is worthy of further study.

## 6.0 DISSERTATION SYNOPSIS

The work presented in this dissertation examined the role of source animal age upon the constructive tissue remodeling induced by surgically placed bioscaffolds composed of mammalian extracellular matrix (ECM); showed that degradation products from ECM bioscaffolds directly promote a constructive M2 macrophage phenotype and that ECM treated macrophages are chemotactic and myogenic for skeletal muscle progenitor cells; described a preclinical model of volumetric muscle loss (VML) and a regenerative medicine approach for treatment that was associated with the recruitment of perivascular stem cells; and validated the translational aspects of the study by showing the ability of surgically placed ECM to recruit progenitor cells and promote skeletal muscle formation in human patients suffering from VML. The major findings for each specific aim are outlined below.

### 6.1 MAJOR FINDINGS

The major findings of the present work were:

**Aim 1:** To evaluate the host remodeling response, including macrophage phenotype induced by extracellular matrix (ECM) scaffolds derived from young and aged source animals.

- Surgically placed ECM bioscaffolds derived from younger animals were associated with a greater M2:M1 macrophage ratio and more favorable constructive tissue remodeling outcomes when compared to ECM bioscaffolds derived from older animals.

**Aim 2:** To determine the ability of ECM to enhance the polarization of macrophages isolated from young and aged subjects.

**Sub-Aim:** To evaluate the effect of ECM and polarized macrophages upon the chemotaxis, mitogenesis, and differentiation of skeletal muscle progenitor cells.

- Degradation products from mammalian ECM directly promote the M2 macrophage phenotype in bone marrow derived macrophages isolated from young and aged subjects.
- ECM treated macrophages are chemotactic and myogenic for perivascular stem cells (PVSC) and skeletal muscle myoblasts.
- Only M1 macrophages are mitogenic for skeletal muscle progenitor cells.
- Degradation products from market weight and young source aged ECM bioscaffolds are chemotactic and myogenic for PVSCs and myoblasts.

**Aim 3:** To determine if an ECM scaffold induced progenitor cell participation and constructive macrophage phenotype correlate with a constructive tissue remodeling outcome in a mouse model of volumetric muscle loss (VML).

- Defects treated with a surgically placed ECM bioscaffold, after 14 days, are associated with a predominant M2 macrophage phenotype and PVSCs outside their

normal perivascular niche, suggesting that they participate in the scaffold remodeling.

- These phenomena correlate with downstream site-appropriate constructive remodeling of skeletal muscle tissue in a preclinical model of VML.
- The translational aspects of the study are validated by the ability of surgically placed ECM to recruit progenitor cells and promote skeletal muscle formation in human patients suffering from VML.

## APPENDIX

### JOURNAL ARTICLES

*Published / Submitted / In Press:*

1. **Sicari BM**, Rubin JP, Dearth CL, Wolf MT, Ambrosio F, Boninger M, Turner NJ, Weber D, Simpson T, Wyse A, Brown EH, Dziki JL, Brown S, Badylak SF. (2013). An acellular biologic scaffold to promote skeletal muscle formation: from preclinical model to clinical implementation. *Submitted*.
2. Goh SK, Bertera S, Olsen P, Candiello JE, Halfter W, Uechi G, Balasubramani M, Johnson SA, **Sicari BM**, Kollar E, Badylak SF, Banerjee I. (2013). Perfusion-decellularized pancreas as a natural 3D scaffold for pancreatic tissue and whole organ engineering. *Biomaterials* 34(28): 6760-72.
3. **Sicari BM**, Dearth CL, Badylak SF. (2013). Tissue engineering and regenerative medicine approaches to enhance the functional response of skeletal muscle injury. *The Anatomic Record* *In Press*.
4. **Sicari BM**, Agrawal V, Siu BF, Dearth CL, Turner NJ, Badylak SF. (2012). A murine model of volumetric muscle loss and a regenerative medicine approach for tissue replacement. *Tissue Eng Part A* 18(19-20): 1941-1948.
5. **Sicari BM**, Johnson SA, Siu BF, Crapo P, Daly KA, Jiang H, Medberry C, Tottey S, Turner N, Badylak SF. (2012) The Effect of Source Animal Age upon the In-Vivo Remodeling Characteristics of an Extracellular Matrix Scaffold. *Biomaterials* 33(22): 5524-5533.
6. **Sicari BM**, Troxell R, Salim F, Tanwir M, Takane KK, Fiaschi-Taesch N. (2012) c-myc and skp2 Coordinate p27 Degradation, Vascular Smooth Muscle Proliferation, and Neointima Formation Induced by the Parathyroid Hormone-Related Protein. *Endocrinology*. 2012 Feb;153(2):861-72.
7. Daly K, Liu S, Agrawal V, Brown B, Huber A, Johnson SA, Reing JE, **Sicari BM**, Wolf MT, Zhang X, Badylak SF. (2011) The Host Response to Endotoxin Contaminated Dermal Matrix. *Tissue Eng Part A* 18(11-12): 1293-1303.

8. Song GJ, Barrick S, Leslie KL, **Sicari B**, Fiaschi-Taesch NM, Bisello A. (2010) EBP50 inhibits the anti-mitogenic action of the parathyroid hormone type 1 receptor in vascular smooth muscle cells. J Mol Cell Cardiol. Dec 2010;49(6):1012-1021
9. Fiaschi-Taesch N, Bigatel TA, **Sicari B**, et al. (2009) Survey of the human pancreatic beta-cell G1/S proteome reveals a potential therapeutic role for cdk-6 and cyclin D1 in enhancing human beta-cell replication and function in vivo. Diabetes. Apr 2009;58(4):882-893.
10. Fiaschi-Taesch N, **Sicari B**, Ubriani K, Cozar-Castellano I, Takane KK, Stewart AF. (2009) Mutant parathyroid hormone-related protein, devoid of the nuclear localization signal, markedly inhibits arterial smooth muscle cell cycle and neointima formation by coordinate up-regulation of p15Ink4b and p27kip1. Endocrinology. Mar 2009;150(3):1429-1439
11. Fiaschi-Taesch NM, Berman DM, **Sicari BM**, Takane KK, Garcia-Ocana A, Ricordi C, Kenyon NS, Stewart AF. (2008) Hepatocyte growth factor enhances engraftment and function of nonhuman primate islets. Diabetes. Oct 2008;57(10):2745-2754.
12. Fiaschi-Taesch NM, Berman DM, **Sicari BM**, et al. (2008) Hepatocyte Growth Factor (HGF) Enhances Engraftment and Function of Non-Human Primate Islets. Diabetes. Jul 15 2008.
13. Cozar-Castellano I, Harb G, Selk K, **Sicari B**, Law B, Zhang P, Scott D, Fiaschi-Taesch N Stewart AF. (2008) Lessons from the first comprehensive molecular characterization of cell cycle control in rodent insulinoma cell lines. Diabetes. Nov 2008;57(11):3056-3068.
14. Fiaschi-Taesch N, **Sicari BM**, Ubriani K, et al. (2006) Cellular mechanism through which parathyroid hormone-related protein induces proliferation in arterial smooth muscle cells: definition of an arterial smooth muscle PTHrP/p27kip1 pathway. Circulation Research. Oct 27 2006;99(9):933-942.

## BOOK CHAPTERS

1. **Sicari BM**, Turner N, Badylak SF. An in vivo model system for evaluation of the host response to biomaterials. Wound Regeneration and Repair: Methods and Protocols. 2013.
2. **Sicari BM**, Zhang L, Londono R, Badylak SF. An assay to quantify chemotactic properties of degradation products from extracellular matrix. Methods Mol Bio. 2013

## PEER REVIEWED ABSTRACTS

1. **Sicari BM**, Dziki JL, Wolf MT, Siu BF, Dearth CL, Turner NJ, Badylak SF. Extracellular matrix bioscaffolds promote a constructive macrophage phenotype. TERMIS NA 2013 "Tissue Engineering and Regenerative Medicine" Atlanta, USA, November 10-13, 2013.
2. **Sicari BM**, Dziki JL, Wolf MT, Siu BF, Dearth CL, Turner NJ, Badylak SF. Endogenous cell therapy by extracellular matrix bioscaffolds. Stem Cell Meeting on the Mesa, San Diego, USA, October 14-16, 2013
3. **Sicari BM**, Brown BN, Kukla KA, Zhang L, Turner NJ, Badylak S. Local macrophage polarization and tissue remodeling following bilateral implantation of ECM scaffold materials in the abdominal wall. *TERMIS World Congress 2012 "Tissue Engineering and Regenerative Medicine" Vienna, Austria, Oral Presentation, September 5-8, 2012*
4. **Sicari BM**, Siu B, Carey L, Turner N, Agrawal V, Badylak S. Macrophage and Progenitor Cell Participation in a Regenerative Medicine Approach to Volumetric Muscle Loss. *TERMIS World Congress 2012 "Tissue Engineering and Regenerative Medicine" Vienna, Austria, September 5-8, 2012.*
5. **Sicari BM**, Siu B, Agrawal V, Turner N, Badylak S. Preclinical and Clinical Evidence of Progenitor Cell Participation in the Remodeling of ECM Scaffolds Extracellular Matrix as a Scaffold for Tissue Replacement Following Volumetric Muscle Loss: Remodeling Characteristics from Animal Models and Human Patients. *Regenerative Medicine Annual Conference and Exposition, Hilton Head, SC, March 14-17, 2012.*
6. **Sicari BM**, Johnson SA, Siu BF, Crapo P, Daly KA, Jiang H, Medberry C, Tottey S, Turner N, Badylak SF. The Effect of Source Animal Age upon the In-Vivo Remodeling Characteristics of an Extracellular Matrix Scaffold. *McGowan Retreat, Farmington PA, 2012.*
7. **Sicari BM**, Agrawal V, Siu B, Turner N, Badylak S. Extracellular Matrix as a Scaffold for Tissue Replacement Following Volumetric Muscle Loss: Remodeling Characteristics from Animal Models and Human Patients. *Tissue Engineering and Regenerative Medicine International Society (TERMIS), North America Annual Conference and Exposition, December 11-14. Oral Presentation, 2011.*
8. **Sicari BM**, Agrawal V, Turner N, Badylak SF. Constructive remodeling by extracellular matrix scaffolds within the skeletal muscle microenvironment. *Regenerative Medicine Annual Conference and Exposition, Hilton Head, SC, March 11-14, 2011*
9. **Sicari BM**, Brown BN, Daly KA, Tottey S, Johnson SA, Badylak SF. Tissue remodeling characteristics of three different extracellular matrix configurations. *McGowan Retreat, Farmington PA, 2010*

10. Fiaschi-Taesch N, Bigatel T, **Sicari B**, Takane KK, Stewart AF. Overexpression of cdk6, A Human Specific  $\beta$  Cell Cdk, Induces Human  $\beta$  Cell Proliferation and Promotes Engraftment and Function of Human Islets. *American Diabetes Association 68<sup>th</sup> Scientific Sessions, June 2008 Oral Presentation.*
11. Fiaschi-Taesch N, Bigatel T, **Sicari B**, Takane KK, Stewart AF. Overexpression of cdk6, A Human Specific  $\beta$  Cell Cdk, Induces Human  $\beta$  Cell Proliferation and Promotes Engraftment and Function of Human Islets. *Upper Midwest Islet Club Meeting (UMIC) at Vanderbilt University, Nashville TN, April 30th to May 2nd 2008, Oral Presentation.*
12. Fiaschi-Taesch N, Berman DM, Takane KK, Ricordi C, **Sicari, B.M.**, Garcia-Ocana A, Kenyon NS, Stewart AF. Hepatocyte Growth Factor (HGF) Markedly Enhances Engraftment and Function of Non-Human Primate (NHP) Islets. *American Diabetes Association 66<sup>th</sup> Scientific Sessions, June 9-16 2006, Oral Presentation.*
13. Fiaschi-Taesch, K. Ubriani, K Takane, **B. M. Sicari**, AF. Stewart. PTHrP induction of VSMC proliferation and neointima formation: a central role for 26S proteasome degradation of p27<sup>kip1</sup>. *Cell Cycle Meeting, Cold Spring Harbor Laboratories, May 17-21 2006, Poster.*
14. Fiaschi-Taesch N, K Ubriani, KK Takane, **B. M. Sicari**, B Law, AF Stewart. PTHrP induction of VSMC proliferation and neointima formation: a central role for 26S proteasome degradation of p27<sup>KIP1</sup>. *American Heart Association, Scientific Session, November 13-16. Oral Presentation, 2005.*
15. Fiaschi-Taesch N, K. R. Ubriani, K. K. Takane, **B. M. Sicari**, B. Law, A. F. Stewart. Nuclear Targeting of PTHrP and Cellular Proliferation: A Central Role for p27<sup>kip1</sup> in Molecular Control of the Cell Cycle. *ASBMR 76<sup>th</sup> Annual Meeting, September 23-27. Oral Presentation, Abstract in J Bone Min Res, 2005.*

## FUNDING

*Active*

1. Grant #: F31 AG042199                      Sicari (PI)    01/03/2012-Present  
     Constructive Remodeling by Extracellular Matrix Scaffolds within the Aging Skeletal Muscle Microenvironment  
     The goal of this project is to investigate the ability of implanted ECM scaffold materials to mitigate age-related changes to the injured skeletal muscle microenvironment.  
     Role: Principal Investigator

## BIBLIOGRAPHY

1. S. F. Badylak, Regenerative medicine and developmental biology: the role of the extracellular matrix. *Anatomical record. Part B, New anatomist* **287**, 36-41 (Nov, 2005).
2. S. F. Badylak, Xenogeneic extracellular matrix as a scaffold for tissue reconstruction. *Transplant immunology* **12**, 367-377 (Apr, 2004).
3. B. Brown, K. Lindberg, J. Reing, D. B. Stolz, S. F. Badylak, The basement membrane component of biologic scaffolds derived from extracellular matrix. *Tissue engineering* **12**, 519-526 (Mar, 2006).
4. M. van der Rest, R. Garrone, Collagen family of proteins. *FASEB journal : official publication of the Federation of American Societies for Experimental Biology* **5**, 2814-2823 (Oct, 1991).
5. V. Agrawal, S. A. Johnson, J. Reing, L. Zhang, S. Tottey, G. Wang, K. K. Hirschi, S. Braunhut, L. J. Gudas, S. F. Badylak, Epimorphic regeneration approach to tissue replacement in adult mammals. *Proceedings of the National Academy of Sciences of the United States of America* **107**, 3351-3355 (Feb 23, 2010).
6. V. Agrawal, J. Kelly, S. Tottey, K. A. Daly, S. A. Johnson, B. F. Siu, J. Reing, S. F. Badylak, An isolated cryptic peptide influences osteogenesis and bone remodeling in an adult mammalian model of digit amputation. *Tissue engineering. Part A* **17**, 3033-3044 (Dec, 2011).
7. V. Agrawal, S. Tottey, S. A. Johnson, J. M. Freund, B. F. Siu, S. F. Badylak, Recruitment of progenitor cells by an extracellular matrix cryptic peptide in a mouse model of digit amputation. *Tissue engineering. Part A* **17**, 2435-2443 (Oct, 2011).
8. A. J. Beattie, T. W. Gilbert, J. P. Guyot, A. J. Yates, S. F. Badylak, Chemoattraction of progenitor cells by remodeling extracellular matrix scaffolds. *Tissue engineering. Part A* **15**, 1119-1125 (May, 2009).
9. E. P. Brennan, J. Reing, D. Chew, J. M. Myers-Irvin, E. J. Young, S. F. Badylak, Antibacterial activity within degradation products of biological scaffolds composed of extracellular matrix. *Tissue engineering* **12**, 2949-2955 (Oct, 2006).

10. E. P. Brennan, X. H. Tang, A. M. Stewart-Akers, L. J. Gudas, S. F. Badylak, Chemoattractant activity of degradation products of fetal and adult skin extracellular matrix for keratinocyte progenitor cells. *Journal of tissue engineering and regenerative medicine* **2**, 491-498 (Dec, 2008).
11. S. Tottey, M. Corselli, E. M. Jeffries, R. Londono, B. Peault, S. F. Badylak, Extracellular matrix degradation products and low-oxygen conditions enhance the regenerative potential of perivascular stem cells. *Tissue engineering. Part A* **17**, 37-44 (Jan, 2011).
12. R. Roberts, J. Gallagher, E. Spooncer, T. D. Allen, F. Bloomfield, T. M. Dexter, Heparan sulphate bound growth factors: a mechanism for stromal cell mediated haemopoiesis. *Nature* **332**, 376-378 (Mar 24, 1988).
13. S. Kagami, S. Kondo, K. Loster, W. Reutter, M. Urushihara, A. Kitamura, S. Kobayashi, Y. Kuroda, Collagen type I modulates the platelet-derived growth factor (PDGF) regulation of the growth and expression of beta1 integrins by rat mesangial cells. *Biochemical and biophysical research communications* **252**, 728-732 (Nov 27, 1998).
14. L. F. Bonewald, Regulation and regulatory activities of transforming growth factor beta. *Critical reviews in eukaryotic gene expression* **9**, 33-44 (1999).
15. J. P. Hodde, R. D. Record, H. A. Liang, S. F. Badylak, Vascular endothelial growth factor in porcine-derived extracellular matrix. *Endothelium : journal of endothelial cell research* **8**, 11-24 (2001).
16. S. L. Voytik-Harbin, A. O. Brightman, M. R. Kraine, B. Waisner, S. F. Badylak, Identification of extractable growth factors from small intestinal submucosa. *Journal of cellular biochemistry* **67**, 478-491 (Dec 15, 1997).
17. A. J. Singer, R. A. Clark, Cutaneous wound healing. *N Engl J Med* **341**, 738-746 (Sep 2, 1999).
18. R. A. Clark, J. M. Lanigan, P. DellaPelle, E. Manseau, H. F. Dvorak, R. B. Colvin, Fibronectin and fibrin provide a provisional matrix for epidermal cell migration during wound reepithelialization. *J Invest Dermatol* **79**, 264-269 (Nov, 1982).
19. M. B. Witte, A. Barbul, General principles of wound healing. *Surg Clin North Am* **77**, 509-528 (Jun, 1997).
20. N. N. Nissen, P. J. Polverini, A. E. Koch, M. V. Volin, R. L. Gamelli, L. A. DiPietro, Vascular endothelial growth factor mediates angiogenic activity during the proliferative phase of wound healing. *Am J Pathol* **152**, 1445-1452 (Jun, 1998).
21. B. N. Brown, J. E. Valentin, A. M. Stewart-Akers, G. P. McCabe, S. F. Badylak, Macrophage phenotype and remodeling outcomes in response to biologic scaffolds with and without a cellular component. *Biomaterials* **30**, 1482-1491 (Mar, 2009).

22. S. F. Badylak, J. E. Valentin, A. K. Ravindra, G. P. McCabe, A. M. Stewart-Akers, Macrophage phenotype as a determinant of biologic scaffold remodeling. *Tissue engineering. Part A* **14**, 1835-1842 (Nov, 2008).
23. T. W. Gilbert, A. M. Stewart-Akers, S. F. Badylak, A quantitative method for evaluating the degradation of biologic scaffold materials. *Biomaterials* **28**, 147-150 (Jan, 2007).
24. B. N. Brown, S. F. Badylak, Expanded applications, shifting paradigms and an improved understanding of host-biomaterial interactions. *Acta biomaterialia* **9**, 4948-4955 (Feb, 2013).
25. S. F. Badylak, B. N. Brown, T. W. Gilbert, K. A. Daly, A. Huber, N. J. Turner, Biologic scaffolds for constructive tissue remodeling. *Biomaterials* **32**, 316-319 (Jan, 2011).
26. D. O. Freytes, J. Martin, S. S. Velankar, A. S. Lee, S. F. Badylak, Preparation and rheological characterization of a gel form of the porcine urinary bladder matrix. *Biomaterials* **29**, 1630-1637 (Apr, 2008).
27. V. Agrawal, B. F. Siu, H. Chao, K. K. Hirschi, E. Raborn, S. A. Johnson, S. Tottey, K. B. Hurley, C. J. Medberry, S. F. Badylak, Partial characterization of the Sox2+ cell population in an adult murine model of digit amputation. *Tissue engineering. Part A* **18**, 1454-1463 (Jul, 2012).
28. S. F. Badylak, K. Park, N. Peppas, G. McCabe, M. Yoder, Marrow-derived cells populate scaffolds composed of xenogeneic extracellular matrix. *Experimental hematology* **29**, 1310-1318 (Nov, 2001).
29. B. N. Brown, R. Londono, S. Tottey, L. Zhang, K. A. Kukla, M. T. Wolf, K. A. Daly, J. E. Reing, S. F. Badylak, Macrophage phenotype as a predictor of constructive remodeling following the implantation of biologically derived surgical mesh materials. *Acta biomaterialia* **8**, 978-987 (Mar, 2012).
30. B. N. Brown, B. D. Ratner, S. B. Goodman, S. Amar, S. F. Badylak, Macrophage polarization: an opportunity for improved outcomes in biomaterials and regenerative medicine. *Biomaterials* **33**, 3792-3802 (May, 2012).
31. J. E. Valentin, A. M. Stewart-Akers, T. W. Gilbert, S. F. Badylak, Macrophage participation in the degradation and remodeling of extracellular matrix scaffolds. *Tissue Eng Part A* **15**, 1687-1694 (Jul, 2009).
32. T. Zantop, T. W. Gilbert, M. C. Yoder, S. F. Badylak, Extracellular matrix scaffolds are repopulated by bone marrow-derived cells in a mouse model of achilles tendon reconstruction. *Journal of orthopaedic research : official publication of the Orthopaedic Research Society* **24**, 1299-1309 (Jun, 2006).

33. M. Crisan, S. Yap, L. Casteilla, C. W. Chen, M. Corselli, T. S. Park, G. Andriolo, B. Sun, B. Zheng, L. Zhang, C. Norotte, P. N. Teng, J. Traas, R. Schugar, B. M. Deasy, S. Badyrak, H. J. Buhring, J. P. Jacobino, L. Lazzari, J. Huard, B. Peault, A perivascular origin for mesenchymal stem cells in multiple human organs. *Cell Stem Cell* **3**, 301-313 (Sep 11, 2008).
34. M. Crisan, M. Corselli, W. C. Chen, B. Peault, Perivascular cells for regenerative medicine. *Journal of cellular and molecular medicine* **16**, 2851-2860 (Dec, 2012).
35. A. Dellavalle, G. Maroli, D. Covarello, E. Azzoni, A. Innocenzi, L. Perani, S. Antonini, R. Sambasivan, S. Brunelli, S. Tajbakhsh, G. Cossu, Pericytes resident in postnatal skeletal muscle differentiate into muscle fibres and generate satellite cells. *Nature communications* **2**, 499 (2011).
36. A. Dellavalle, M. Sampaolesi, R. Tonlorenzi, E. Tagliafico, B. Sacchetti, L. Perani, A. Innocenzi, B. G. Galvez, G. Messina, R. Morosetti, S. Li, M. Belicchi, G. Peretti, J. S. Chamberlain, W. E. Wright, Y. Torrente, S. Ferrari, P. Bianco, G. Cossu, Pericytes of human skeletal muscle are myogenic precursors distinct from satellite cells. *Nature cell biology* **9**, 255-267 (Mar, 2007).
37. J. Takebe, C. M. Champagne, S. Offenbacher, K. Ishibashi, L. F. Cooper, Titanium surface topography alters cell shape and modulates bone morphogenetic protein 2 expression in the J774A.1 macrophage cell line. *J Biomed Mater Res A* **64**, 207-216 (Feb 1, 2003).
38. J. Lu, M. Descamps, J. Dejou, G. Koubi, P. Hardouin, J. Lemaitre, J. P. Proust, The biodegradation mechanism of calcium phosphate biomaterials in bone. *J Biomed Mater Res* **63**, 408-412 (2002).
39. R. S. Labow, D. Sa, L. A. Matheson, J. P. Santerre, Polycarbonate-urethane hard segment type influences esterase substrate specificity for human-macrophage-mediated biodegradation. *J Biomater Sci Polym Ed* **16**, 1167-1177 (2005).
40. I. M. Khouw, P. B. van Wachem, L. F. de Leij, M. J. van Luyn, Inhibition of the tissue reaction to a biodegradable biomaterial by monoclonal antibodies to IFN-gamma. *J Biomed Mater Res* **41**, 202-210 (Aug, 1998).
41. W. G. Brodbeck, J. Patel, G. Voskerician, E. Christenson, M. S. Shive, Y. Nakayama, T. Matsuda, N. P. Ziats, J. M. Anderson, Biomaterial adherent macrophage apoptosis is increased by hydrophilic and anionic substrates in vivo. *Proc Natl Acad Sci U S A* **99**, 10287-10292 (Aug 6, 2002).
42. K. Kedzierska, R. Azzam, P. Ellery, J. Mak, A. Jaworowski, S. M. Crowe, Defective phagocytosis by human monocyte/macrophages following HIV-1 infection: underlying mechanisms and modulation by adjunctive cytokine therapy. *Journal of clinical virology*

- : the official publication of the Pan American Society for Clinical Virology **26**, 247-263 (Feb, 2003).
43. A. Aderem, D. M. Underhill, Mechanisms of phagocytosis in macrophages. *Annual review of immunology* **17**, 593-623 (1999).
  44. J. S. Savill, A. H. Wyllie, J. E. Henson, M. J. Walport, P. M. Henson, C. Haslett, Macrophage phagocytosis of aging neutrophils in inflammation. Programmed cell death in the neutrophil leads to its recognition by macrophages. *The Journal of clinical investigation* **83**, 865-875 (Mar, 1989).
  45. A. Mantovani, S. K. Biswas, M. R. Galdiero, A. Sica, M. Locati, Macrophage plasticity and polarization in tissue repair and remodelling. *The Journal of pathology* **229**, 176-185 (Jan, 2013).
  46. A. Mantovani, A. Sica, M. Locati, Macrophage polarization comes of age. *Immunity* **23**, 344-346 (Oct, 2005).
  47. A. Mantovani, A. Sica, S. Sozzani, P. Allavena, A. Vecchi, M. Locati, The chemokine system in diverse forms of macrophage activation and polarization. *Trends in immunology* **25**, 677-686 (Dec, 2004).
  48. A. Mantovani, S. Sozzani, M. Locati, P. Allavena, A. Sica, Macrophage polarization: tumor-associated macrophages as a paradigm for polarized M2 mononuclear phagocytes. *Trends in immunology* **23**, 549-555 (Nov, 2002).
  49. F. O. Martinez, A. Sica, A. Mantovani, M. Locati, Macrophage activation and polarization. *Frontiers in bioscience : a journal and virtual library* **13**, 453-461 (2008).
  50. D. M. Mosser, J. P. Edwards, Exploring the full spectrum of macrophage activation. *Nature reviews. Immunology* **8**, 958-969 (Dec, 2008).
  51. D. M. Mosser, X. Zhang, Activation of murine macrophages. *Current protocols in immunology / edited by John E. Coligan ... [et al.]* **Chapter 14**, Unit 14 12 (Nov, 2008).
  52. B. M. Carlson, Regeneration fo the completely excised gastrocnemius muscle in the frog and rat from minced muscle fragments. *Journal of morphology* **125**, 447-472 (Aug, 1968).
  53. B. M. Carlson, J. A. Faulkner, The regeneration of skeletal muscle fibers following injury: a review. *Medicine and science in sports and exercise* **15**, 187-198 (1983).
  54. J. Huard, Y. Li, F. H. Fu, Muscle injuries and repair: current trends in research. *J Bone Joint Surg Am* **84-A**, 822-832 (May, 2002).

55. S. B. Charge, M. A. Rudnicki, Cellular and molecular regulation of muscle regeneration. *Physiol Rev* **84**, 209-238 (Jan, 2004).
56. S. Grefte, A. M. Kuijpers-Jagtman, R. Torensma, J. W. Von den Hoff, Skeletal muscle development and regeneration. *Stem Cells Dev* **16**, 857-868 (Oct, 2007).
57. J. G. Tidball, S. A. Villalta, Regulatory interactions between muscle and the immune system during muscle regeneration. *American journal of physiology. Regulatory, integrative and comparative physiology* **298**, R1173-1187 (May, 2010).
58. A. C. Wozniak, J. Kong, E. Bock, O. Pilipowicz, J. E. Anderson, Signaling satellite-cell activation in skeletal muscle: markers, models, stretch, and potential alternate pathways. *Muscle Nerve* **31**, 283-300 (Mar, 2005).
59. P. S. Zammit, T. A. Partridge, Z. Yablonka-Reuveni, The skeletal muscle satellite cell: the stem cell that came in from the cold. *The journal of histochemistry and cytochemistry : official journal of the Histochemistry Society* **54**, 1177-1191 (Nov, 2006).
60. T. J. Hawke, D. J. Garry, Myogenic satellite cells: physiology to molecular biology. *J Appl Physiol* **91**, 534-551 (Aug, 2001).
61. A. Mauro, Satellite cell of skeletal muscle fibers. *The Journal of biophysical and biochemical cytology* **9**, 493-495 (Feb, 1961).
62. A. R. Muir, A. H. Kanji, D. Allbrook, The structure of the satellite cells in skeletal muscle. *J Anat* **99**, 435-444 (Jul, 1965).
63. X. Shi, D. J. Garry, Muscle stem cells in development, regeneration, and disease. *Genes Dev* **20**, 1692-1708 (Jul 1, 2006).
64. M. A. Khan, Corticosteroid therapy in Duchenne muscular dystrophy. *Journal of the neurological sciences* **120**, 8-14 (Dec 1, 1993).
65. A. Y. Manzur, T. Kuntzer, M. Pike, A. Swan, Glucocorticoid corticosteroids for Duchenne muscular dystrophy. *Cochrane database of systematic reviews*, CD003725 (2008).
66. B. Balaban, D. J. Matthews, G. H. Clayton, T. Carry, Corticosteroid treatment and functional improvement in Duchenne muscular dystrophy: long-term effect. *American journal of physical medicine & rehabilitation / Association of Academic Physiatrists* **84**, 843-850 (Nov, 2005).
67. S. H. Lin, D. C. Chuang, Y. Hattori, H. C. Chen, Traumatic major muscle loss in the upper extremity: reconstruction using functioning free muscle transplantation. *Journal of reconstructive microsurgery* **20**, 227-235 (Apr, 2004).

68. C. Fan, P. Jiang, L. Fu, P. Cai, L. Sun, B. Zeng, Functional reconstruction of traumatic loss of flexors in forearm with gastrocnemius myocutaneous flap transfer. *Microsurgery* **28**, 71-75 (2008).
69. M. D. Vekris, A. E. Beris, M. G. Lykissas, A. V. Korompilias, A. D. Vekris, P. N. Soucacos, Restoration of elbow function in severe brachial plexus paralysis via muscle transfers. *Injury* **39 Suppl 3**, S15-22 (Sep, 2008).
70. J. Huard, J. P. Bouchard, R. Roy, C. Labrecque, G. Dansereau, B. Lemieux, J. P. Tremblay, Myoblast transplantation produced dystrophin-positive muscle fibres in a 16-year-old patient with Duchenne muscular dystrophy. *Clinical science* **81**, 287-288 (Aug, 1991).
71. J. Huard, J. P. Bouchard, R. Roy, F. Malouin, G. Dansereau, C. Labrecque, N. Albert, C. L. Richards, B. Lemieux, J. P. Tremblay, Human myoblast transplantation: preliminary results of 4 cases. *Muscle & nerve* **15**, 550-560 (May, 1992).
72. P. Seale, M. A. Rudnicki, A new look at the origin, function, and "stem-cell" status of muscle satellite cells. *Developmental biology* **218**, 115-124 (Feb 15, 2000).
73. J. R. Mendell, J. T. Kissel, A. A. Amato, W. King, L. Signore, T. W. Prior, Z. Sahenk, S. Benson, P. E. McAndrew, R. Rice, et al., Myoblast transfer in the treatment of Duchenne's muscular dystrophy. *The New England journal of medicine* **333**, 832-838 (Sep 28, 1995).
74. B. F. Grogan, J. R. Hsu, C. Skeletal Trauma Research, Volumetric muscle loss. *The Journal of the American Academy of Orthopaedic Surgeons* **19 Suppl 1**, S35-37 (2011).
75. R. M. Grady, H. Teng, M. C. Nichol, J. C. Cunningham, R. S. Wilkinson, J. R. Sanes, Skeletal and cardiac myopathies in mice lacking utrophin and dystrophin: a model for Duchenne muscular dystrophy. *Cell* **90**, 729-738 (Aug 22, 1997).
76. B. Peault, M. Rudnicki, Y. Torrente, G. Cossu, J. P. Tremblay, T. Partridge, E. Gussoni, L. M. Kunkel, J. Huard, Stem and progenitor cells in skeletal muscle development, maintenance, and therapy. *Molecular therapy : the journal of the American Society of Gene Therapy* **15**, 867-877 (May, 2007).
77. T. A. Partridge, J. E. Morgan, G. R. Coulton, E. P. Hoffman, L. M. Kunkel, Conversion of mdx myofibres from dystrophin-negative to -positive by injection of normal myoblasts. *Nature* **337**, 176-179 (Jan 12, 1989).
78. J. P. Tremblay, J. P. Bouchard, F. Malouin, D. Theau, F. Cottrell, H. Collin, A. Rouche, S. Gilgenkrantz, N. Abbadi, M. Tremblay, et al., Myoblast transplantation between monozygotic twin girl carriers of Duchenne muscular dystrophy. *Neuromuscular disorders : NMD* **3**, 583-592 (Sep-Nov, 1993).

79. J. P. Tremblay, F. Malouin, R. Roy, J. Huard, J. P. Bouchard, A. Satoh, C. L. Richards, Results of a triple blind clinical study of myoblast transplantations without immunosuppressive treatment in young boys with Duchenne muscular dystrophy. *Cell transplantation* **2**, 99-112 (Mar-Apr, 1993).
80. G. Karpati, D. Ajdukovic, D. Arnold, R. B. Gledhill, R. Guttmann, P. Holland, P. A. Koch, E. Shoubridge, D. Spence, M. Vanasse, et al., Myoblast transfer in Duchenne muscular dystrophy. *Annals of neurology* **34**, 8-17 (Jul, 1993).
81. E. Gussoni, G. K. Pavlath, A. M. Lanctot, K. R. Sharma, R. G. Miller, L. Steinman, H. M. Blau, Normal dystrophin transcripts detected in Duchenne muscular dystrophy patients after myoblast transplantation. *Nature* **356**, 435-438 (Apr 2, 1992).
82. R. G. Miller, K. R. Sharma, G. K. Pavlath, E. Gussoni, M. Mynhier, A. M. Lanctot, C. M. Greco, L. Steinman, H. M. Blau, Myoblast implantation in Duchenne muscular dystrophy: the San Francisco study. *Muscle & nerve* **20**, 469-478 (Apr, 1997).
83. B. Guerette, I. Asselin, D. Skuk, M. Entman, J. P. Tremblay, Control of inflammatory damage by anti-LFA-1: increase success of myoblast transplantation. *Cell transplantation* **6**, 101-107 (Mar-Apr, 1997).
84. J. Huard, G. Acsadi, A. Jani, B. Massie, G. Karpati, Gene transfer into skeletal muscles by isogenic myoblasts. *Human gene therapy* **5**, 949-958 (Aug, 1994).
85. D. Skuk, B. Roy, M. Goulet, J. P. Tremblay, Successful myoblast transplantation in primates depends on appropriate cell delivery and induction of regeneration in the host muscle. *Experimental neurology* **155**, 22-30 (Jan, 1999).
86. B. Guerette, I. Asselin, J. T. Vilquin, R. Roy, J. P. Tremblay, Lymphocyte infiltration following allo- and xenomyoblast transplantation in mice. *Transplantation proceedings* **26**, 3461-3462 (Dec, 1994).
87. O. Hardiman, R. M. Sklar, R. H. Brown, Jr., Direct effects of cyclosporin A and cyclophosphamide on differentiation of normal human myoblasts in culture. *Neurology* **43**, 1432-1434 (Jul, 1993).
88. F. Hong, J. Lee, J. W. Song, S. J. Lee, H. Ahn, J. J. Cho, J. Ha, S. S. Kim, Cyclosporin A blocks muscle differentiation by inducing oxidative stress and inhibiting the peptidyl-prolyl-cis-trans isomerase activity of cyclophilin A: cyclophilin A protects myoblasts from cyclosporin A-induced cytotoxicity. *FASEB journal : official publication of the Federation of American Societies for Experimental Biology* **16**, 1633-1635 (Oct, 2002).
89. M. Cerletti, S. Jurga, C. A. Witczak, M. F. Hirshman, J. L. Shadrach, L. J. Goodyear, A. J. Wagers, Highly efficient, functional engraftment of skeletal muscle stem cells in dystrophic muscles. *Cell* **134**, 37-47 (Jul 11, 2008).

90. A. Sacco, R. Doyonnas, P. Kraft, S. Vitorovic, H. M. Blau, Self-renewal and expansion of single transplanted muscle stem cells. *Nature* **456**, 502-506 (Nov 27, 2008).
91. D. Skuk, M. Goulet, B. Roy, P. Chapdelaine, J. P. Bouchard, R. Roy, F. J. Dugre, M. Sylvain, J. G. Lachance, L. Deschenes, H. Senay, J. P. Tremblay, Dystrophin expression in muscles of duchenne muscular dystrophy patients after high-density injections of normal myogenic cells. *Journal of neuropathology and experimental neurology* **65**, 371-386 (Apr, 2006).
92. I. Riederer, E. Negroni, M. Bencze, A. Wolff, A. Aamiri, J. P. Di Santo, S. D. Silva-Barbosa, G. Butler-Browne, W. Savino, V. Mouly, Slowing down differentiation of engrafted human myoblasts into immunodeficient mice correlates with increased proliferation and migration. *Molecular therapy : the journal of the American Society of Gene Therapy* **20**, 146-154 (Jan, 2012).
93. I. Kinoshita, R. Roy, F. J. Dugre, C. Gravel, B. Roy, M. Goulet, I. Asselin, J. P. Tremblay, Myoblast transplantation in monkeys: control of immune response by FK506. *Journal of neuropathology and experimental neurology* **55**, 687-697 (Jun, 1996).
94. I. Kinoshita, J. T. Vilquin, B. Guerette, I. Asselin, R. Roy, J. P. Tremblay, Very efficient myoblast allotransplantation in mice under FK506 immunosuppression. *Muscle & nerve* **17**, 1407-1415 (Dec, 1994).
95. D. Skuk, B. Roy, M. Goulet, P. Chapdelaine, J. P. Bouchard, R. Roy, F. J. Dugre, J. G. Lachance, L. Deschenes, S. Helene, M. Sylvain, J. P. Tremblay, Dystrophin expression in myofibers of Duchenne muscular dystrophy patients following intramuscular injections of normal myogenic cells. *Molecular therapy : the journal of the American Society of Gene Therapy* **9**, 475-482 (Mar, 2004).
96. D. Skuk, M. Goulet, B. Roy, V. Piette, C. H. Cote, P. Chapdelaine, J. Y. Hogrel, M. Paradis, J. P. Bouchard, M. Sylvain, J. G. Lachance, J. P. Tremblay, First test of a "high-density injection" protocol for myogenic cell transplantation throughout large volumes of muscles in a Duchenne muscular dystrophy patient: eighteen months follow-up. *Neuromuscular disorders : NMD* **17**, 38-46 (Jan, 2007).
97. Y. Torrente, M. Belicchi, M. Sampaolesi, F. Pisati, M. Meregalli, G. D'Antona, R. Tonlorenzi, L. Porretti, M. Gavina, K. Mamchaoui, M. A. Pellegrino, D. Furling, V. Mouly, G. S. Butler-Browne, R. Bottinelli, G. Cossu, N. Bresolin, Human circulating AC133(+) stem cells restore dystrophin expression and ameliorate function in dystrophic skeletal muscle. *The Journal of clinical investigation* **114**, 182-195 (Jul, 2004).
98. E. Negroni, I. Riederer, S. Chaouch, M. Belicchi, P. Razini, J. Di Santo, Y. Torrente, G. S. Butler-Browne, V. Mouly, In vivo myogenic potential of human CD133+ muscle-derived stem cells: a quantitative study. *Molecular therapy : the journal of the American Society of Gene Therapy* **17**, 1771-1778 (Oct, 2009).

99. Y. Torrente, M. Belicchi, C. Marchesi, G. Dantona, F. Cogiamanian, F. Pisati, M. Gavina, R. Giordano, R. Tonlorenzi, G. Fagiolari, C. Lamperti, L. Porretti, R. Lopa, M. Sampaolesi, L. Vicentini, N. Grimoldi, F. Tiberio, V. Songa, P. Baratta, A. Prella, L. Forzenigo, M. Guglieri, O. Pansarasa, C. Rinaldi, V. Mouly, G. S. Butler-Browne, G. P. Comi, P. Biondetti, M. Moggio, S. M. Gaini, N. Stocchetti, A. Priori, M. G. D'Angelo, A. Turconi, R. Bottinelli, G. Cossu, P. Rebulli, N. Bresolin, Autologous transplantation of muscle-derived CD133+ stem cells in Duchenne muscle patients. *Cell transplantation* **16**, 563-577 (2007).
100. J. Y. Lee, Z. Qu-Petersen, B. Cao, S. Kimura, R. Jankowski, J. Cummins, A. Usas, C. Gates, P. Robbins, A. Wernig, J. Huard, Clonal isolation of muscle-derived cells capable of enhancing muscle regeneration and bone healing. *The Journal of cell biology* **150**, 1085-1100 (Sep 4, 2000).
101. Z. Qu-Petersen, B. Deasy, R. Jankowski, M. Ikezawa, J. Cummins, R. Pruchnic, J. Mytinger, B. Cao, C. Gates, A. Wernig, J. Huard, Identification of a novel population of muscle stem cells in mice: potential for muscle regeneration. *The Journal of cell biology* **157**, 851-864 (May 27, 2002).
102. M. Lavasani, A. Lu, H. Peng, J. Cummins, J. Huard, Nerve growth factor improves the muscle regeneration capacity of muscle stem cells in dystrophic muscle. *Human gene therapy* **17**, 180-192 (Feb, 2006).
103. K. L. Urish, J. B. Vella, M. Okada, B. M. Deasy, K. Tobita, B. B. Keller, B. Cao, J. D. Piganelli, J. Huard, Antioxidant levels represent a major determinant in the regenerative capacity of muscle stem cells. *Molecular biology of the cell* **20**, 509-520 (Jan, 2009).
104. L. Drowley, M. Okada, S. Beckman, J. Vella, B. Keller, K. Tobita, J. Huard, Cellular antioxidant levels influence muscle stem cell therapy. *Molecular therapy : the journal of the American Society of Gene Therapy* **18**, 1865-1873 (Oct, 2010).
105. E. R. Andreeva, I. M. Pugach, D. Gordon, A. N. Orekhov, Continuous subendothelial network formed by pericyte-like cells in human vascular bed. *Tissue & cell* **30**, 127-135 (Feb, 1998).
106. M. A. Goodell, K. Brose, G. Paradis, A. S. Conner, R. C. Mulligan, Isolation and functional properties of murine hematopoietic stem cells that are replicating in vivo. *The Journal of experimental medicine* **183**, 1797-1806 (Apr 1, 1996).
107. E. Gussoni, Y. Soneoka, C. D. Strickland, E. A. Buzney, M. K. Khan, A. F. Flint, L. M. Kunkel, R. C. Mulligan, Dystrophin expression in the mdx mouse restored by stem cell transplantation. *Nature* **401**, 390-394 (Sep 23, 1999).
108. E. Bachrach, S. Li, A. L. Perez, J. Schienda, K. Liadaki, J. Volinski, A. Flint, J. Chamberlain, L. M. Kunkel, Systemic delivery of human microdystrophin to regenerating

- mouse dystrophic muscle by muscle progenitor cells. *Proceedings of the National Academy of Sciences of the United States of America* **101**, 3581-3586 (Mar 9, 2004).
109. A. Asakura, M. A. Rudnicki, Side population cells from diverse adult tissues are capable of in vitro hematopoietic differentiation. *Experimental hematology* **30**, 1339-1345 (Nov, 2002).
  110. Y. Jiang, B. N. Jahagirdar, R. L. Reinhardt, R. E. Schwartz, C. D. Keene, X. R. Ortiz-Gonzalez, M. Reyes, T. Lenvik, T. Lund, M. Blackstad, J. Du, S. Aldrich, A. Lisberg, W. C. Low, D. A. Largaespada, C. M. Verfaillie, Pluripotency of mesenchymal stem cells derived from adult marrow. *Nature* **418**, 41-49 (Jul 4, 2002).
  111. P. A. Zuk, M. Zhu, H. Mizuno, J. Huang, J. W. Futrell, A. J. Katz, P. Benhaim, H. P. Lorenz, M. H. Hedrick, Multilineage cells from human adipose tissue: implications for cell-based therapies. *Tissue engineering* **7**, 211-228 (Apr, 2001).
  112. D. T. Shih, D. C. Lee, S. C. Chen, R. Y. Tsai, C. T. Huang, C. C. Tsai, E. Y. Shen, W. T. Chiu, Isolation and characterization of neurogenic mesenchymal stem cells in human scalp tissue. *Stem cells* **23**, 1012-1020 (Aug, 2005).
  113. P. S. In 't Anker, S. A. Scherjon, C. Kleijburg-van der Keur, G. M. de Groot-Swings, F. H. Claas, W. E. Fibbe, H. H. Kanhai, Isolation of mesenchymal stem cells of fetal or maternal origin from human placenta. *Stem cells* **22**, 1338-1345 (2004).
  114. A. Erices, P. Conget, J. J. Minguell, Mesenchymal progenitor cells in human umbilical cord blood. *British journal of haematology* **109**, 235-242 (Apr, 2000).
  115. M. F. Pittenger, A. M. Mackay, S. C. Beck, R. K. Jaiswal, R. Douglas, J. D. Mosca, M. A. Moorman, D. W. Simonetti, S. Craig, D. R. Marshak, Multilineage potential of adult human mesenchymal stem cells. *Science* **284**, 143-147 (Apr 2, 1999).
  116. D. Woodbury, E. J. Schwarz, D. J. Prockop, I. B. Black, Adult rat and human bone marrow stromal cells differentiate into neurons. *Journal of neuroscience research* **61**, 364-370 (Aug 15, 2000).
  117. B. E. Petersen, W. C. Bowen, K. D. Patrene, W. M. Mars, A. K. Sullivan, N. Murase, S. S. Boggs, J. S. Greenberger, J. P. Goff, Bone marrow as a potential source of hepatic oval cells. *Science* **284**, 1168-1170 (May 14, 1999).
  118. P. A. Dreyfus, F. Chretien, B. Chazaud, Y. Kirova, P. Caramelle, L. Garcia, G. Butler-Browne, R. K. Gherardi, Adult bone marrow-derived stem cells in muscle connective tissue and satellite cell niches. *The American journal of pathology* **164**, 773-779 (Mar, 2004).

119. T. R. Brazelton, M. Nystrom, H. M. Blau, Significant differences among skeletal muscles in the incorporation of bone marrow-derived cells. *Developmental biology* **262**, 64-74 (Oct 1, 2003).
120. R. E. Bittner, C. Schofer, K. Weipoltshammer, S. Ivanova, B. Streubel, E. Hauser, M. Freilinger, H. Hoger, A. Elbe-Burger, F. Wachtler, Recruitment of bone-marrow-derived cells by skeletal and cardiac muscle in adult dystrophic mdx mice. *Anatomy and embryology* **199**, 391-396 (May, 1999).
121. G. Ferrari, G. Cusella-De Angelis, M. Coletta, E. Paolucci, A. Stornaiuolo, G. Cossu, F. Mavilio, Muscle regeneration by bone marrow-derived myogenic progenitors. *Science* **279**, 1528-1530 (Mar 6, 1998).
122. T. Winkler, P. von Roth, G. Matziolis, M. Mehta, C. Perka, G. N. Duda, Dose-response relationship of mesenchymal stem cell transplantation and functional regeneration after severe skeletal muscle injury in rats. *Tissue engineering. Part A* **15**, 487-492 (Mar, 2009).
123. Q. Liu, Z. Chen, T. Terry, J. M. McNatt, J. T. Willerson, P. Zoldhelyi, Intra-arterial transplantation of adult bone marrow cells restores blood flow and regenerates skeletal muscle in ischemic limbs. *Vascular and endovascular surgery* **43**, 433-443 (Oct-Nov, 2009).
124. S. W. Feng, X. L. Lu, Z. S. Liu, Y. N. Zhang, T. Y. Liu, J. L. Li, M. J. Yu, Y. Zeng, C. Zhang, Dynamic distribution of bone marrow-derived mesenchymal stromal cells and change of pathology after infusing into mdx mice. *Cytotherapy* **10**, 254-264 (2008).
125. E. J. Gang, R. Darabi, D. Bosnakovski, Z. Xu, K. E. Kamm, M. Kyba, R. C. Perlingeiro, Engraftment of mesenchymal stem cells into dystrophin-deficient mice is not accompanied by functional recovery. *Experimental cell research* **315**, 2624-2636 (Sep 10, 2009).
126. D. Cizkova, J. Vavrova, S. Micuda, S. Filip, E. Brckova, L. Bruckova, J. Mokry, Role of transplanted bone marrow cells in response to skeletal muscle injury. *Folia biologica* **57**, 232-241 (2011).
127. B. M. Strem, K. C. Hicok, M. Zhu, I. Wulur, Z. Alfonso, R. E. Schreiber, J. K. Fraser, M. H. Hedrick, Multipotential differentiation of adipose tissue-derived stem cells. *The Keio journal of medicine* **54**, 132-141 (Sep, 2005).
128. G. Di Rocco, M. G. Iachininoto, A. Tritarelli, S. Straino, A. Zacheo, A. Germani, F. Crea, M. C. Capogrossi, Myogenic potential of adipose-tissue-derived cells. *Journal of cell science* **119**, 2945-2952 (Jul 15, 2006).
129. C. H. Pinheiro, J. C. de Queiroz, L. Guimaraes-Ferreira, K. F. Vitzel, R. T. Nachbar, L. G. de Sousa, A. L. de Souza-Jr, M. T. Nunes, R. Curi, Local injections of adipose-derived mesenchymal stem cells modulate inflammation and increase angiogenesis ameliorating

- the dystrophic phenotype in dystrophin-deficient skeletal muscle. *Stem cell reviews* **8**, 363-374 (Jun, 2012).
130. Y. Kang, C. Park, D. Kim, C. M. Seong, K. Kwon, C. Choi, Unsorted human adipose tissue-derived stem cells promote angiogenesis and myogenesis in murine ischemic hindlimb model. *Microvascular research* **80**, 310-316 (Dec, 2010).
  131. S. Kern, H. Eichler, J. Stoeve, H. Kluter, K. Bieback, Comparative analysis of mesenchymal stem cells from bone marrow, umbilical cord blood, or adipose tissue. *Stem cells* **24**, 1294-1301 (May, 2006).
  132. M. Pesce, A. Orlandi, M. G. Iachininoto, S. Straino, A. R. Torella, V. Rizzuti, G. Pompilio, G. Bonanno, G. Scambia, M. C. Capogrossi, Myoendothelial differentiation of human umbilical cord blood-derived stem cells in ischemic limb tissues. *Circulation research* **93**, e51-62 (Sep 5, 2003).
  133. K. Y. Kong, J. Ren, M. Kraus, S. P. Finklestein, R. H. Brown, Jr., Human umbilical cord blood cells differentiate into muscle in sjl muscular dystrophy mice. *Stem cells* **22**, 981-993 (2004).
  134. J. K. Koponen, T. Kekarainen, E. H. S. A. Laitinen, J. Nystedt, J. Laine, S. Yla-Herttuala, Umbilical cord blood-derived progenitor cells enhance muscle regeneration in mouse hindlimb ischemia model. *Molecular therapy : the journal of the American Society of Gene Therapy* **15**, 2172-2177 (Dec, 2007).
  135. D. Montarras, J. Morgan, C. Collins, F. Relaix, S. Zaffran, A. Cumano, T. Partridge, M. Buckingham, Direct isolation of satellite cells for skeletal muscle regeneration. *Science* **309**, 2064-2067 (Sep 23, 2005).
  136. L. Song, R. S. Tuan, Transdifferentiation potential of human mesenchymal stem cells derived from bone marrow. *FASEB journal : official publication of the Federation of American Societies for Experimental Biology* **18**, 980-982 (Jun, 2004).
  137. Y. Fan, M. Maley, M. Beilharz, M. Grounds, Rapid death of injected myoblasts in myoblast transfer therapy. *Muscle & nerve* **19**, 853-860 (Jul, 1996).
  138. F. D. Camargo, S. M. Chambers, E. Drew, K. M. McNagny, M. A. Goodell, Hematopoietic stem cells do not engraft with absolute efficiencies. *Blood* **107**, 501-507 (Jan 15, 2006).
  139. H. Glimm, I. H. Oh, C. J. Eaves, Human hematopoietic stem cells stimulated to proliferate in vitro lose engraftment potential during their S/G(2)/M transit and do not reenter G(0). *Blood* **96**, 4185-4193 (Dec 15, 2000).
  140. M. Gnecci, H. He, O. D. Liang, L. G. Melo, F. Morello, H. Mu, N. Noiseux, L. Zhang, R. E. Pratt, J. S. Ingwall, V. J. Dzau, Paracrine action accounts for marked protection of

- ischemic heart by Akt-modified mesenchymal stem cells. *Nature medicine* **11**, 367-368 (Apr, 2005).
141. C. E. Murry, H. Reinecke, L. M. Pabon, Regeneration gaps: observations on stem cells and cardiac repair. *Journal of the American College of Cardiology* **47**, 1777-1785 (May 2, 2006).
  142. B. Gharaibeh, M. Lavasani, J. H. Cummins, J. Huard, Terminal differentiation is not a major determinant for the success of stem cell therapy - cross-talk between muscle-derived stem cells and host cells. *Stem cell research & therapy* **2**, 31 (2011).
  143. M. Perez-Illarbe, O. Agbulut, B. Pelacho, C. Ciorba, E. San Jose-Eneriz, M. Desnos, A. A. Hagege, P. Aranda, E. J. Andreu, P. Menasche, F. Prosper, Characterization of the paracrine effects of human skeletal myoblasts transplanted in infarcted myocardium. *European journal of heart failure* **10**, 1065-1072 (Nov, 2008).
  144. M. Gnechchi, Z. Zhang, A. Ni, V. J. Dzau, Paracrine mechanisms in adult stem cell signaling and therapy. *Circulation research* **103**, 1204-1219 (Nov 21, 2008).
  145. A. Arthur, A. Zannettino, S. Gronthos, The therapeutic applications of multipotential mesenchymal/stromal stem cells in skeletal tissue repair. *Journal of cellular physiology* **218**, 237-245 (Feb, 2009).
  146. S. Ota, K. Uehara, M. Nozaki, T. Kobayashi, S. Terada, K. Tobita, F. H. Fu, J. Huard, Intramuscular transplantation of muscle-derived stem cells accelerates skeletal muscle healing after contusion injury via enhancement of angiogenesis. *The American journal of sports medicine* **39**, 1912-1922 (Sep, 2011).
  147. M. L. Springer, A. S. Chen, P. E. Kraft, M. Bednarski, H. M. Blau, VEGF gene delivery to muscle: potential role for vasculogenesis in adults. *Molecular cell* **2**, 549-558 (Nov, 1998).
  148. M. L. Springer, C. R. Ozawa, A. Banfi, P. E. Kraft, T. K. Ip, T. R. Brazelton, H. M. Blau, Localized arteriole formation directly adjacent to the site of VEGF-induced angiogenesis in muscle. *Molecular therapy : the journal of the American Society of Gene Therapy* **7**, 441-449 (Apr, 2003).
  149. B. M. Deasy, J. M. Feduska, T. R. Payne, Y. Li, F. Ambrosio, J. Huard, Effect of VEGF on the regenerative capacity of muscle stem cells in dystrophic skeletal muscle. *Molecular therapy : the journal of the American Society of Gene Therapy* **17**, 1788-1798 (Oct, 2009).
  150. R. Shah, A. C. Sinanan, J. C. Knowles, N. P. Hunt, M. P. Lewis, Craniofacial muscle engineering using a 3-dimensional phosphate glass fibre construct. *Biomaterials* **26**, 1497-1505 (May, 2005).

151. M. Koning, M. C. Harmsen, M. J. van Luyn, P. M. Werker, Current opportunities and challenges in skeletal muscle tissue engineering. *Journal of tissue engineering and regenerative medicine* **3**, 407-415 (Aug, 2009).
152. C. A. Rossi, M. Pozzobon, P. De Coppi, Advances in musculoskeletal tissue engineering: moving towards therapy. *Organogenesis* **6**, 167-172 (Jul-Sep, 2010).
153. K. A. Athanasiou, G. G. Niederauer, C. M. Agrawal, Sterilization, toxicity, biocompatibility and clinical applications of polylactic acid/polyglycolic acid copolymers. *Biomaterials* **17**, 93-102 (Jan, 1996).
154. M. K. Smith, M. C. Peters, T. P. Richardson, J. C. Garbern, D. J. Mooney, Locally enhanced angiogenesis promotes transplanted cell survival. *Tissue engineering* **10**, 63-71 (Jan-Feb, 2004).
155. L. D. Harris, B. S. Kim, D. J. Mooney, Open pore biodegradable matrices formed with gas foaming. *Journal of biomedical materials research* **42**, 396-402 (Dec 5, 1998).
156. M. C. Peters, P. J. Polverini, D. J. Mooney, Engineering vascular networks in porous polymer matrices. *Journal of biomedical materials research* **60**, 668-678 (Jun 15, 2002).
157. L. Thorrez, J. Shansky, L. Wang, L. Fast, T. VandenDriessche, M. Chuah, D. Mooney, H. Vandenburgh, Growth, differentiation, transplantation and survival of human skeletal myofibers on biodegradable scaffolds. *Biomaterials* **29**, 75-84 (Jan, 2008).
158. A. K. Saxena, J. Marler, M. Benvenuto, G. H. Willital, J. P. Vacanti, Skeletal muscle tissue engineering using isolated myoblasts on synthetic biodegradable polymers: preliminary studies. *Tissue engineering* **5**, 525-532 (Dec, 1999).
159. J. S. Choi, S. J. Lee, G. J. Christ, A. Atala, J. J. Yoo, The influence of electrospun aligned poly(epsilon-caprolactone)/collagen nanofiber meshes on the formation of self-aligned skeletal muscle myotubes. *Biomaterials* **29**, 2899-2906 (Jul, 2008).
160. S. F. Badylak, D. O. Freytes, T. W. Gilbert, Extracellular matrix as a biological scaffold material: Structure and function. *Acta biomaterialia* **5**, 1-13 (Jan, 2009).
161. M. J. Bissell, J. Aggeler, Dynamic reciprocity: how do extracellular matrix and hormones direct gene expression? *Prog Clin Biol Res* **249**, 251-262 (1987).
162. H. K. Kleinman, D. Philp, M. P. Hoffman, Role of the extracellular matrix in morphogenesis. *Curr Opin Biotechnol* **14**, 526-532 (Oct, 2003).
163. F. Rosso, A. Giordano, M. Barbarisi, A. Barbarisi, From cell-ECM interactions to tissue engineering. *J Cell Physiol* **199**, 174-180 (May, 2004).

164. G. A. Di Lullo, S. M. Sweeney, J. Korkko, L. Ala-Kokko, J. D. San Antonio, Mapping the ligand-binding sites and disease-associated mutations on the most abundant protein in the human, type I collagen. *The Journal of biological chemistry* **277**, 4223-4231 (Feb 8, 2002).
165. Y. R. Shih, C. N. Chen, S. W. Tsai, Y. J. Wang, O. K. Lee, Growth of mesenchymal stem cells on electrospun type I collagen nanofibers. *Stem cells* **24**, 2391-2397 (Nov, 2006).
166. L. Heckmann, J. Fiedler, T. Mattes, M. Dauner, R. E. Brenner, Interactive effects of growth factors and three-dimensional scaffolds on multipotent mesenchymal stromal cells. *Biotechnology and applied biochemistry* **49**, 185-194 (Mar, 2008).
167. Y. Zhang, S. Thorn, J. N. DaSilva, M. Lamoureux, R. A. DeKemp, R. S. Beanlands, M. Ruel, E. J. Suuronen, Collagen-based matrices improve the delivery of transplanted circulating progenitor cells: development and demonstration by ex vivo radionuclide cell labeling and in vivo tracking with positron-emission tomography. *Circulation. Cardiovascular imaging* **1**, 197-204 (Nov, 2008).
168. W. Dai, S. L. Hale, G. L. Kay, A. J. Jyrala, R. A. Kloner, Delivering stem cells to the heart in a collagen matrix reduces relocation of cells to other organs as assessed by nanoparticle technology. *Regenerative medicine* **4**, 387-395 (May, 2009).
169. V. Kroehne, I. Heschel, F. Schugner, D. Lasrich, J. W. Bartsch, H. Jockusch, Use of a novel collagen matrix with oriented pore structure for muscle cell differentiation in cell culture and in grafts. *Journal of cellular and molecular medicine* **12**, 1640-1648 (Sep-Oct, 2008).
170. J. Ma, K. Holden, J. Zhu, H. Pan, Y. Li, The application of three-dimensional collagen-scaffolds seeded with myoblasts to repair skeletal muscle defects. *Journal of biomedicine & biotechnology* **2011**, 812135 (2011).
171. S. Carnio, E. Serena, C. A. Rossi, P. De Coppi, N. Elvassore, L. Vitiello, Three-dimensional porous scaffold allows long-term wild-type cell delivery in dystrophic muscle. *Journal of tissue engineering and regenerative medicine* **5**, 1-10 (Jan, 2011).
172. R. Stern, A. A. Asari, K. N. Sugahara, Hyaluronan fragments: an information-rich system. *European journal of cell biology* **85**, 699-715 (Aug, 2006).
173. W. Wang, M. Fan, L. Zhang, S. H. Liu, L. Sun, C. Y. Wang, Compatibility of hyaluronic acid hydrogel and skeletal muscle myoblasts. *Biomedical materials* **4**, 025011 (Apr, 2009).
174. C. A. Rossi, M. Flaibani, B. Blaauw, M. Pozzobon, E. Figallo, C. Reggiani, L. Vitiello, N. Elvassore, P. De Coppi, In vivo tissue engineering of functional skeletal muscle by freshly isolated satellite cells embedded in a photopolymerizable hydrogel. *FASEB*

*journal : official publication of the Federation of American Societies for Experimental Biology* **25**, 2296-2304 (Jul, 2011).

175. P. M. Crapo, T. W. Gilbert, S. F. Badylak, An overview of tissue and whole organ decellularization processes. *Biomaterials* **32**, 3233-3243 (Apr, 2011).
176. A. J. Engler, M. A. Griffin, S. Sen, C. G. Bonnemann, H. L. Sweeney, D. E. Discher, Myotubes differentiate optimally on substrates with tissue-like stiffness: pathological implications for soft or stiff microenvironments. *The Journal of cell biology* **166**, 877-887 (Sep 13, 2004).
177. A. J. Engler, S. Sen, H. L. Sweeney, D. E. Discher, Matrix elasticity directs stem cell lineage specification. *Cell* **126**, 677-689 (Aug 25, 2006).
178. M. M. Stern, R. L. Myers, N. Hammam, K. A. Stern, D. Eberli, S. B. Kritchevsky, S. Soker, M. Van Dyke, The influence of extracellular matrix derived from skeletal muscle tissue on the proliferation and differentiation of myogenic progenitor cells ex vivo. *Biomaterials* **30**, 2393-2399 (Apr, 2009).
179. E. K. Merritt, M. V. Cannon, D. W. Hammers, L. N. Le, R. Gokhale, A. Sarathy, T. J. Song, M. T. Tierney, L. J. Suggs, T. J. Walters, R. P. Farrar, Repair of traumatic skeletal muscle injury with bone-marrow-derived mesenchymal stem cells seeded on extracellular matrix. *Tissue engineering. Part A* **16**, 2871-2881 (Sep, 2010).
180. G. Moon du, G. Christ, J. D. Stitzel, A. Atala, J. J. Yoo, Cyclic mechanical preconditioning improves engineered muscle contraction. *Tissue Eng Part A* **14**, 473-482 (Apr, 2008).
181. B. T. Corona, M. A. Machingal, T. Criswell, M. Vadhavkar, A. C. Dannahower, C. Bergman, W. Zhao, G. J. Christ, Further development of a tissue engineered muscle repair construct in vitro for enhanced functional recovery following implantation in vivo in a murine model of volumetric muscle loss injury. *Tissue Eng Part A* **18**, 1213-1228 (Jun, 2012).
182. M. A. Machingal, B. T. Corona, T. J. Walters, V. Kesireddy, C. N. Koval, A. Dannahower, W. Zhao, J. J. Yoo, G. J. Christ, A tissue-engineered muscle repair construct for functional restoration of an irrecoverable muscle injury in a murine model. *Tissue engineering. Part A* **17**, 2291-2303 (Sep, 2011).
183. C. A. Powell, B. L. Smiley, J. Mills, H. H. Vandenburg, Mechanical stimulation improves tissue-engineered human skeletal muscle. *Am J Physiol Cell Physiol* **283**, C1557-1565 (Nov, 2002).
184. G. H. Borschel, R. G. Dennis, W. M. Kuzon, Jr., Contractile skeletal muscle tissue-engineered on an acellular scaffold. *Plast Reconstr Surg* **113**, 595-602; discussion 603-594 (Feb, 2004).

185. T. Zantop, T. W. Gilbert, M. C. Yoder, S. F. Badylak, Extracellular matrix scaffolds are repopulated by bone marrow-derived cells in a mouse model of achilles tendon reconstruction. *J Orthop Res* **24**, 1299-1309 (Jun, 2006).
186. J. E. Reing, L. Zhang, J. Myers-Irvin, K. E. Cordero, D. O. Freytes, E. Heber-Katz, K. Bedelbaeva, D. McIntosh, A. Dewilde, S. J. Braunhut, S. F. Badylak, Degradation products of extracellular matrix affect cell migration and proliferation. *Tissue engineering. Part A* **15**, 605-614 (Mar, 2009).
187. G. E. Davis, K. J. Bayless, M. J. Davis, G. A. Meininger, Regulation of tissue injury responses by the exposure of matricryptic sites within extracellular matrix molecules. *Am J Pathol* **156**, 1489-1498 (May, 2000).
188. A. Sarikaya, R. Record, C. C. Wu, B. Tullius, S. Badylak, M. Ladisch, Antimicrobial activity associated with extracellular matrices. *Tissue Eng* **8**, 63-71 (Feb, 2002).
189. F. Li, W. Li, S. Johnson, D. Ingram, M. Yoder, S. Badylak, Low-molecular-weight peptides derived from extracellular matrix as chemoattractants for primary endothelial cells. *Endothelium* **11**, 199-206 (May-Aug, 2004).
190. S. L. Voytik-Harbin, A. O. Brightman, B. Waisner, C. H. Lamar, S. F. Badylak, Application and evaluation of the alamarBlue assay for cell growth and survival of fibroblasts. *In Vitro Cell Dev Biol Anim* **34**, 239-246 (Mar, 1998).
191. R. D. Record, D. Hillegonds, C. Simmons, R. Tullius, F. A. Rickey, D. Elmore, S. F. Badylak, In vivo degradation of <sup>14</sup>C-labeled small intestinal submucosa (SIS) when used for urinary bladder repair. *Biomaterials* **22**, 2653-2659 (Oct, 2001).
192. T. W. Gilbert, A. M. Stewart-Akers, A. Simmons-Byrd, S. F. Badylak, Degradation and remodeling of small intestinal submucosa in canine Achilles tendon repair. *J Bone Joint Surg Am* **89**, 621-630 (Mar, 2007).
193. A. J. Allman, T. B. McPherson, S. F. Badylak, L. C. Merrill, B. Kallakury, C. Sheehan, R. H. Raeder, D. W. Metzger, Xenogeneic extracellular matrix grafts elicit a TH2-restricted immune response. *Transplantation* **71**, 1631-1640 (Jun 15, 2001).
194. S. F. Badylak, D. A. Vorp, A. R. Spievack, A. Simmons-Byrd, J. Hanke, D. O. Freytes, A. Thapa, T. W. Gilbert, A. Nieponice, Esophageal reconstruction with ECM and muscle tissue in a dog model. *J Surg Res* **128**, 87-97 (Sep, 2005).
195. S. F. Badylak, T. Hoppo, A. Nieponice, T. W. Gilbert, J. M. Davison, B. A. Jobe, Esophageal preservation in five male patients after endoscopic inner-layer circumferential resection in the setting of superficial cancer: a regenerative medicine approach with a biologic scaffold. *Tissue engineering. Part A* **17**, 1643-1650 (Jun, 2011).

196. J. D. Wood, A. Simmons-Byrd, A. R. Spievack, S. F. Badylak, Use of a particulate extracellular matrix bioscaffold for treatment of acquired urinary incontinence in dogs. *J Am Vet Med Assoc* **226**, 1095-1097 (Apr 1, 2005).
197. R. S. Sutherland, L. S. Baskin, S. W. Hayward, G. R. Cunha, Regeneration of bladder urothelium, smooth muscle, blood vessels and nerves into an acellular tissue matrix. *J Urol* **156**, 571-577 (Aug, 1996).
198. K. A. Robinson, J. Li, M. Mathison, A. Redkar, J. Cui, N. A. Chronos, R. G. Matheny, S. F. Badylak, Extracellular matrix scaffold for cardiac repair. *Circulation* **112**, I135-143 (Aug 30, 2005).
199. T. Ota, T. W. Gilbert, D. Schwartzman, C. F. McTiernan, T. Kitajima, Y. Ito, Y. Sawa, S. F. Badylak, M. A. Zenati, A fusion protein of hepatocyte growth factor enhances reconstruction of myocardium in a cardiac patch derived from porcine urinary bladder matrix. *J Thorac Cardiovasc Surg* **136**, 1309-1317 (Nov, 2008).
200. N. J. Turner, A. J. Yates, Jr., D. J. Weber, I. R. Qureshi, D. B. Stolz, T. W. Gilbert, S. F. Badylak, Xenogeneic extracellular matrix as an inductive scaffold for regeneration of a functioning musculotendinous junction. *Tissue engineering. Part A* **16**, 3309-3317 (Nov, 2010).
201. V. J. Mase, Jr., J. R. Hsu, S. E. Wolf, J. C. Wenke, D. G. Baer, J. Owens, S. F. Badylak, T. J. Walters, Clinical application of an acellular biologic scaffold for surgical repair of a large, traumatic quadriceps femoris muscle defect. *Orthopedics* **33**, 511 (Jul, 2010).
202. J. E. Valentin, N. J. Turner, T. W. Gilbert, S. F. Badylak, Functional skeletal muscle formation with a biologic scaffold. *Biomaterials* **31**, 7475-7484 (Oct, 2010).
203. K. M. Clarke, G. C. Lantz, S. K. Salisbury, S. F. Badylak, M. C. Hiles, S. L. Voytik, Intestine submucosa and polypropylene mesh for abdominal wall repair in dogs. *J Surg Res* **60**, 107-114 (Jan, 1996).
204. K. A. Daly, M. Wolf, S. A. Johnson, S. F. Badylak, A rabbit model of peripheral compartment syndrome with associated rhabdomyolysis and a regenerative medicine approach for treatment. *Tissue Eng Part C Methods* **17**, 631-640 (Jun, 2011).
205. V. Agrawal, B. N. Brown, A. J. Beattie, T. W. Gilbert, S. F. Badylak, Evidence of innervation following extracellular matrix scaffold-mediated remodelling of muscular tissues. *J Tissue Eng Regen Med* **3**, 590-600 (Dec, 2009).
206. S. Badylak, K. Kokini, B. Tullius, A. Simmons-Byrd, R. Morff, Morphologic study of small intestinal submucosa as a body wall repair device. *J Surg Res* **103**, 190-202 (Apr, 2002).

207. J. P. Iannotti, M. J. Codsì, Y. W. Kwon, K. Derwin, J. Ciccone, J. J. Brems, Porcine small intestine submucosa augmentation of surgical repair of chronic two-tendon rotator cuff tears. A randomized, controlled trial. *J Bone Joint Surg Am* **88**, 1238-1244 (Jun, 2006).
208. S. Tottey, S. A. Johnson, P. M. Crapo, J. E. Reing, L. Zhang, H. Jiang, C. J. Medberry, B. Reines, S. F. Badylak, The effect of source animal age upon extracellular matrix scaffold properties. *Biomaterials* **32**, 128-136 (Jan, 2011).
209. N. J. Turner, S. A. Johnson, S. F. Badylak, A histomorphologic study of the normal healing response following digit amputation in C57bl/6 and MRL/MpJ mice. *Archives of histology and cytology* **73**, 103-111 (2010).
210. M. T. Wolf, K. A. Daly, J. E. Reing, S. F. Badylak, Biologic scaffold composed of skeletal muscle extracellular matrix. *Biomaterials* **33**, 2916-2925 (Apr, 2012).
211. Sicari, B., et al., Extracellular Matrix as a Scaffold for Tissue Replacement Following Volumetric Muscle Loss: Remodeling Characteristics from Animal Models and Human Patients., in Tissue Engineering and Regenerative Medicine International Society, North America Annual Conference and Exposition, December 11-14. Oral Presentation, 2011.2011.
212. A. Nieponice, T. W. Gilbert, S. A. Johnson, N. J. Turner, S. F. Badylak, Bone marrow-derived cells participate in the long-term remodeling in a mouse model of esophageal reconstruction. *The Journal of surgical research*, (Oct 6, 2012).
213. P. V. Kochupura, E. U. Azeloglu, D. J. Kelly, S. V. Doronin, S. F. Badylak, I. B. Krukenkamp, I. S. Cohen, G. R. Gaudette, Tissue-engineered myocardial patch derived from extracellular matrix provides regional mechanical function. *Circulation* **112**, I144-149 (Aug 30, 2005).
214. S. F. Badylak, P. V. Kochupura, I. S. Cohen, S. V. Doronin, A. E. Saltman, T. W. Gilbert, D. J. Kelly, R. A. Ignatz, G. R. Gaudette, The use of extracellular matrix as an inductive scaffold for the partial replacement of functional myocardium. *Cell transplantation* **15 Suppl 1**, S29-40 (2006).
215. L. Arnold, A. Henry, F. Poron, Y. Baba-Amer, N. van Rooijen, A. Plonquet, R. K. Gherardi, B. Chazaud, Inflammatory monocytes recruited after skeletal muscle injury switch into antiinflammatory macrophages to support myogenesis. *The Journal of experimental medicine* **204**, 1057-1069 (May 14, 2007).
216. Y. P. Li, TNF-alpha is a mitogen in skeletal muscle. *American journal of physiology. Cell physiology* **285**, C370-376 (Aug, 2003).
217. D. Ruffell, F. Mourkioti, A. Gambardella, P. Kirstetter, R. G. Lopez, N. Rosenthal, C. Nerlov, A CREB-C/EBPbeta cascade induces M2 macrophage-specific gene expression

- and promotes muscle injury repair. *Proceedings of the National Academy of Sciences of the United States of America* **106**, 17475-17480 (Oct 13, 2009).
218. J. G. Tidball, M. Wehling-Henricks, Macrophages promote muscle membrane repair and muscle fibre growth and regeneration during modified muscle loading in mice in vivo. *J Physiol* **578**, 327-336 (Jan 1, 2007).
  219. J. S. Burchfield, M. Iwasaki, M. Koyanagi, C. Urbich, N. Rosenthal, A. M. Zeiher, S. Dimmeler, Interleukin-10 from transplanted bone marrow mononuclear cells contributes to cardiac protection after myocardial infarction. *Circulation research* **103**, 203-211 (Jul 18, 2008).
  220. K. Le Blanc, O. Ringden, Immunomodulation by mesenchymal stem cells and clinical experience. *Journal of internal medicine* **262**, 509-525 (Nov, 2007).
  221. A. I. Caplan, J. E. Dennis, Mesenchymal stem cells as trophic mediators. *Journal of cellular biochemistry* **98**, 1076-1084 (Aug 1, 2006).
  222. B. M. Sicari, S. A. Johnson, B. F. Siu, P. M. Crapo, K. A. Daly, H. Jiang, C. J. Medberry, S. Tottey, N. J. Turner, S. F. Badylak, The effect of source animal age upon the in vivo remodeling characteristics of an extracellular matrix scaffold. *Biomaterials* **33**, 5524-5533 (Aug, 2012).
  223. A. Ayyildiz, K. T. Akgul, E. Huri, B. Nuhoglu, B. Kilicoglu, H. Ustun, M. Gurdal, C. Germiyanoglu, Use of porcine small intestinal submucosa in bladder augmentation in rabbit: long-term histological outcome. *ANZ journal of surgery* **78**, 82-86 (Jan-Feb, 2008).
  224. C. G. Zalavras, R. Gardocki, E. Huang, M. Stevanovic, T. Hedman, J. Tibone, Reconstruction of large rotator cuff tendon defects with porcine small intestinal submucosa in an animal model. *Journal of shoulder and elbow surgery / American Shoulder and Elbow Surgeons ... [et al.]* **15**, 224-231 (Mar-Apr, 2006).
  225. J. E. Adams, M. E. Zobitz, J. S. Reach, Jr., K. N. An, S. P. Steinmann, Rotator cuff repair using an acellular dermal matrix graft: an in vivo study in a canine model. *Arthroscopy : the journal of arthroscopic & related surgery : official publication of the Arthroscopy Association of North America and the International Arthroscopy Association* **22**, 700-709 (Jul, 2006).
  226. M. H. Zheng, J. Chen, Y. Kirilak, C. Willers, J. Xu, D. Wood, Porcine small intestine submucosa (SIS) is not an acellular collagenous matrix and contains porcine DNA: possible implications in human implantation. *Journal of biomedical materials research. Part B, Applied biomaterials* **73**, 61-67 (Apr, 2005).

227. T. Doede, M. Bondartschuk, C. Joerck, E. Schulze, M. Goernig, Unsuccessful alloplastic esophageal replacement with porcine small intestinal submucosa. *Artificial organs* **33**, 328-333 (Apr, 2009).
228. J. R. Walton, N. K. Bowman, Y. Khatib, J. Linklater, G. A. Murrell, Restore orthobiologic implant: not recommended for augmentation of rotator cuff repairs. *The Journal of bone and joint surgery. American volume* **89**, 786-791 (Apr, 2007).
229. T. J. Keane, R. Londono, N. J. Turner, S. F. Badylak, Consequences of ineffective decellularization of biologic scaffolds on the host response. *Biomaterials* **33**, 1771-1781 (Feb, 2012).
230. L. Ansaloni, P. Cambrini, F. Catena, S. Di Saverio, S. Gagliardi, F. Gazzotti, J. P. Hodde, D. W. Metzger, L. D'Alessandro, A. D. Pinna, Immune response to small intestinal submucosa (surgisis) implant in humans: preliminary observations. *J Invest Surg* **20**, 237-241 (Jul-Aug, 2007).
231. L. L. Pu, Small intestinal submucosa (Surgisis) as a bioactive prosthetic material for repair of abdominal wall fascial defect. *Plast Reconstr Surg* **115**, 2127-2131 (Jun, 2005).
232. N. A. Kissane, K. M. Itani, A decade of ventral incisional hernia repairs with biologic acellular dermal matrix: what have we learned? *Plast Reconstr Surg* **130**, 194S-202S (Nov, 2012).
233. W. W. Hope, D. Griner, A. Adams, W. B. Hooks, T. V. Clancy, Use and indications of human acellular dermis in ventral hernia repair at a community hospital. *Plast Surg Int* **2012**, 918345 (2012).
234. E. Lullove, Acellular fetal bovine dermal matrix in the treatment of nonhealing wounds in patients with complex comorbidities. *J Am Podiatr Med Assoc* **102**, 233-239 (May-Jun, 2012).
235. J. A. Niezgoda, C. C. Van Gils, R. G. Frykberg, J. P. Hodde, Randomized clinical trial comparing OASIS Wound Matrix to Regranex Gel for diabetic ulcers. *Adv Skin Wound Care* **18**, 258-266 (Jun, 2005).
236. K. A. Derwin, S. F. Badylak, S. P. Steinmann, J. P. Iannotti, Extracellular matrix scaffold devices for rotator cuff repair. *Journal of shoulder and elbow surgery / American Shoulder and Elbow Surgeons ... [et al.]* **19**, 467-476 (Apr, 2010).
237. S. P. Badhe, T. M. Lawrence, F. D. Smith, P. G. Lunn, An assessment of porcine dermal xenograft as an augmentation graft in the treatment of extensive rotator cuff tears. *J Shoulder Elbow Surg* **17**, 35S-39S (Jan-Feb, 2008).
238. I. Wong, J. Burns, S. Snyder, Arthroscopic GraftJacket repair of rotator cuff tears. *J Shoulder Elbow Surg* **19**, 104-109 (Mar, 2010).

239. A. Cheng, M. Saint-Cyr, Comparison of different ADM materials in breast surgery. *Clin Plast Surg* **39**, 167-175 (Apr, 2012).
240. M. M. Mofid, M. S. Meininger, M. S. Lacey, Veritas(R) bovine pericardium for immediate breast reconstruction: a xenograft alternative to acellular dermal matrix products. *Eur J Plast Surg* **35**, 717-722 (Oct, 2012).
241. A. O. Momoh, A. M. Kamat, C. E. Butler, Reconstruction of the pelvic floor with human acellular dermal matrix and omental flap following anterior pelvic exenteration. *J Plast Reconstr Aesthet Surg* **63**, 2185-2187 (Dec, 2010).
242. J. G. Han, Z. J. Wang, Z. G. Gao, H. M. Xu, Z. H. Yang, M. L. Jin, Pelvic floor reconstruction using human acellular dermal matrix after cylindrical abdominoperineal resection. *Dis Colon Rectum* **53**, 219-223 (Feb, 2010).
243. A. C. Weiser, I. Franco, D. B. Herz, R. I. Silver, E. F. Reda, Single layered small intestinal submucosa in the repair of severe chordee and complicated hypospadias. *J Urol* **170**, 1593-1595; discussion 1595 (Oct, 2003).
244. C. P. Carpenter, L. N. Daniali, N. P. Shah, M. Granick, M. L. Jordan, Distal urethral reconstruction with AlloDerm: a case report and review of the literature. *Can J Urol* **19**, 6207-6210 (Apr, 2012).
245. Sicari, B., et al., Extracellular Matrix as a Scaffold for Tissue Replacement Following Volumetric Muscle Loss: Remodeling Characteristics from Animal Models and Human Patients., in Tissue Engineering and Regenerative Medicine International Society, North America Annual Conference and Exposition, December 11-14. Oral Presentation, 2011.2011.
246. S. Gordon, P. R. Taylor, Monocyte and macrophage heterogeneity. *Nature reviews. Immunology* **5**, 953-964 (Dec, 2005).
247. D. M. Mosser, The many faces of macrophage activation. *J Leukoc Biol* **73**, 209-212 (Feb, 2003).
248. R. D. Stout, C. Jiang, B. Matta, I. Tietzel, S. K. Watkins, J. Suttles, Macrophages sequentially change their functional phenotype in response to changes in microenvironmental influences. *J Immunol* **175**, 342-349 (Jul 1, 2005).
249. Y. Kharraz, J. Guerra, C. J. Mann, A. L. Serrano, P. Munoz-Canoves, Macrophage plasticity and the role of inflammation in skeletal muscle repair. *Mediators of inflammation* **2013**, 491497 (2013).

250. M. Saclier, S. Cuvellier, M. Magnan, R. Mounier, B. Chazaud, Monocyte/macrophage interactions with myogenic precursor cells during skeletal muscle regeneration. *The FEBS journal* **280**, 4118-4130 (Sep, 2013).
251. D. R. Thomas, Loss of skeletal muscle mass in aging: examining the relationship of starvation, sarcopenia and cachexia. *Clin Nutr* **26**, 389-399 (Aug, 2007).
252. I. Janssen, D. S. Shepard, P. T. Katzmarzyk, R. Roubenoff, The healthcare costs of sarcopenia in the United States. *J Am Geriatr Soc* **52**, 80-85 (Jan, 2004).
253. E. Marzetti, C. Leeuwenburgh, Skeletal muscle apoptosis, sarcopenia and frailty at old age. *Exp Gerontol* **41**, 1234-1238 (Dec, 2006).
254. A. S. Brack, M. J. Conboy, S. Roy, M. Lee, C. J. Kuo, C. Keller, T. A. Rando, Increased Wnt signaling during aging alters muscle stem cell fate and increases fibrosis. *Science* **317**, 807-810 (Aug 10, 2007).
255. G. Goldspink, Age-related muscle loss and progressive dysfunction in mechanosensitive growth factor signaling. *Ann N Y Acad Sci* **1019**, 294-298 (Jun, 2004).
256. M. D. Grounds, Age-associated changes in the response of skeletal muscle cells to exercise and regeneration. *Ann N Y Acad Sci* **854**, 78-91 (Nov 20, 1998).
257. I. M. Conboy, M. J. Conboy, G. M. Smythe, T. A. Rando, Notch-mediated restoration of regenerative potential to aged muscle. *Science* **302**, 1575-1577 (Nov 28, 2003).
258. I. M. Conboy, T. A. Rando, Aging, stem cells and tissue regeneration: lessons from muscle. *Cell Cycle* **4**, 407-410 (Mar, 2005).
259. S. I. Zacks, M. F. Sheff, Age-related impeded regeneration of mouse minced anterior tibial muscle. *Muscle Nerve* **5**, 152-161 (Feb, 1982).
260. I. M. Conboy, M. J. Conboy, A. J. Wagers, E. R. Girma, I. L. Weissman, T. A. Rando, Rejuvenation of aged progenitor cells by exposure to a young systemic environment. *Nature* **433**, 760-764 (Feb 17, 2005).
261. R. Solana, R. Tarazona, I. Gayoso, O. Lesur, G. Dupuis, T. Fulop, Innate immunosenescence: effect of aging on cells and receptors of the innate immune system in humans. *Seminars in immunology* **24**, 331-341 (Oct, 2012).
262. A. C. Shaw, S. Joshi, H. Greenwood, A. Panda, J. M. Lord, Aging of the innate immune system. *Current opinion in immunology* **22**, 507-513 (Aug, 2010).
263. P. Yoon, K. T. Keylock, M. E. Hartman, G. G. Freund, J. A. Woods, Macrophage hypo-responsiveness to interferon-gamma in aged mice is associated with impaired signaling through Jak-STAT. *Mech Ageing Dev* **125**, 137-143 (Feb, 2004).

264. E. D. Boehmer, J. Goral, D. E. Faunce, E. J. Kovacs, Age-dependent decrease in Toll-like receptor 4-mediated proinflammatory cytokine production and mitogen-activated protein kinase expression. *J Leukoc Biol* **75**, 342-349 (Feb, 2004).
265. R. L. Chelvarajan, S. M. Collins, J. M. Van Willigen, S. Bondada, The unresponsiveness of aged mice to polysaccharide antigens is a result of a defect in macrophage function. *J Leukoc Biol* **77**, 503-512 (Apr, 2005).
266. S. Antonaci, E. Jirillo, M. T. Ventura, A. R. Garofalo, L. Bonomo, Non-specific immunity in aging: deficiency of monocyte and polymorphonuclear cell-mediated functions. *Mech Ageing Dev* **24**, 367-375 (Mar, 1984).
267. J. Plowden, M. Renshaw-Hoelscher, C. Engleman, J. Katz, S. Sambhara, Innate immunity in aging: impact on macrophage function. *Aging Cell* **3**, 161-167 (Aug, 2004).
268. J. Lloberas, A. Celada, Effect of aging on macrophage function. *Exp Gerontol* **37**, 1325-1331 (Dec, 2002).
269. E. Ortega, J. J. Garcia, M. De la Fuente, Modulation of adherence and chemotaxis of macrophages by norepinephrine. Influence of ageing. *Mol Cell Biochem* **203**, 113-117 (Jan, 2000).
270. G. S. Ashcroft, M. A. Horan, M. W. Ferguson, Aging is associated with reduced deposition of specific extracellular matrix components, an upregulation of angiogenesis, and an altered inflammatory response in a murine incisional wound healing model. *J Invest Dermatol* **108**, 430-437 (Apr, 1997).
271. M. Renshaw, J. Rockwell, C. Engleman, A. Gewirtz, J. Katz, S. Sambhara, Cutting edge: impaired Toll-like receptor expression and function in aging. *J Immunol* **169**, 4697-4701 (Nov 1, 2002).
272. Y. Shimada, H. Ito, Heterogeneous aging of macrophage-lineage cells in the capacity for TNF production and self renewal in C57BL/6 mice. *Mech Ageing Dev* **87**, 183-195 (Jun 25, 1996).
273. R. L. Chelvarajan, Y. Liu, D. Popa, M. L. Getchell, T. V. Getchell, A. J. Stromberg, S. Bondada, Molecular basis of age-associated cytokine dysregulation in LPS-stimulated macrophages. *J Leukoc Biol* **79**, 1314-1327 (Jun, 2006).
274. W. Burgess, Q. Liu, J. Zhou, Q. Tang, A. Ozawa, R. VanHoy, S. Arkins, R. Dantzer, K. W. Kelley, The immune-endocrine loop during aging: role of growth hormone and insulin-like growth factor-I. *Neuroimmunomodulation* **6**, 56-68 (Jan-Apr, 1999).

275. S. Mahbub, C. R. Deburghgraeve, E. J. Kovacs, Advanced age impairs macrophage polarization. *Journal of interferon & cytokine research : the official journal of the International Society for Interferon and Cytokine Research* **32**, 18-26 (Jan, 2012).
276. N. J. Turner, A. J. Yates, D. J. Weber, I. R. Qureshi, D. B. Stolz, T. W. Gilbert, S. F. Badylak, Xenogeneic Extracellular Matrix as an Inductive Scaffold for Regeneration of a Functioning Musculotendinous Junction. *Tissue Eng Part A*, (Aug 1, 2010).
277. S. A. Brigido, S. F. Boc, R. C. Lopez, Effective management of major lower extremity wounds using an acellular regenerative tissue matrix: a pilot study. *Orthopedics* **27**, s145-149 (Jan, 2004).
278. A. Nieponice, K. McGrath, I. Qureshi, E. J. Beckman, J. D. Luketich, T. W. Gilbert, S. F. Badylak, An extracellular matrix scaffold for esophageal stricture prevention after circumferential EMR. *Gastrointest Endosc* **69**, 289-296 (Feb, 2009).
279. A. Nieponice, T. W. Gilbert, S. F. Badylak, Reinforcement of esophageal anastomoses with an extracellular matrix scaffold in a canine model. *Ann Thorac Surg* **82**, 2050-2058 (Dec, 2006).
280. P. G. De Deyne, S. M. Kladakis, Bioscaffolds in tissue engineering: a rationale for use in the reconstruction of musculoskeletal soft tissues. *Clin Podiatr Med Surg* **22**, 521-532, v (Oct, 2005).
281. P. Akhyari, H. Kamiya, A. Haverich, M. Karck, A. Lichtenberg, Myocardial tissue engineering: the extracellular matrix. *Eur J Cardiothorac Surg* **34**, 229-241 (Aug, 2008).
282. U. Rowlatt, Intrauterine wound healing in a 20 week human fetus. *Virchows Arch A Pathol Anat Histol* **381**, 353-361 (Mar 23, 1979).
283. A. J. Cowin, M. P. Brosnan, T. M. Holmes, M. W. Ferguson, Endogenous inflammatory response to dermal wound healing in the fetal and adult mouse. *Dev Dyn* **212**, 385-393 (Jul, 1998).
284. J. Hopkinson-Woolley, D. Hughes, S. Gordon, P. Martin, Macrophage recruitment during limb development and wound healing in the embryonic and foetal mouse. *J Cell Sci* **107** (Pt 5), 1159-1167 (May, 1994).
285. J. Brock, K. Midwinter, J. Lewis, P. Martin, Healing of incisional wounds in the embryonic chick wing bud: characterization of the actin purse-string and demonstration of a requirement for Rho activation. *J Cell Biol* **135**, 1097-1107 (Nov, 1996).
286. P. Martin, J. Lewis, Actin cables and epidermal movement in embryonic wound healing. *Nature* **360**, 179-183 (Nov 12, 1992).

287. T. Sawai, N. Usui, K. Sando, Y. Fukui, S. Kamata, A. Okada, N. Taniguchi, N. Itano, K. Kimata, Hyaluronic acid of wound fluid in adult and fetal rabbits. *J Pediatr Surg* **32**, 41-43 (Jan, 1997).
288. D. C. West, D. M. Shaw, P. Lorenz, N. S. Adzick, M. T. Longaker, Fibrotic healing of adult and late gestation fetal wounds correlates with increased hyaluronidase activity and removal of hyaluronan. *Int J Biochem Cell Biol* **29**, 201-210 (Jan, 1997).
289. D. J. Whitby, M. W. Ferguson, The extracellular matrix of lip wounds in fetal, neonatal and adult mice. *Development* **112**, 651-668 (Jun, 1991).
290. M. T. Longaker, D. J. Whitby, M. W. Ferguson, M. R. Harrison, T. M. Crombleholme, J. C. Langer, K. C. Cochrum, E. D. Verrier, R. Stern, Studies in fetal wound healing: III. Early deposition of fibronectin distinguishes fetal from adult wound healing. *J Pediatr Surg* **24**, 799-805 (Aug, 1989).
291. B. P. Toole, T. N. Wight, M. I. Tammi, Hyaluronan-cell interactions in cancer and vascular disease. *J Biol Chem* **277**, 4593-4596 (Feb 15, 2002).
292. M. T. Longaker, E. S. Chiu, N. S. Adzick, M. Stern, M. R. Harrison, R. Stern, Studies in fetal wound healing. V. A prolonged presence of hyaluronic acid characterizes fetal wound fluid. *Ann Surg* **213**, 292-296 (Apr, 1991).
293. H. N. Lovvorn Iii, D. T. Cheung, M. E. Nimni, N. Perelman, J. M. Estes, N. S. Adzick, Relative distribution and crosslinking of collagen distinguish fetal from adult sheep wound repair. *Journal of Pediatric Surgery* **34**, 218-223 (1999).
294. S. F. Badylak, The extracellular matrix as a biologic scaffold material. *Biomaterials* **28**, 3587-3593 (Sep, 2007).
295. A. V. Boruch, A. Nieponice, I. R. Qureshi, T. W. Gilbert, S. F. Badylak, Constructive remodeling of biologic scaffolds is dependent on early exposure to physiologic bladder filling in a canine partial cystectomy model. *J Surg Res* **161**, 217-225 (Jun 15, 2010).
296. W. H. Eaglstein, V. Falanga, Tissue engineering and the development of Apligraf a human skin equivalent. *Adv Wound Care* **11**, 1-8 (Jul-Aug, 1998).
297. N. Bhattacharya, Fetal cell/tissue therapy in adult disease: a new horizon in regenerative medicine. *Clin Exp Obstet Gynecol* **31**, 167-173 (2004).
298. S. F. Badylak, G. C. Lantz, A. Coffey, L. A. Geddes, Small intestinal submucosa as a large diameter vascular graft in the dog. *The Journal of surgical research* **47**, 74-80 (Jul, 1989).
299. L. Kamentsky, T. R. Jones, A. Fraser, M. A. Bray, D. J. Logan, K. L. Madden, V. Ljosa, C. Rueden, K. W. Eliceiri, A. E. Carpenter, Improved structure, function and

- compatibility for CellProfiler: modular high-throughput image analysis software. *Bioinformatics* **27**, 1179-1180 (Apr 15, 2011).
300. M. R. Lamprecht, D. M. Sabatini, A. E. Carpenter, CellProfiler: free, versatile software for automated biological image analysis. *Biotechniques* **42**, 71-75 (Jan, 2007).
  301. D. T. Butcher, T. Alliston, V. M. Weaver, A tense situation: forcing tumour progression. *Nat Rev Cancer* **9**, 108-122 (Feb, 2009).
  302. S. Calve, S. J. Odelberg, H. G. Simon, A transitional extracellular matrix instructs cell behavior during muscle regeneration. *Dev Biol* **344**, 259-271 (Aug 1, 2010).
  303. H. N. Lovvorn, 3rd, D. T. Cheung, M. E. Nimni, N. Perelman, J. M. Estes, N. S. Adzick, Relative distribution and crosslinking of collagen distinguish fetal from adult sheep wound repair. *J Pediatr Surg* **34**, 218-223 (Jan, 1999).
  304. F. O. Martinez, S. Gordon, M. Locati, A. Mantovani, Transcriptional profiling of the human monocyte-to-macrophage differentiation and polarization: new molecules and patterns of gene expression. *J Immunol* **177**, 7303-7311 (Nov 15, 2006).
  305. B. N. Brown, R. Londono, S. Tottey, L. Zhang, K. A. Kukla, M. T. Wolf, K. A. Daly, J. E. Reing, S. F. Badylak, Macrophage phenotype as a predictor of constructive remodeling following the implantation of biologically derived surgical mesh materials. *Acta Biomater*, (Dec 2, 2011).
  306. D. M. Underhill, A. Ozinsky, K. D. Smith, A. Aderem, Toll-like receptor-2 mediates mycobacteria-induced proinflammatory signaling in macrophages. *Proceedings of the National Academy of Sciences of the United States of America* **96**, 14459-14463 (Dec 7, 1999).
  307. C. D. Mills, K. Kincaid, J. M. Alt, M. J. Heilman, A. M. Hill, M-1/M-2 macrophages and the Th1/Th2 paradigm. *Journal of immunology* **164**, 6166-6173 (Jun 15, 2000).
  308. J. M. Wainwright, R. Hashizume, K. L. Fujimoto, N. T. Remlinger, C. Pesyna, W. R. Wagner, K. Tobita, T. W. Gilbert, S. F. Badylak, Right ventricular outflow tract repair with a cardiac biologic scaffold. *Cells, tissues, organs* **195**, 159-170 (2012).
  309. D. Shi, H. Reinecke, C. E. Murry, B. Torok-Storb, Myogenic fusion of human bone marrow stromal cells, but not hematopoietic cells. *Blood* **104**, 290-294 (Jul 1, 2004).
  310. M. L. Novak, T. J. Koh, Phenotypic transitions of macrophages orchestrate tissue repair. *The American journal of pathology* **183**, 1352-1363 (Nov, 2013).
  311. X. Wang, H. Wu, Z. Zhang, S. Liu, J. Yang, X. Chen, M. Fan, X. Wang, Effects of interleukin-6, leukemia inhibitory factor, and ciliary neurotrophic factor on the proliferation and differentiation of adult human myoblasts. *Cellular and molecular neurobiology* **28**, 113-124 (Jan, 2008).

312. B. Deng, M. Wehling-Henricks, S. A. Villalta, Y. Wang, J. G. Tidball, IL-10 triggers changes in macrophage phenotype that promote muscle growth and regeneration. *Journal of immunology* **189**, 3669-3680 (Oct 1, 2012).
313. M. Hill, A. Wernig, G. Goldspink, Muscle satellite (stem) cell activation during local tissue injury and repair. *J Anat* **203**, 89-99 (Jul, 2003).
314. T. L. Adair-Kirk, J. J. Atkinson, D. G. Kelley, R. H. Arch, J. H. Miner, R. M. Senior, A chemotactic peptide from laminin alpha 5 functions as a regulator of inflammatory immune responses via TNF alpha-mediated signaling. *J Immunol* **174**, 1621-1629 (Feb 1, 2005).
315. T. A. Lew, J. A. Walker, J. C. Wenke, L. H. Blackbourne, R. G. Hale, Characterization of craniomaxillofacial battle injuries sustained by United States service members in the current conflicts of Iraq and Afghanistan. *J Oral Maxillofac Surg* **68**, 3-7 (Jan, 2010).
316. M. T. Mazurek, J. R. Ficke, The scope of wounds encountered in casualties from the global war on terrorism: from the battlefield to the tertiary treatment facility. *J Am Acad Orthop Surg* **14**, S18-23 (2006).
317. B. D. Owens, J. F. Kragh, Jr., J. C. Wenke, J. Macaitis, C. E. Wade, J. B. Holcomb, Combat wounds in operation Iraqi Freedom and operation Enduring Freedom. *J Trauma* **64**, 295-299 (Feb, 2008).
318. S. J. Mannion, E. Chaloner, Principles of war surgery. *BMJ* **330**, 1498-1500 (Jun 25, 2005).
319. G. Bowyer, Debridement of extremity war wounds. *J Am Acad Orthop Surg* **14**, S52-56 (2006).
320. M. Deutinger, R. Kuzbari, T. Paternostro-Sluga, M. Quittan, A. Zauner-Dungl, A. Wörseg, B. Todoroff, J. Holle, Donor-site morbidity of the gracilis flap. *Plastic and reconstructive surgery* **95**, 1240-1244 (Jun, 1995).
321. Y. Kimata, K. Uchiyama, S. Ebihara, M. Sakuraba, H. Iida, T. Nakatsuka, K. Harii, Anterolateral thigh flap donor-site complications and morbidity. *Plastic and reconstructive surgery* **106**, 584-589 (Sep, 2000).
322. D. J. Kelly, A. B. Rosen, A. J. Schuldt, P. V. Kochupura, S. V. Doronin, I. A. Potapova, E. U. Azeloglu, S. F. Badylak, P. R. Brink, I. S. Cohen, G. R. Gaudette, Increased myocyte content and mechanical function within a tissue-engineered myocardial patch following implantation. *Tissue Eng Part A* **15**, 2189-2201 (Aug, 2009).

323. D. O. Freytes, S. F. Badylak, T. J. Webster, L. A. Geddes, A. E. Rundell, Biaxial strength of multilaminated extracellular matrix scaffolds. *Biomaterials* **25**, 2353-2361 (May, 2004).
324. M. Kitzmann, G. Carnac, M. Vandromme, M. Primig, N. J. Lamb, A. Fernandez, The muscle regulatory factors MyoD and myf-5 undergo distinct cell cycle-specific expression in muscle cells. *J Cell Biol* **142**, 1447-1459 (Sep 21, 1998).
325. C. A. Collins, I. Olsen, P. S. Zammit, L. Heslop, A. Petrie, T. A. Partridge, J. E. Morgan, Stem cell function, self-renewal, and behavioral heterogeneity of cells from the adult muscle satellite cell niche. *Cell* **122**, 289-301 (Jul 29, 2005).
326. J. Rantanen, T. Hurme, R. Lukka, J. Heino, H. Kalimo, Satellite cell proliferation and the expression of myogenin and desmin in regenerating skeletal muscle: evidence for two different populations of satellite cells. *Lab Invest* **72**, 341-347 (Mar, 1995).
327. J. Dhawan, T. A. Rando, Stem cells in postnatal myogenesis: molecular mechanisms of satellite cell quiescence, activation and replenishment. *Trends Cell Biol* **15**, 666-673 (Dec, 2005).
328. H. C. Olguin, B. B. Olwin, Pax-7 up-regulation inhibits myogenesis and cell cycle progression in satellite cells: a potential mechanism for self-renewal. *Dev Biol* **275**, 375-388 (Nov 15, 2004).
329. D. Sun, C. O. Martinez, O. Ochoa, L. Ruiz-Willhite, J. R. Bonilla, V. E. Centonze, L. L. Waite, J. E. Michalek, L. M. McManus, P. K. Shireman, Bone marrow-derived cell regulation of skeletal muscle regeneration. *FASEB J* **23**, 382-395 (Feb, 2009).
330. A. S. de la Garza-Rodea, I. van der Velde, H. Boersma, M. A. Goncalves, D. W. van Bekkum, A. A. de Vries, S. Knaan-Shanzer, Long-term contribution of human bone marrow mesenchymal stromal cells to skeletal muscle regeneration in mice. *Cell Transplant* **20**, 217-231 (2011).
331. C. Drapeau, D. Antarr, H. Ma, Z. Yang, L. Tang, R. M. Hoffman, D. J. Schaeffer, Mobilization of bone marrow stem cells with StemEnhance improves muscle regeneration in cardiotoxin-induced muscle injury. *Cell Cycle* **9**, 1819-1823 (May, 2010).
332. K. Ojima, A. Uezumi, H. Miyoshi, S. Masuda, Y. Morita, A. Fukase, A. Hattori, H. Nakauchi, Y. Miyagoe-Suzuki, S. Takeda, Mac-1(low) early myeloid cells in the bone marrow-derived SP fraction migrate into injured skeletal muscle and participate in muscle regeneration. *Biochem Biophys Res Commun* **321**, 1050-1061 (Sep 3, 2004).
333. R. Couteaux, J. C. Mira, A. d'Albis, Regeneration of muscles after cardiotoxin injury. I. Cytological aspects. *Biol Cell* **62**, 171-182 (1988).

334. H. M. Price, E. L. Howes, Jr., J. M. Blumberg, Ultrastructural Alterations in Skeletal Muscle Fibers Injured by Cold. II. Cells on the Sarcolemmal Tube: Observations on "Discontinuous" Regeneration and Myofibril Formation. *Lab Invest* **13**, 1279-1302 (Oct, 1964).
335. G. L. Warren, C. P. Ingalls, S. J. Shah, R. B. Armstrong, Uncoupling of in vivo torque production from EMG in mouse muscles injured by eccentric contractions. *The Journal of physiology* **515** ( Pt 2), 609-619 (Mar 1, 1999).
336. D. A. Lowe, G. L. Warren, C. P. Ingalls, D. B. Boorstein, R. B. Armstrong, Muscle function and protein metabolism after initiation of eccentric contraction-induced injury. *J Appl Physiol* **79**, 1260-1270 (Oct, 1995).
337. J. E. Valentin, J. S. Badylak, G. P. McCabe, S. F. Badylak, Extracellular matrix bioscaffolds for orthopaedic applications. A comparative histologic study. *J Bone Joint Surg Am* **88**, 2673-2686 (Dec, 2006).
338. S. F. Badylak, T. W. Gilbert, Immune response to biologic scaffold materials. *Semin Immunol* **20**, 109-116 (Apr, 2008).
339. E. Vorotnikova, D. McIntosh, A. Dewilde, J. Zhang, J. E. Reing, L. Zhang, K. Cordero, K. Bedelbaeva, D. Gourevitch, E. Heber-Katz, S. F. Badylak, S. J. Braunhut, Extracellular matrix-derived products modulate endothelial and progenitor cell migration and proliferation in vitro and stimulate regenerative healing in vivo. *Matrix Biol* **29**, 690-700 (Oct, 2010).
340. H. Yin, F. Price, M. A. Rudnicki, Satellite cells and the muscle stem cell niche. *Physiol Rev* **93**, 23-67 (Jan, 2013).
341. J. M. Beiner, P. Jokl, Muscle contusion injuries: current treatment options. *J Am Acad Orthop Surg* **9**, 227-237 (Jul-Aug, 2001).
342. T. A. Jarvinen, T. L. Jarvinen, M. Kaariainen, H. Kalimo, M. Jarvinen, Muscle injuries: biology and treatment. *Am J Sports Med* **33**, 745-764 (May, 2005).
343. S. Ciciliot, S. Schiaffino, Regeneration of mammalian skeletal muscle. Basic mechanisms and clinical implications. *Curr Pharm Des* **16**, 906-914 (2010).
344. G. L. Warren, M. Summan, X. Gao, R. Chapman, T. Hulderman, P. P. Simeonova, Mechanisms of skeletal muscle injury and repair revealed by gene expression studies in mouse models. *J Physiol* **582**, 825-841 (Jul 15, 2007).
345. B. Leitgeb, Structural investigation of endomorphins by experimental and theoretical methods: hunting for the bioactive conformation. *Chemistry & biodiversity* **4**, 2703-2724 (Dec, 2007).

346. M. Klinkenberg, S. Fischer, T. Kremer, F. Hernekamp, M. Lehnhardt, A. Daigeler, Comparison of anterolateral thigh, lateral arm, and parascapular free flaps with regard to donor-site morbidity and aesthetic and functional outcomes. *Plastic and reconstructive surgery* **131**, 293-302 (Feb, 2013).
347. M. H. Snow, An autoradiographic study of satellite cell differentiation into regenerating myotubes following transplantation of muscles in young rats. *Cell Tissue Res* **186**, 535-540 (Jan 31, 1978).
348. M. A. LaBarge, H. M. Blau, Biological progression from adult bone marrow to mononucleate muscle stem cell to multinucleate muscle fiber in response to injury. *Cell* **111**, 589-601 (Nov 15, 2002).
349. A. T. Palermo, M. A. Labarge, R. Doyonnas, J. Pomerantz, H. M. Blau, Bone marrow contribution to skeletal muscle: a physiological response to stress. *Dev Biol* **279**, 336-344 (Mar 15, 2005).
350. F. Relaix, D. Rocancourt, A. Mansouri, M. Buckingham, A Pax3/Pax7-dependent population of skeletal muscle progenitor cells. *Nature* **435**, 948-953 (Jun 16, 2005).
351. R. W. Ten Broek, S. Grefte, J. W. Von den Hoff, Regulatory factors and cell populations involved in skeletal muscle regeneration. *J Cell Physiol* **224**, 7-16 (Jul, 2010).
352. B. Chazaud, M. Brigitte, H. Yacoub-Youssef, L. Arnold, R. Gherardi, C. Sonnet, P. Lafuste, F. Chretien, Dual and beneficial roles of macrophages during skeletal muscle regeneration. *Exerc Sport Sci Rev* **37**, 18-22 (Jan, 2009).
353. M. J. Bissell, H. G. Hall, G. Parry, How does the extracellular matrix direct gene expression? *J Theor Biol* **99**, 31-68 (Nov 7, 1982).
354. N. Boudreau, C. Myers, M. J. Bissell, From laminin to lamin: regulation of tissue-specific gene expression by the ECM. *Trends Cell Biol* **5**, 1-4 (Jan, 1995).
355. D. Ingber, Extracellular matrix and cell shape: potential control points for inhibition of angiogenesis. *J Cell Biochem* **47**, 236-241 (Nov, 1991).
356. B. Perniconi, A. Costa, P. Aulino, L. Teodori, S. Adamo, D. Coletti, The pro-myogenic environment provided by whole organ scale acellular scaffolds from skeletal muscle. *Biomaterials* **32**, 7870-7882 (Nov, 2011).
357. B. M. Sicari, V. Agrawal, B. F. Siu, C. J. Medberry, C. L. Dearth, N. J. Turner, S. F. Badylak, A murine model of volumetric muscle loss and a regenerative medicine approach for tissue replacement. *Tissue Eng Part A* **18**, 1941-1948 (Oct, 2012).

358. E. K. Merritt, D. W. Hammers, M. Tierney, L. J. Suggs, T. J. Walters, R. P. Farrar, Functional assessment of skeletal muscle regeneration utilizing homologous extracellular matrix as scaffolding. *Tissue Eng Part A* **16**, 1395-1405 (Apr, 2010).
359. J. G. Smith, A. J. Smith, R. M. Shelton, P. R. Cooper, Recruitment of dental pulp cells by dentine and pulp extracellular matrix components. *Exp Cell Res* **318**, 2397-2406 (Nov 1, 2012).
360. C. W. Chen, E. Montelatici, M. Crisan, M. Corselli, J. Huard, L. Lazzari, B. Peault, Perivascular multi-lineage progenitor cells in human organs: regenerative units, cytokine sources or both? *Cytokine & growth factor reviews* **20**, 429-434 (Oct-Dec, 2009).
361. B. T. Corona, X. Wu, C. L. Ward, J. S. McDaniel, C. R. Rathbone, T. J. Walters, The promotion of a functional fibrosis in skeletal muscle with volumetric muscle loss injury following the transplantation of muscle-ECM. *Biomaterials* **34**, 3324-3335 (Apr, 2013).